UNIVERSIDAD DE OVIEDO

Programa de Doctorado: Diseño, Construcción y Fabricación en la Ingeniería.

Tesis Doctoral

Modelizado y calibración en dinámica estructural

Rodolfo Alonso Camblor

Septiembre de 2015

Justificación

Oviedo, 11 de septiembre de 2015

Presidente/a de la Comisión Académica del Programa de Doctorado Diseño, construcción y fabricación en la ingeniería / Director/a de Departamento CONSTRUCCION E INGENIERIA DE FABRICACION

UNIVERSIDAD DE OVIEDO
Departamento de Construcción
e Ingeniería de Fabricación

Fdo.: Rocío Fernández

Contra la presente resolución podrá interponer recurso de alzada ente el Excmo. Sr. Rector Magfco. de esta Universidad en el plazo de un mes a contar desde el siguiente a la recepción de la presente resolución, de acuerdo con lo previsto en el artículo 114 de la Ley 30/92, de 26 de noviembre, del Régimen Jurídico de las Administraciones Públicas y Procedimiento Administrativo Común (B.O.E. de 27 de noviembre), modificada por la Ley 4/1999, de 13 de enero (B.OE. de 14 de enero)

SRA. PRESIDENTA DEL CENTRO INTERNACIONAL DE POSTGRADO

RESUMEN DEL CONTENIDO DE TESIS DOCTORAL

1.- Título de la Tesis	
Español/Otro Idioma: Modelizado y calibración en dinámica estructural	Inglés: Modelling and updating in structural dynamics

2.- Autor	
Nombre: Rodolfo Alonso Cambior	DNI/Pasaporte/NIE:
Programa de Doctorado: Diseño, Construcción y Fabricación en la Ingeniería	
Órgano responsable: Departamento de Construcción e Ingeniería de Fabricación	

RESUMEN (en español)

En las aplicaciones de ingeniería civil, los pórticos se calculan generalmente mediante modelos lineales. De esta forma se simplifica significativamente el modelizado, el cálculo y la extracción de propiedades dinámicas. Sin embargo, la linealidad raramente sucede en la realidad. Las estructuras siempre contienen cierto grado de no linealidad. Así pues, debe utilizarse un enfoque no lineal siempre que se requieran predicciones precisas del modelo. En esta tesis se estudian y resuelven varios aspectos relativos al modelizado y calibración lineal y no lineal de estructuras porticadas. Estos están recogidos en tres diferentes publicaciones en revistas especializadas.

La primera publicación incluye un pórtico a pequeña escala ensayado dinámicamente en una serie de diferentes configuraciones obtenidas mediante cambios de masa y la introducción de daño controlado. Se pretende un modelizado por elementos finitos con sentido físico para la configuración inicial. El modelo se calibra mediante una red neuronal, siendo las entradas de la red las frecuencias naturales del pórtico. El proceso de calibración se hace más preciso y robusto mediante un procedimiento regresivo, que constituye una contribución original de este estudio. Se desarrolló un novedoso modelo analítico simplificado para calcular la reducción de rigidez a flexión de las vigas debido al daño impuesto. Los resultados experimentales de las restantes configuraciones se utilizaron para validar el modelo de elementos finitos readaptado y el analítico de daño. Los resultados obtenidos fueron exitosos. El modelo readaptado reproduce de forma precisa las frecuencias identificadas en todas las configuraciones. El estudio estadístico de la transmisión de errores proporcionó unos estrechos intervalos de confianza para todos los parámetros identificados.

En el segundo artículo se propone un método para la calibración de modelos, tanto analíticos como de elementos finitos. Se plantea como la minimización de una función de error definida en el dominio del tiempo. La minimización se lleva a cabo mediante un novedoso algoritmo estocástico adaptativo, que constituye la principal contribución de este artículo. La solución se busca de forma iterativa muestreando los parámetros a calibrar en un espacio acotado. Se elige la función Beta, que es coherente con el carácter acotado del espacio de búsqueda, para el muestreo. Las características de las distribuciones se modifican en cada paso del proceso dependiendo de los resultados en los pasos anteriores. El método se probó mediante simulaciones con un modelo analítico y con resultados experimentales. Los últimos procedieron de un modelo de puente a pequeña escala ensayado sísmicamente. En estos casos particulares el funcionamiento del algoritmo propuesto fue mejor que el de otros algoritmos estocásticos de carácter general. El caso experimental fue especialmente mal condicionado. En estas

desfavorables condiciones, el algoritmo fue capaz de calibrar simultáneamente los parámetros de rigidez y amortiguamiento de un modelo no lineal.
En el tercer artículo se presenta la identificación modal no lineal de un pórtico de acero de cuatro plantas. En él se incluyen tanto los aspectos experimentales como los analíticos. Se aislaron experimentalmente los dos primeros modos de flexión del pórtico mediante una excitación simple mono armónica. Se midió la subsecuente vibración libre y se utilizó para la identificación. Se desarrolló un procedimiento original de filtraje para superar los inconvenientes los filtros de paso banda normalmente utilizados y mejorar la exactitud de las señales. Los resultados de la identificación no paramétrica revelaron que la estructura es débilmente no lineal en rigidez y fuertemente no lineal en amortiguamiento, mientras que las formas modales permanecen lineales dentro del rango de las medidas. Se demostró que los modos lineales son compatibles con la rigidez no lineal siempre que la no linealidad esté uniformemente distribuida a lo largo de la estructura. El comportamiento global de la estructura es no lineal para desplazamientos modales bajos y tiende hacia la linealidad a medida que el desplazamiento aumenta. Se propusieron leyes no lineales asintóticas para el modelizado de la rigidez y el amortiguamiento modales. Esta es otra contribución original en este trabajo. El modelo no lineal propuesto se ajustó a los resultados experimentales en el dominio del tiempo utilizando el algoritmo previamente desarrollado. Los resultados fueron excelentes con errores de ajuste tres órdenes de magnitud inferiores a los de un modelo lineal.

RESUMEN (en Inglés)

Linear models are commonly chosen for analysing the framed structures used in civil engineering applications. This approach strongly simplifies the modelling, analysis and extraction of dynamic properties. However, linearity seldom occurs in reality. Structures always contain some degree of nonlinearity. Therefore, a nonlinear approach should be used when more accurate predictions are required. Several issues related to the linear and nonlinear modelling and calibration of framed structures are addressed in this thesis. They are related to three different papers.
The first paper includes a small-scale steel frame dynamically tested in a series of different configurations obtained from the original one by changing masses and causing structural damage. Finite element modelling with physical meaning is tried for the original undamaged configuration. The finite element model is updated through a neural network, the natural frequencies of the model being the net input. The updating process is made more accurate and robust by using a regressive procedure, which constitutes an original contribution of this study. A novel simplified analytical model has been developed to evaluate the reduction of bending stiffness of the beams due to damage. The experimental results of the rest of configurations have been used to validate both the updated finite element model and the damage one. The results obtained are successful. The updated model accurately reproduces the low frequencies identified experimentally for all the configurations. The statistical study of the transmission of errors yields narrow confidence intervals for all the identified parameters.
A method in propounded in the second paper to updated finite element and analytical models. It is posed as the minimization of an error function defined in the time domain. The minimization is carried out by a novel adaptive sampling algorithm, which

constitutes the main contribution in this paper. The solution is searched by sampling the parameters to be updated in a bounded space in an iterative form. The Beta distribution, which is consistent with the bounded character of the search space, is chosen for the sampling. The characteristics of the distributions are changed in each step of the process depending on the results of the previous ones. The method was tested through a simulated dynamic model and an experimental case. The latter was a small-scale model of a continuous bridge seismically tested. In these particular cases, the performance of the proposed algorithm was better than those of the other related stochastic algorithms. The experimental case was especially ill-conditioned. Under these unfavourable conditions, the algorithm was capable to calibrate simultaneously the stiffness and damping parameters of a nonlinear model.

The nonlinear modal identification of a four-storey steel frame is presented in the third paper. It includes both the experimental and the analytical aspects. The first two bending modes of the frame were experientially isolated by a single-point mono-harmonic excitation. The subsequent free decay vibration was measured and used for identification purposes. An original filtering procedure was developed in order to overcome the drawbacks of the common band-pass filters and to enhance the accuracy of the signals. The results of the nonparametric identification reveal that the structure is weakly nonlinear in stiffness and strongly nonlinear in damping, while the mode shapes remain linear within the range of measurements. It is proved that these linear mode shapes are compatible with the nonlinear stiffness as long as the nonlinearity is uniformly distributed across the structure. The global behaviour of the structure is nonlinear for low modal displacements and tends to linearity for large displacements. Asymptotic nonlinear laws defined in the modal space where proposed to model both the stiffness and the damping. This is another original contribution of this paper. The proposed nonlinear model was fitted to the experimental data in the time domain by using the algorithm previously developed. Results were excellent with fitting errors three orders of magnitude lower than those of a pure linear model.

SR. DIRECTOR DE DEPARTAMENTO DE_____/
SR. PRESIDENTE DE LA COMISIÓN ACADÉMICA DEL PROGRAMA DE DOCTORADO EN _____

INFORME PARA LA PRESENTACIÓN DE TESIS DOCTORAL COMO COMPENDIO DE PUBLICACIONES

Año Académico:_2015/2016

1.- Datos personales del autor de la Tesis		
Apellidos: ALONSO CAMBLOR	Nombre: RODOLFO	
DNI/Pasaporte/NIE:	Teléfono:	Correo electrónico:

2.- Datos académicos	
Programa de Doctorado cursado: Diseño, Construcción y Fabricación en la Ingeniería	
Órgano responsable: Departamento de Construcción e Ingeniería de Fabricación	
Departamento/Instituto en el que presenta la Tesis Doctoral: Departamento de Construcción e Ingeniería de Fabricación	
Título definitivo de la Tesis	
Español: Modelizado y calibración en dinámica estructural	Inglés: Modelling and updating in structural dynamics
Rama de conocimiento: Ingeniería	

3.- Director/es de la Tesis	
D: José Luis Zapico Valle	DNI/Pasaporte/NIE: 10548268P
Departamento/Instituto: Departamento de Construcción e Ingeniería de Fabricación	

4.- Informe
La tesis se presenta como compendio de tres publicaciones en las que se estudian de forma progresiva diferentes aspectos de la misma unidad temática. Los tres artículos pertenecen a revistas indexadas en el JCR con índices de impacto elevados y posicionados dentro del primer cuartil en el campo de la ingeniería. La calidad de las publicaciones así como el grado de implicación del doctorando en la investigación son suficientes para la presentación de la tesis en el formato indicado.

Gijón, 3 de septiembre de 2015

Director de la Tesis Doctoral

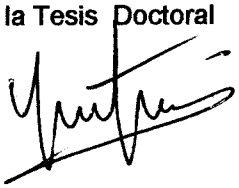

Fdo.: José Luis Zapico Valle

ACEPTACIÓN COAUTORES PRESENTACIÓN TRABAJOS FORMANDO PARTE DE TESIS DOCTORAL COMO COMPENDIO DE PUBLICACIONES

1.- Datos personales del coautor		
Apellidos: González Buelga	Nombre: Alicia	
DNI/Pasaporte/NIE	Teléfono	Correo electrónico

2.- Publicaciones que formarán parte de la tesis y de las que es coautor
Finite element model updating of a small steel frame using neural networks. *Smart Materials and Structures*, 17 (2008) 045016 (11pp).

ACEPTACIÓN:	
Acepto que las publicaciones anteriores formen parte de la tesis doctoral titulada: Modelizado y Calibración en Dinámica Estructural Y elaborada por D. Rodolfo Alonso Camblor Gijón, 31 de julio de 2015 Firma	

ACEPTACIÓN COAUTORES PRESENTACIÓN TRABAJOS FORMANDO PARTE DE TESIS DOCTORAL COMO COMPENDIO DE PUBLICACIONES

1.- Datos personales del coautor		
Apellidos: **González Martínez**	Nombre: **María Placeres**	
DNI/Pasaporte/NIE	Teléfono	Correo electrónico

2.- Publicaciones que formarán parte de la tesis y de las que es coautor

Finite element model updating of a small steel frame using neural networks. *Smart Materials and Structures*, 17 (2008) 045016 (11pp)..

A new method for finite element model updating in structural dynamics. *Mechanical Systems and Signal Processing*, 24 (2010) 2137-59.

ACEPTACIÓN:

Acepto que las publicaciones anteriores formen parte de la tesis doctoral titulada:
Modelizado y Calibración en Dinámica Estructural

Y elaborada por D. Rodolfo Alonso Camblor

Gijón, 29 de Julio de 2015

Fdo. María Placeres González Martínez

ACEPTACIÓN COAUTORES PRESENTACIÓN TRABAJOS FORMANDO PARTE DE TESIS DOCTORAL COMO COMPENDIO DE PUBLICACIONES

1.- Datos personales del coautor		
Apellidos: Zapico Valle	Nombre: José Luis	
DNI/Pasaporte/NIE:	Teléfono	Correo electrónico

2.- Publicaciones que formarán parte de la tesis y de las que es coautor

Finite element model updating of a small steel frame using neural networks. *Smart Materials and Structures*, 17 (2008) 045016 (11pp)..

A new method for finite element model updating in structural dynamics. *Mechanical Systems and Signal Processing*, 24 (2010) 2137-59.

Nonlinear modal identification of a steel frame. *Engineering Structures*, 56 (2013) 246-259.

ACEPTACIÓN:

Acepto que las publicaciones anteriores formen parte de la tesis doctoral titulada:
Modelizado y Calibración en Dinámica Estructural

Y elaborada por D. Rodolfo Alonso Camblor

Gijón , 29 de julio de 2015

Firma

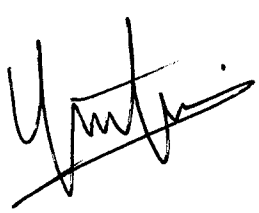

ACEPTACIÓN COAUTORES PRESENTACIÓN TRABAJOS FORMANDO PARTE DE TESIS DOCTORAL COMO COMPENDIO DE PUBLICACIONES

1.- Datos personales del coautor		
Apellidos: García Diéguez	Nombre: Marta	
DNI/Pasaporte/NIE	Teléfono	Correo electrónico

2.- Publicaciones que formarán parte de la tesis y de las que es coautor
A new method for finite element model updating in structural dynamics. *Mechanical Systems and Signal Processing*, 24 (2010) 2137–59. Nonlinear modal identification of a steel frame. *Engineering Structures*, 56 (2013) 246–259.

ACEPTACIÓN:	
Acepto que las publicaciones anteriores formen parte de la tesis doctoral titulada: Modelizado y Calibración en Dinámica Estructural Y elaborada por D. Rodolfo Alonso Camblor Gijón, 29 Julio 2015 Firma	

Esta tesis se presenta como compendio de publicaciones para la obtención del título de Doctor por la Universidad de Oviedo.

Los artículos que forman parte de esta tesis y han sido publicados en revistas indexadas en el Journal Citation Report (JRC) son:

1. Finite element model updating of a small steel frame using neural networks.
   J. L. Zapico, A. González-Buelga, M. P. González and R. Alonso.
   Smart Materials and Structures. 17 (2008) 045016 (11pp).
   Índice de impacto (2009): 1,749.
   Instruments & instrumentation (12/58, Q1).

2. A new method for finite element model updating in structural dynamics.
   J. L. Zapico-Valle, R. Alonso-Camblor, M. P. González-Martínez, M. García-Diéguez.
   Mechanical Systems and Signal Processing. 24 (2010) 2137-2159.
   Índice de impacto (2011): 1,824.
   Engineering, mechanical (15/122, Q1).

3. Nonlinear modal identification of a steel frame.
   J. L. Zapico-Valle, M. García-Diéguez, R. Alonso-Camblor.
   Engineering Structures. 56 (2013) 246-259.
   Índice de impacto (2014): 1,838.
   Engineering, civil (21/124, Q1).

Resumen

En las aplicaciones de ingeniería civil, los pórticos se calculan generalmente mediante modelos lineales. De esta forma se simplifica significativamente el modelizado, el cálculo y la extracción de propiedades dinámicas. Sin embargo, la linealidad raramente sucede en la realidad. Las estructuras siempre contienen cierto grado de no linealidad. Así pues, debe utilizarse un enfoque no lineal siempre que se requieran predicciones precisas del modelo. En esta tesis se estudian y resuelven varios aspectos relativos al modelizado y calibración lineal y no lineal de estructuras porticadas. Estos están recogidos en tres diferentes publicaciones en revistas especializadas.

La primera publicación incluye un pórtico a pequeña escala ensayado dinámicamente en una serie de diferentes configuraciones obtenidas mediante cambios de masa y la introducción de daño controlado. Se pretende un modelizado por elementos finitos con sentido físico para la configuración inicial. El modelo se calibra mediante una red neuronal, siendo las entradas de la red las frecuencias naturales del pórtico. El proceso de calibración se hace más preciso y robusto mediante un procedimiento regresivo, que constituye una contribución original de este estudio. Se desarrolló un novedoso modelo analítico simplificado para calcular la reducción de rigidez a flexión de las vigas debido al daño impuesto. Los resultados experimentales de las restantes configuraciones se utilizaron para validar el modelo de elementos finitos readaptado y el analítico de daño. Los resultados obtenidos fueron exitosos. El modelo readaptado reproduce de forma precisa las frecuencias identificadas en todas las configuraciones. El estudio estadístico de la transmisión de errores proporcionó unos estrechos intervalos de confianza para todos los parámetros identificados.

En el segundo artículo se propone un método para la calibración de modelos, tanto analíticos como de elementos finitos. Se plantea como la minimización de una función de error definida en el dominio del tiempo. La minimización se lleva a cabo mediante un novedoso algoritmo estocástico adaptativo, que constituye la principal contribución de este artículo. La solución se busca de forma iterativa muestreando los parámetros a calibrar en un espacio acotado. Se elige la función Beta, que es coherente con el carácter acotado del espacio de búsqueda, para el muestreo. Las características de las distribuciones se modifican en cada paso del proceso dependiendo de los resultados en los pasos anteriores. El método se probó mediante simulaciones con un modelo analítico

y con resultados experimentales. Los últimos procedieron de un modelo de puente a pequeña escala ensayado sísmicamente. En estos casos particulares el funcionamiento del algoritmo propuesto fue mejor que el de otros algoritmos estocásticos de carácter general. El caso experimental fue especialmente mal condicionado. En estas desfavorables condiciones, el algoritmo fue capaz de calibrar simultáneamente los parámetros de rigidez y amortiguamiento de un modelo no lineal.

En el tercer artículo se presenta la identificación modal no lineal de un pórtico de acero de cuatro plantas. En él se incluyen tanto los aspectos experimentales como los analíticos. Se aislaron experimentalmente los dos primeros modos de flexión del pórtico mediante una excitación simple mono armónica. Se midió la subsecuente vibración libre y se utilizó para la identificación. Se desarrolló un procedimiento original de filtraje para superar los inconvenientes los filtros de paso banda normalmente utilizados y mejorar la exactitud de las señales. Los resultados de la identificación no paramétrica revelaron que la estructura es débilmente no lineal en rigidez y fuertemente no lineal en amortiguamiento, mientras que las formas modales permanecen lineales dentro del rango de las medidas. Se demostró que los modos lineales son compatibles con la rigidez no lineal siempre que la no linealidad esté uniformemente distribuida a lo largo de la estructura. El comportamiento global de la estructura es no lineal para desplazamientos modales bajos y tiende hacia la linealidad a medida que el desplazamiento aumenta. Se propusieron leyes no lineales asintóticas para el modelizado de la rigidez y el amortiguamiento modales. Esta es otra contribución original en este trabajo. El modelo no lineal propuesto se ajustó a los resultados experimentales en el dominio del tiempo utilizando el algoritmo previamente desarrollado. Los resultados fueron excelentes con errores de ajuste tres órdenes de magnitud inferiores a los de un modelo lineal.

Abstract

Linear models are commonly chosen for analysing the framed structures used in civil engineering applications. This approach strongly simplifies the modelling, analysis and extraction of dynamic properties. However, linearity seldom occurs in reality. Structures always contain some degree of nonlinearity. Therefore, a nonlinear approach should be used when more accurate predictions are required. Several issues related to the linear and nonlinear modelling and calibration of framed structures are addressed in this thesis. They are related to three different papers.

The first paper includes a small-scale steel frame dynamically tested in a series of different configurations obtained from the original one by changing masses and causing structural damage. Finite element modelling with physical meaning is tried for the original undamaged configuration. The finite element model is updated through a neural network, the natural frequencies of the model being the net input. The updating process is made more accurate and robust by using a regressive procedure, which constitutes an original contribution of this study. A novel simplified analytical model has been developed to evaluate the reduction of bending stiffness of the beams due to damage. The experimental results of the rest of configurations have been used to validate both the updated finite element model and the damage one. The results obtained are successful. The updated model accurately reproduces the low frequencies identified experimentally for all the configurations. The statistical study of the transmission of errors yields narrow confidence intervals for all the identified parameters.

A method in propounded in the second paper to updated finite element and analytical models. It is posed as the minimization of an error function defined in the time domain. The minimization is carried out by a novel adaptive sampling algorithm, which constitutes the main contribution in this paper. The solution is searched by sampling the parameters to be updated in a bounded space in an iterative form. The Beta distribution, which is consistent with the bounded character of the search space, is chosen for the sampling. The characteristics of the distributions are changed in each step of the process depending on the results of the previous ones. The method was tested through a simulated dynamic model and an experimental case. The latter was a small-scale model of a continuous bridge seismically tested. In these particular cases, the performance of the proposed algorithm was better than those of the other related stochastic algorithms.

The experimental case was especially ill-conditioned. Under these unfavourable conditions, the algorithm was capable to calibrate simultaneously the stiffness and damping parameters of a nonlinear model.

The nonlinear modal identification of a four-storey steel frame is presented in the third paper. It includes both the experimental and the analytical aspects. The first two bending modes of the frame were experientially isolated by a single-point mono-harmonic excitation. The subsequent free decay vibration was measured and used for identification purposes. An original filtering procedure was developed in order to overcome the drawbacks of the common band-pass filters and to enhance the accuracy of the signals. The results of the nonparametric identification reveal that the structure is weakly nonlinear in stiffness and strongly nonlinear in damping, while the mode shapes remain linear within the range of measurements. It is proved that these linear mode shapes are compatible with the nonlinear stiffness as long as the nonlinearity is uniformly distributed across the structure. The global behaviour of the structure is nonlinear for low modal displacements and tends to linearity for large displacements. Asymptotic nonlinear laws defined in the modal space where proposed to model both the stiffness and the damping. This is another original contribution of this paper. The proposed nonlinear model was fitted to the experimental data in the time domain by using the algorithm previously developed. Results were excellent with fitting errors three orders of magnitude lower than those of a pure linear model.

Índice general

Acrónimos

Entrada	Descripción	Pág.
FRFs	Funciones de Respuesta en Frecuencia	9, 10, 15, 16
MEF	Modelo de Elementos Finitos	9, 10, 14
RMEF	Readaptación de Modelos de elementos Finitos	9, 10, 15, 16, 18, 19
MAC	Modal Assurance Criterion	10
CMCM	Cross Model-Cross Mode	11
SEA	Substructure Energy Approach	12
IESM	Inverse Eigensentitivity Method	14, 15, 16, 18
RFM	Response Function Method	15, 17
ROCP	Reduced Order Characteristic Polynomial	16
MUBE	Model Updating using Base Excitation	16, 17
SA	Simulated Annealing	17
GA	Genetic Algorithm	17
BSA	Blended Simulated Annealing	17
PSO	Particle Swarm Optimization	17
RSM	Response Surface Methodology	18
ISO	International Organization for Standardization	20
SHM	Structural Health Monitoring	20, 21
RFSM	Restoring Force Surface Method	21, 22
NNMs	Nonlinear Normal Modes	22

CMA-ES	Covariance Matrix Adaptation Evolution Strategy	29, 30
MLF	Moving Linear Fitting	33,34

1. Introducción

En términos generales se entiende por modelización la acción de crear un esquema teórico, conocido como modelo, que describa cierta realidad física. Cabe destacar que los hechos físicos reales son únicos e irrepetibles. Ya Heráclito afirmaba: “Ningún hombre puede cruzar el mismo río dos veces, porque ni el hombre ni el agua serán los mismos”. Por eso quizá la realidad física sea inaprehensible en su totalidad y su descripción constituye un problema filosófico complejo con muchos posibles enfoques. En ingeniería se suele adoptar un enfoque pragmático guiado por la utilidad, más que por la veracidad. Esto significa que, dado cierto nivel de aproximación a la realidad, el modelo más apropiado en cada aplicación es aquel que tenga la menor complejidad y que proporcione la solución más rápidamente y al menor coste posible. Los modelos en ingeniería se formulan generalmente en términos matemáticos, como pueden ser sistemas de ecuaciones diferenciales. El lenguaje simbólico de las matemáticas es muy apropiado para expresar conceptos de gran complejidad. El modelizado implica la selección y cuantificación de las variables y relaciones de un sistema físico capaces de representarlo al nivel de detalle requerido. En el caso de estructuras y sistemas mecánicos, el proceso de modelizado requiere de los ingenieros una notable perspicacia para apreciar los aspectos fundamentales del comportamiento físico. Las matemáticas son una herramienta para expresar lo previamente intuido. El modelizado, pues, constituye una mezcla equilibrada entre intuición y deducción. Una descripción magistral de este proceso fue realizada por el insigne ingeniero francés Eugène Freyssinet: “Sólo existen en mí dos fuentes de información: la percepción directa de los hechos y la intuición, en la que veo la expresión y el resumen de todas las experiencias acumuladas por la vida en el subconsciente de los seres, desde la primera célula. Bien entendido, es preciso que la intuición sea controlada por la experiencia. Pero cuando se halla en contradicción con el resultado de un cálculo hago revisar el cálculo, y mis colaboradores aseguran que, a fin de cuentas, es siempre el cálculo el que está equivocado”. Posteriormente matizó la cuestión de esta forma: “Entiéndanme bien: yo no niego la grandeza ni la belleza de las matemáticas, ellas han proporcionado a los Einstein y a los De Broglie el lenguaje con el cual han escrito la más grandiosa epopeya que los hombres hayan concebido jamás. Tampoco desconozco su utilidad práctica en

nuestra profesión; yo no me he abstenido de utilizarlas en su oportunidad. Pero no debemos nunca olvidar que ellas no nos proporcionan sino medios de cambiar la forma de los datos que ya poseemos, y que, por grande que sea el interés y la utilidad de esas transformaciones, no hallamos nunca, al final de un cálculo, más que lo que hemos puesto en él al iniciarlo".

El modelizado es fundamental en la práctica de la ingeniería de estructuras y sistemas mecánicos. En la fase de diseño el modelo permite predecir la respuesta de la estructura a las solicitaciones previstas y a partir de ella modificar sucesivamente su diseño hasta que se satisfagan las condiciones de seguridad y seviciabilidad al mínimo coste posible. El modelo también es necesario en sentido inverso para para inferir a partir de resultados de ensayos el estado de una estructura en servicio y su evolución, pues las estructuras tienden a degradarse y desgastarse en el tiempo, o para evaluar la integridad estructural tras una solicitación excepcional, como un choque, terremoto, huracán, etc. En este caso los parámetros del modelo se readaptan hasta que su respuesta se aproxime suficientemente a la medida experimentalmente. El cálculo, tanto en sentido directo como inverso, requiere la resolución de muchas operaciones matemáticas, que aumentan exponencialmente con la complejidad del modelo, y constituye una tarea significativa de la práctica ingenieril.

Los modelos utilizados en ingeniería estructural estuvieron inicialmente limitados por los procedimientos de cálculo matemático disponibles. Estos se realizaban manualmente y así resultaban lentos y poco fiables. Para ser aplicables en estas condiciones, los modelos tenían que ser sencillos, con poco nivel de detalle. Se utilizaban generalmente modelos lineales en régimen estático y las uniones entre elementos se modelizaban o totalmente rígidas o totalmente flexibles. Otra particularidad en este período inicial es que los métodos de modelizado y cálculo se adaptaban a las características de cada estructura, no se planteaban métodos generales aplicables a la mayoría de los casos.

La invención de los ordenadores a mediados del siglo pasado, y su rápida evolución posterior, supuso una auténtica revolución a la que la ingeniería estructural no fue ajena. El ordenador permite realizar operaciones matemáticas de forma muy rápida, con gran precisión y almacenar grandes volúmenes de datos para su posterior utilización. Una vez disponible esta potente herramienta de cálculo, los métodos manuales se abandonaron y se retomaron los métodos de cálculo matriciales, que habían sido formulados siglos atrás por Navier y Cauchy, pero no se habían utilizado porque

requieren la solución de extensos sistemas de ecuaciones inviable por procedimientos manuales. El más popular es el método de los desplazamientos, que es aplicable a estructuras formadas por barras interconectadas a través de nodos. La idea básica en este método consiste en reducir el continuo considerando solamente los grados de libertad de los nodos. La matriz de rigidez, que relaciona desplazamientos con fuerzas nodales, se obtiene a partir de las matrices de rigidez de cada barra, para las que existen soluciones analíticas exactas. Los desplazamientos nodales correspondientes a un estado de carga dado se obtienen resolviendo el sistema de ecuaciones derivado de la relación citada. Finalmente, los efectos en cada barra se siguen de los desplazamientos nodales y las matrices de rigidez individuales. Para la resolución de estos extensos sistemas de ecuaciones también se retomaron antiguos algoritmos (Gauss, Cholesky, etc.), que fueron desarrollados y adaptados a las nuevas circunstancias, y se crearon nuevos algoritmos. El método es totalmente general y una vez transcrito a un código informático es aplicable a cualquier estructura formada por barras.

Las demandas de la industria aeroespacial motivaron la extensión del método de los desplazamientos a estructuras bidimensionales. El esquema intuitivo adoptado por los ingenieros estructurales en este caso consistió en dividir artificialmente la superficie media de la estructura en un número finito de elementos a través de líneas imaginarias. De ahí que se designen como elementos finitos. Los elementos se suponen conectados a un número discreto de puntos comunes situados en los contornos y cuyos desplazamientos constituyen las variables del problema. Estos elementos y puntos son el correlato de las barras y nodos de las estructuras reticuladas. Al contrario que las barras, no se conocen soluciones analíticas generales para el campo de desplazamientos en el interior de los elementos bidimensionales. Así que se aproximan mediante un conjunto de funciones de interpolación dependientes de los desplazamientos nodales. Las funciones de interpolación junto las leyes constitutivas del material permiten obtener las matrices de rigidez de los elementos. A partir de aquí se sigue el método de los desplazamientos para calcular la respuesta de la estructura a una solicitación dada.

Este procedimiento intuitivo de los ingenieros fue posteriormente retomado por los matemáticos con mayor rigor analítico e incorporando ciertos enfoques de aproximación previos con objeto de garantizar la convergencia de la solución. Entre ellos intervino el matemático Richard Courant que advertía de la necesaria simbiosis entre la intuición y el razonamiento deductivo: “La evidencia empírica nunca puede establecer la existencia

matemática; ni puede la necesidad de una demostración de existencia ser descartada por un físico como rigor innecesario. Sólo una prueba matemática de existencia puede asegurar que la descripción matemática de un fenómeno tiene sentido". De todo ello surgió el llamado método de los elementos finitos. Éste es un método general para aproximar cualquier problema físico descrito mediante ecuaciones diferenciales, que son transformadas en sistemas de ecuaciones algebraicas y resueltas numéricamente con la ayuda del ordenador. Los códigos informáticos de cálculo, conocidos como modelos numéricos o modelos software, incluyen subrutinas para la ejecución de operaciones repetitivas en función de ciertos parámetros. La ejecución de estas subrutinas está organizada mediante un programa principal. La gran cantidad de datos necesaria para la definición numérica del problema físico y los también numerosos datos de salida generados se tratan y almacenan mediante programas específicos de pre y postprocesado. El método permite el cálculo de todo tipo de estructuras incluyendo aquellas con geometrías tridimensionales muy complejas. Las opciones de cálculo son inmensas. Se pueden abordar problemas con no linealidades tanto materiales como geométricas. El cálculo dinámico en el dominio del tiempo es otra de las posibles opciones. También es aplicable en problemas combinados como la interacción fluido estructura. La evolución creciente del método y el desarrollo de los ordenadores personales en las últimas décadas propiciaron su uso generalizado, constituyendo una herramienta imprescindible para cálculo estructural en la actualidad. Con esta potente herramienta de cálculo se han podido atender las demandas de reducción de peso y aumento de fiabilidad requeridas en el sector aeroespacial. La optimización estructural fue posteriormente extendida a otros sectores: transporte, ingeniería civil y construcción. Como resultado se consiguen diseños estructurales cada vez más competitivos y fiables.

La potencia de cálculo y coherencia matemática conseguidos no garantizan, sin embargo, el éxito en la aplicación del método de los elementos finitos. Como se ha comentado al inicio de esta sección, el modelo de cálculo debe satisfacer otra condición esencial: ser capaz de reproducir la realidad física que se modeliza. Para que esto se cumpla el modelo debe recoger las relaciones entre variables físicas más significativas en el caso que se trate. Además de la completitud de las variables y sus relaciones, los valores numéricos de los parámetros del modelo deben ser próximos a los reales. El proceso de acercamiento a la realidad se conoce como readaptación de modelos, *model*

updating en la literatura en inglés. Ésta constituye una tarea fundamental para conseguir el máximo provecho del modelo en sus aplicaciones. Le readaptación se basa en datos empíricos obtenidos mediante ensayos en estructuras reales. De estos datos se infiere la estructura idónea del modelo de cálculo. Esta tarea no se puede automatizar, sino que es el resultado de la intuición física y experiencia previa de los ingenieros estructurales. Por otra parte, la calibración de los parámetros del modelo está condicionada por la naturaleza de los datos experimentales. Estos son generalmente incompletos, pues están limitados a un número restringido de grados de libertad y a un rango limitado de frecuencias. Además, los datos contienen errores que son propios del sistema de medida y del posterior tratamiento de las señales. Todas estas peculiaridades hacen que la readaptación de modelos sea una tarea muy compleja, para cuya solución no existe un algoritmo general, en la que la experiencia adquirida en el estudio de casos particulares resulta muy útil en tratamiento de casos posteriores similares.

2. Objetivos generales

Esta tesis se une al campo de la readaptación de modelos estructurales con la intención de alcanzar las siguientes metas:

a) Desarrollar procedimientos aplicables a estructuras porticadas en servicio para la obtención de datos experimentales.

b) Establecer procedimientos de preprocesado de las señales experimentales capaces de reducir los errores de medida y a la vez mantener el máximo de información.

c) Crear modelos avanzados que describan el comportamiento dinámico de estructuras porticadas.

d) Implantar procedimientos para la calibración de tales modelos en función de las señales experimentales.

3. Estado del arte

El análisis dinámico trata de comprender, evaluar, analizar y modificar (si se requiere) el comportamiento dinámico de una estructura, el cual puede representarse en términos de frecuencias naturales, modos de vibración, índices de amortiguamiento, funciones de respuesta en frecuencia (FRFs), etc. El análisis dinámico de las estructuras se puede llevar a cabo por la vía experimental [9], o bien por medio de una aproximación teórica [25]. La aplicación de la vía teórica implica la necesidad de creación de un modelo analítico del sistema bien sea a través de un método clásico [26] o a través del método de elementos finitos [27]. La aplicación de un método clásico se limita a sistemas simples mientras que se prefiere el empleo del método de elementos finitos a sistemas estructurales reales más complejos. El modelo creado no puede reproducir con toda exactitud la respuesta dinámica de las estructuras. A pesar de que los datos experimentales procedentes de la respuesta dinámica de la estructura poseen errores que pueden provocar una baja correlación entre éstos y las predicciones del modelo analítico, la principal causa de esta diferencia entre respuestas analíticas y experimentales se debe según Friswell and Mottershead [3] a errores en el propio modelo de elementos finitos (MEF). Estos errores se deben principalmente a la mala definición de las condiciones de contorno, valores inadecuados de las propiedades del material, incorrecta discretización o baja calidad del mallado, dificultad de modelización de formas complejas, asunción de simplificaciones como amortiguamiento lineal en vez de no lineal, modelizado incorrecto de las uniones y errores de redondeo en los cálculos efectuados.

Se hace necesario readaptar el modelo de elementos finitos para que su respuesta se ajuste a la respuesta dinámica real obtenida experimentalmente. Este proceso de corrección del modelo es lo que se conoce como readaptación de modelos de elementos finitos (RMEF). En las técnicas de readaptación de modelos las respuestas experimental y la proporcionada por el modelo se comparan, se correlacionan y se compatibilizan dimensionalmente para tener la seguridad que el modelo escogido es válido para su posterior calibración sin necesidad de recurrir a un nuevo modelo de elementos finitos. Existen diversas metodologías para comparar y correlacionar las respuestas proporcionadas por el modelo con las obtenidas experimentalmente. Cabe destacar el

Modal Assurance Criterion (MAC), desarrollado por Allemag and Brown [33], que se fundamenta en establecer una correlación entre los modos de vibración obtenidos de la respuesta dinámica de la estructura y los proporcionados por el modelo analítico de elementos finitos (MEF). El hecho de disponer de un conjunto de datos experimentales de dimensiones claramente inferior al conjunto de datos obtenidos del modelo analítico de elementos finitos, implica que se está ante un problema con datos incompletos y por tanto se deben hacer compatibles los conjuntos de datos que se van a comparar en el proceso de calibración del modelo analítico. Para lograr esta compatibilidad dimensional se recurre a reducir el número de grados de libertad del modelo analítico, pues generalmente se mide un reducido número de modos de vibración, o bien realizar una expansión modal de los modos de vibración para estimar los modos en los grados de libertad en los que no se han realizado mediciones.

El campo de readaptación de modelos tuvo un fuerte impulso desde los 90 hasta la actualidad a raíz de los requerimientos de la industria aeroespacial. Se han publicado numerosos artículos, revisiones del estado del arte y libros. Entre ellos, cabe destacar [3], [24], [2]. Los primeros procedimientos de RMEF se deben a Ewins [25]. Estos son los métodos directos basados, en parte, en la teoría de control. Se parte de las matrices de rigidez, masa y amortiguamiento generadas a través de un MEF que se modifican directamente de forma que reproduzcan exactamente las características modales de las estructura. La comparación de las FRF es difícil puesto que el amortiguamiento está presente en los datos modales experimentales extraídos de la estructura y en general no se incluye en los modelos analíticos de elementos finitos [2]. La ventaja que tienen estos métodos directos es que reproducen exactamente los datos modales obtenidos experimentalmente por medio de operaciones analíticas matriciales directas, lo que los hace muy eficientes y rápidos. El inconveniente radica en que sólo son aplicables a sistemas lineales, se reproducen señales de ruido y modos espúreos y, además, es necesario realizar unos procedimientos de ensayo y análisis modal muy refinados. Las técnicas directas de calibración se fundamentan en el uso de tres conjuntos de valores: los datos modales experimentales, las matrices de masa y rigidez del modelo analítico. Se considera conocido de forma precisa uno de dicho conjunto de valores y los otros dos restantes se ajustan a partir de los valores del conjunto conocido. Baruch and Bar-Ithack [29] desarrollaron un método directo de readaptación en el que se considera correcta la matriz de masa del modelo analítico y la matriz de rigidez se ajusta

considerando los modos de vibración corregidos y las frecuencias de los ensayos experimentales. Berman and Nagy [30] cuestionaron el uso de la masa como parámetro fijo y propusieron en su lugar los datos modales experimentales, de manera que se ajustan las matrices de masa y rigidez. El método de Berman and Nagy [30] fue ampliado por Caesar [31], mediante la incorporación de restricciones adicionales que preservan la masa total del sistema y las fuerzas de interconexión. Chen et al. [34] llegaron a ajustar simultáneamente las matrices de masa y rigidez del sistema. Shidu and Ewins [35] desarrollaron un método directo basado en la matriz de error, que es útil cuando los errores que se deducen del modelo analítico son pequeños. Kabe [36] propuso un método directo que mantiene el ancho de banda de las matrices durante el proceso de calibración del modelo gracias a la identificación en la etapa inicial de los términos nulos en las mismas y obligándoles a permanecer a cero durante el proceso de readaptación. En varios ejemplos simulados, Farhat and Hemez [37] propusieron una técnica de readaptación de modelos en la que se emplea una metodología de sensibilidad de elemento a elemento que es bastante robusta. Friswell et al. [38] desarrollaron un procedimiento de readaptación simultánea de las matrices de rigidez y amortiguamiento partiendo de la base de que la matriz de masa sea correcta. Xiamin [39] logró una técnica de aproximación matricial usando descomposición en valores singulares que es particularmente útil cuando las diferencias entre la respuesta experimental y la del modelo analítico son muy grandes. Recientemente, Carvalho et al. [32] desarrollaron un método que puede identificar y prevenir la aparición de modos espúreos en los resultados calibrados. Todas estas metodologías directas de ajuste de modelos tienen como objetivo eliminar el desajuste existente entre la respuesta experimental medida y la proporcionada por el modelo de elementos finitos sin preocuparse de realizar corrección o ajuste alguno sobre las propiedades físicas de los sistemas de matrices. Así pues, las matrices obtenidas tras el proceso de readaptación del modelo por medio de técnicas directas son, en general, totalmente pobladas y guardan poca relación con la conectividad física de la estructura.

En la actualidad se han realizado algunas investigaciones orientadas a desarrollar metodologías del tipo directo para la readaptación de modelos a través del ajuste de las propiedades físicas del modelo de elementos finitos. Hu et al. [40] presentaron el método de *cross-model-cross-mode* (CMCM) que presenta unos resultados satisfactorios para ejemplos simulados del modelo de edificio a cortante y el del pórtico

tridimensional. Este método tiene el inconveniente de necesitar información modal espacial experimental completa. Fang et al. [41] propusieron un método denominado *Substructure Energy Approach* (SEA) en el que se subdivide el sistema principal en subsistemas, de los cuales solamente se identifican y readaptan los críticos en vez de todo el sistema en su conjunto, y gracias a ello se puede superar el inconveniente de no disponer de toda la información modal espacial experimental. Este método se verificó en la readaptación de modelos sencillos tipo sistema masa-muelle y celosías bi y tridimensionales empleando datos experimentales simulados. Jacquelin et al. [42] desarrollaron una técnica directa probabilística de readaptación de modelos que tiene en cuenta las incertidumbres de los datos experimentales. Jiang et al. [43] redujeron el proceso de readaptación de modelos al problema de la mejor aproximación tipo, siendo válida su utilización en ejemplos numéricos de sistemas no amortiguados, no habiendo sido probado en ejemplos simulados de sistemas amortiguados y tampoco lo ha sido con resultados experimentales reales.

El mayor inconveniente de los métodos directos es que son meramente representacionales, esto es, se trata de un modelo matemático puro basado en el ajuste de los elementos de las matrices, que reproduce la respuesta pero sin significado físico. Se rompe la conectividad de las matrices y el cambio en los términos de las mismas no puede traducirse en los propios elementos de la estructura. Ya Berman [28] indicaba que con estas operaciones matriciales no se podía llegar a un modelo con sentido físico.

Los requerimientos de la industria hicieron que los métodos de readaptación evolucionasen hacia otro tipo de estrategias considerando el sentido físico del modelo. Este grupo de metodologías se conocen en la literatura como métodos iterativos. Con los métodos iterativos no solamente se busca acercar la respuesta analítica a la experimental, sino dotar al modelo de un mayor sentido físico. Para lograr este objetivo son básicas dos tareas. Primero, la identificación de las carencias conceptuales del modelo que sean significativas para el uso al que se le asignan, por ejemplo, si las uniones de una estructura son flexibles y se modelizan como rígidas no están reproduciendo adecuadamente la realidad física. Estas carencias en el modelo suelen localizarse en los puntos de discontinuidad de las estructuras como son las uniones y los apoyos. También es típico el caso del amortiguamiento, que suele modelizarse como amortiguamiento lineal, pero que raramente se da esta condición en la realidad. La segunda tarea consiste en la calibración de los parámetros del modelo. Algunos

parámetros son muy conocidos de ensayos y estudios previos y su margen de variación es muy pequeño. Tal es el caso de algunas propiedades físicas como la densidad del material o propiedades elásticas como el módulo de elasticidad. Sin embargo, otros son más desconocidos y es necesario su calibración o ajuste. Sirva como ejemplo la rigidez a flexión de una unión que puede variar de cero (articulada) a infinito (rígida).

La identificación de carencias conceptuales de modelizado y la selección de parámetros a calibrar son tareas muy difíciles que no pueden ser automatizadas. Cada caso requiere un estudio particular y las soluciones se obtienen después de un proceso de ensayo y error en el que la experiencia y la intuición son fundamentales [2]. Bajo estas circunstancias, la experiencia ganada en el estudio de un caso particular puede utilizarse de manera ventajosa en el estudio de posteriores casos similares.

La información necesaria para desarrollar estas tareas proviene de ensayos experimentales, generalmente dinámicos, realizados sobre estructuras. Las señales utilizadas pueden venir expresadas en el domino del tiempo, de la frecuencia, y el modal. Los datos de los ensayos deben ser lo más informativos posibles. Los datos experimentales son incompletos porque no contienen a todos los grados de libertad de la estructura e incluyen un rango limitado de modos de vibración.

Los parámetros que se eligen para readaptar deben cumplir dos condiciones: que sean inciertos, y que los datos disponibles sean sensibles a dichos parámetros. El número de parámetros a calibrar debe ser el menor posible porque se debe llegar a un sistema de bien condicionado.

En estas técnicas los parámetros elegidos se calibran de forma iterativa de modo tal que se minimiza cierta función de error, que tiene en cuenta las diferencias entre las respuestas experimentales y analítica, como se indica en Figura 1.

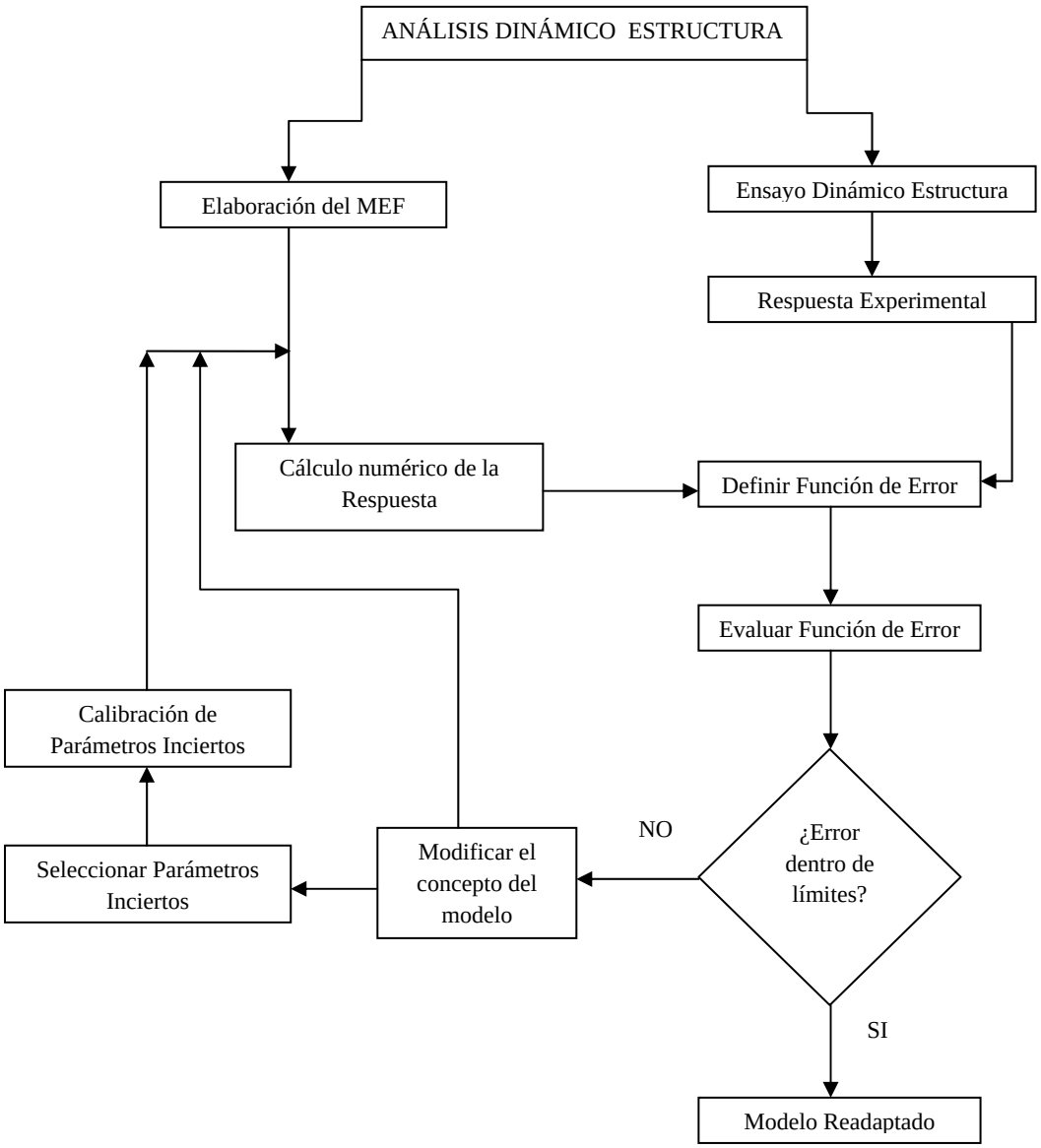

Figura 1. Esquema de método iterativo de readaptación de modelos de elementos finitos.

Estas técnicas se iniciaron en 1974, cuando Collins et al. [44] propusieron el *Inverse Eigensensitive Method* (IESM). Después Chen y Garba [45] utilizaron la técnica de matriz de perturbación para calcular las sensibilidades a los datos modales. Este método fue posteriormente mejorado por Kim et al. [46] incluyendo sensibilidades de segundo orden. Después Lin et al. [47] mejoraron la convergencia de este método empleando los datos modales del modelo de elementos finitos y los experimentales para el cálculo de los coeficientes de la matriz de sensibilidad. Esto también permitió la aplicación del método a casos con errores grandes.

En la IESM se utilizan datos modales como frecuencias, modos e índices de amortiguamiento para construir la función de error. Los datos modales se obtienen a través de la realización de análisis modal a las FRFs. El análisis modal añade ciertos errores a los datos modales extraídos, que son posteriormente transmitidos a los resultados del proceso de RMEF. Para evitar este problema se pueden utilizar directamente en la readaptación las FRF medidas usando el llamado *Response Function Method* (RFM), propuesto por Lin and Ewins [48]. RFM no requiere practicar ninguna extracción modal en las medidas experimentales, eliminando así las posibilidades de error. Modak et al. [49] aplicaron la RFM a una viga biempotrada y a una estructura porticada simple en forma de F. La eficiencia del IESM y RFM fue probada por Imregun et al. [51] y por Modak et al. [50]. Para el caso de modos incompletos y sin ruido, RFM proporciona mejores resultados que el IESM, mientras que este último funciona mejor con datos contaminados con ruido, particularmente cuando el rango de readaptación cubre un gran número de modos. Además, si el número de frecuencias no es elegido adecuadamente, entonces el RFM no es capaz de converger hacia la solución.

Posteriormente, Arora et al. [52] [53] propusieron dos técnicas para extender el RFM básico y así ampliar la aplicabilidad del método considerando el amortiguamiento. La primera técnica propuesta combina la RFM con el método de identificación de amortiguamiento de Pilkey [54]. Esta técnica incluye dos pasos. En un primer paso se readapta sólo la masa y rigidez, mientras que el amortiguamiento se readapta en un segundo paso en el que se emplean la masa y rigidez readaptadas en el primero. La segunda técnica considera los parámetros del modelo y las matrices del sistema en forma compleja para así conseguir modos complejos de estructuras amortiguadas. Posteriormente se compararon las dos técnicas y se encontró que la basada en parámetros complejos proporciona mejores resultados que la otra. Arora [55] también comparó la precisión del RFM básico con el método directo de Berman and Nagy [30] encontrando que el funcionamiento del RFM básico fue superior al del método directo en términos de precisión de las FRF. Recientemente el RFM básico [56] fue extendido por Pradhan and Modak [57] dando lugar al RFM normal, que está basado en la estimación de las FRF normales calculadas exclusivamente a través de las matrices de masa y rigidez. El RFM normal fue posteriormente utilizado por Pradhan and Modak [58] para la identificación de la matriz de amortiguamiento a partir de las FRF experimentales. En el 2000, Modak et al. [59] desarrollaron una técnica de RMEF

basada en optimización restringida. Se evaluó el funcionamiento de esta técnica aplicándola a una viga biapoyada. Esta técnica es computacionalmente más costosa que la IESM pero es capaz de resolver la dificultad que puede surgir de la gran diferencia de las sensibilidades entre las frecuencias naturales y de los modos de vibración. Después aplicaron esta técnica a una viga biapoyada y a una estructura porticada en forma de F [60].

Atalla and Inman [61] utilizaron redes neuronales para readaptar un pórtico flexible. En este método, la red neuronal se entrena y valida utilizando las respuestas del modelo de elementos finitos. La red una vez entrenada puede posteriormente emplearse para obtener los parámetros readaptados tomando las respuestas experimentales como entradas de la red. Una vez que la red está entrenada adecuadamente, los cálculos basados en la red son mucho más rápidos que los de las técnicas convencionales de optimización, independientemente de la complejidad de la estrucutura real. La readaptación de modelos basada en redes neuronales es muy robusta frente al ruido presente en las señales [62]. La principal limitación de este método es que requiere un gran número de datos para el entrenamiento de la red. Sin embargo, este problema puede superarse usando el método de los vectores ortogonales para reducir el número de datos de entrenamiento [4] [63].

Si sólo se miden frecuencias naturales debido a las limitaciones experimentales, la RMEF también puede ejecutarse utilizando el método conocido como *Reduced Order Characteristic Polynomial* (ROCP) propuesto por Li [64]. En esta publicación se aplica el método ROCP para la readptación de una estructura de tipo viga con movimiento restringido en un extremo. En este método se define un polinomio en términos de frecuencias medidas, frecuencias analíticas, modos analíticos y parámetros de readaptación. Suponiendo que las frecuencias naturales medidas son las raíces del polinomio se derivan una serie de ecuaciones no lineales. La resolución de este sistema de ecuaciones no lineales proporciona los valores de los parámetros readaptados.

En ocasiones resulta muy difícil medir con precisión las FRF debido al pequeño tamaño o la fragilidad de la estructura. En estos casos se puede aplicar el método conocido como *Model Updating using Base Excitation* (MUBE) propuesto por Lin and Zhu [65]. En este artículo MUBE se utilizó para readaptar una viga en voladizo y una celosía funcionando satisfactoriamente. En este método, la base de la estructura se excita con una fuerza de entrada aleatoria y desconocida mediante un excitador eléctromagnético.

La respuesta en desplazamiento medida se utiliza para la readaptación del modelo. Este método es muy apropiado cuando la fuerza de excitación es desconocida o difícil de medir. Jamshidi and Ashory [66] compararon el funcionamiento del MUBE y del RFM empleando datos experimentales incompletos y con presencia de ruido, descubrieron que los resultados de readaptación conseguidos con MUBE eran mejores que los obtenidos empleando RFM.

El problema de readaptación de estructuras reales es muy complejo debido a la presencia de no linealidades, amortiguamiento, errores de medida, y un elevado número de parámetros a readaptar. En estas condiciones las técnicas tradicionales de readaptación pueden no converger o permanecer atrapadas en un mínimo local en vez de encontrar el mínimo global de la función de error. En estas situaciones se aconseja el uso de técnicas de optimización capaces de encontrar el óptimo global incluso para un problema de optimización complicado. Los métodos estocásticos son una alternativa para resolver estos problemas de optimización global. En ellos se busca la solución en un espacio dado de una forma aleatoria controlada aprovechando la información adquirida de iteraciones previas. Estos métodos tratan de mejorar la eficacia en la localización del mínimo global, ya que el tiempo de computación es prohibitivo para la búsqueda aleatoria pura, sin perder fiabilidad [7]. Levin and Lieven [10] aplicaron el método *Simulated Annealing* (SA) y el *Genetic Algorithm* (GA) para readaptar casos simulados y experimentales. Probaron diferentes versiones de GA y desarrollaron una variante del SA, que se llama *Blended Simulated Annealing* (BSA). Se descubrió que el BSA funcionaba mejor que el GA en los casos estudiados. Tanto el SA como el GA son métodos de optimización muy robustos que pueden superar mínimos locales de funciones de error altamente multimodales. Por otra parte son muy lentos cuando se comparan con los métodos determinísticos. Además su precisión es muy limitada, tienden a proporcionar soluciones en un en un amplio entorno del mínimo global. Hay algunas estrategias híbridas que combinan GA y búsqueda local [8] [11] para mejorar los resultados. Algunos algoritmos emergentes como la *Particle Swarm Optimization* (PSO) se han incorporado a este campo [67]. Se trata de un algoritmo muy simple y robusto. Sin embargo, los valores de sus parámetros óptimos tienen una gran dependencia del tipo de aplicación y tienen que ser calibrados fuera de línea. Se han propuesto estrategias híbridas que incluyen la readaptación de los parámetros en línea del método [12]. Así mismo Kwon and Lin [68] propusieron una técnica de

readaptación robusta utilizando el método de Taguchi con la que obtuvieron buenos resultados de readaptación de modelos de elementos finitos. En la formulación de la función de error se utilizan datos en el dominio de la frecuencia y el modal. Esta técnica es muy robusta frente a varios tipos de ruido porque los parámetros se optimizan de tal forma que se maximiza la ratio de señal-ruido.

Debido a su naturaleza, las técnicas iterativas son computacionalmente ineficientes, particularmente si se aplican a modelos de elementos finitos de grandes estructuras. En este sentido Guo and Zhan [69] sugieren una técnica de readaptación de elementos finitos basada en la *Response Surface Methodology* (RSM). Con esta técnica no se requieren cálculos de elementos finitos en cada iteración, haciéndola así computacionalmente eficiente. En este método se crea una superficie de respuesta n-dimensional tomando como variables independientes los parámetros a readaptar y como variables dependientes las respuestas dinámicas del modelo de elementos finitos. Los valores calibrados de los parámetros del modelo se obtienen utilizando la superficie de respuesta y las respuestas medidas minimizando la función de error. La RMEF basada en RSM está considerada tan precisa como el método basado en IESM, y además más robusto y eficiente. Posteriormente Ren and Chen [70] aplicaron el RSM así como el IESM a un puente de hormigón prefabricado y compararon la convergencia de la función de error por ambas técnicas. El estudio mostró que para un número de iteraciones dado, la función de error alcanza valores más bajos empleando la RSM. En la versión de RSM tradicional, las señales experimentales medidas son primero transformadas a uno o más parámetros de respuesta como las frecuencias naturales. Esto reduce la información en los datos de entrenamiento empleados para desarrollar los modelos de superficie de respuesta. Para salvar este problema Shahidi and Pakzad [71] utilizaron datos en el dominio del tiempo para la técnica basada en RSM. La técnica basada en datos en el dominio del tiempo ayudó a extraer más información de las señales medidas y compensar el error presente en el meta modelo. La eficiencia del RSM fue mejorada posteriormente por Chakraborty and Sen [72] desarrollando una técnica adaptativa reemplazando el método de mínimos cuadrados por el método de mínimos cuadrados móvil.

Cabe destacar que un modelo de elementos finitos de una estructura real contiene un gran número de parámetros. Si todos ellos se seleccionan para la calibración, entonces el problema de readaptación se vuelve muy complejo y costoso en términos de tiempo.

Un número elevado de parámetros a calibrar también produce un mal condicionamiento del problema quedando atrapado en muchos mínimos locales [73] [2]. Fissette et al. [74] proponen un método basado en balance de fuerzas para identificar y seleccionar solamente unos pocos e importantes parámetros de calibración. Este método puede utilizarse para localización de errores y después los parámetros a calibrar se seleccionan solamente de las regiones donde aparecen los errores. Waters [75] propuso un método de balance de fuerzas modificado en el que se supone que las regiones de error no son necesariamente una indicación de errores de modelizado. Kim and Park [76] desarrollaron un procedimiento automático de selección de parámetros. Este método fue validado aplicándolo a un modelo de elementos finitos de una cubierta de un disco duro conteniendo 1115 elementos finitos y 6732 grados de libertad. Después de aplicar la primera fase del procedimiento automático de selección de parámetros se encontró que el número de parámetros se había reducido a 150 y tras aplicar la segunda fase del procedimiento propuesto se redujo drásticamente a 20. Algunos de los parámetros físicos de la estructura como pueden ser la densidad, módulo de elasticidad, no tienen un valor único en todo el volumen una estructura real. Adhikari and Frisswell [77] propusieron una distribución espacial de estos parámetros expresando los parámetros a calibrar como campos aleatorios espacialmente correlacionados.

Si se realizan una serie de estructuras idénticas, cada parámetro tiene un valor diferente en cada estructura. Esta variabilidad en aparentemente idénticos especímenes puede proceder de muchas fuentes como tolerancias geométricas, procesos de fabricación, etc. Así pues, cada parámetro material tiene una naturaleza estocástica con una media y una varianza. Mares et al. [1] tuvo en cuenta esta naturaleza estocástica de los parámetros de los materiales durante el RMEF usando un ejemplo simulado y obteniendo resultados bastante satisfactorios. La elipse de dispersiones del modelo analítico readaptado se sobrepone bastante próxima a la elipse de dispersión experimental. Mottershead et al. [78] llevaron a cabo el RMEF estocástico en una serie de estructuras físicas. El enfoque estocástico de la readaptación de elementos finitos requiere un gran número de ensayos y volumen de datos. Para reducir el número de ensayos y el volumen de datos se puede adoptar el enfoque utilizado por Khodaparast et al. [79] en el que el valor de los parámetros se expresa en términos de intervalos de confianza.

Las estructuras porticadas se utilizan extensivamente en las aplicaciones de ingeniería civil como los edificios y construcciones industriales. El diseño, posterior control y

monitorizado de estas estructuras está basado en modelos matemáticos, experimentos y experiencias previas. Normalmente se utilizan modelos lineales para el análisis de estas estructuras en las aplicaciones ingenieriles. Este enfoque simplifica el modelizado, el análisis y la extracción de propiedades modales. Sin embargo, la linealidad es la excepción más que la regla en la realidad. Las estructuras siempre contienen cierto grado de no linealidad debido al comportamiento del material, las interfaces de la estructura, las inestabilidades, etc. [13]. Por tanto, se introduce un error sistemático con el modelizado lineal y debe utilizarse un enfoque no lineal cuando se requieren predicciones más precisas.

Este es el caso que se presenta cuando se analiza la respuesta dinámica de una estructura cerca de sus resonancias. En estas condiciones, las fuerzas elásticas e inerciales se contrarrestan y la respuesta está gobernada principalmente por el amortiguamiento. Por estas razones, en la referencia [14] se recomienda realizar ensayos dinámicos para lograr modelos precisos de amortiguamiento con los que comprobar la serviciabilidad de pasarelas. El código ISO [15] también recomienda la elección de un modelo apropiado de amortiguamiento y su calibración a través de experimentos para comprobar la serviciabilidad de edificios y pasillos frente a vibraciones. Los códigos avanzados de diseño dinámico [16] incluyen varios criterios de funcionamiento para estructuras porticadas de acero. Para el nivel de ocupación inmediata, se recomienda que no haya daño significativo en la estructura. Esto significa que la estructura debe permanecer en el rango elástico durante la excitación sísmica. En estas condiciones la respuesta sísmica de la estructura depende exclusivamente del amortiguamiento, pues no existen mecanismos disipativos debidos al daño. Por tanto, es fundamental un apropiado modelizado y calibración del amortiguamiento para este nivel de funcionamiento. Estos son sólo unos ejemplos en los que el amortiguamiento podría ser un factor significativo en el análisis dinámico.

Debido a razones económicas y de seguridad, en muchos casos debe comprobarse el funcionamiento de las estructuras en servicio. Como las estructuras tienden a degradarse cuando envejecen, su integridad también debe ser monitorizada continua o periódicamente. Después de un evento excepcional, como puede ser una sobrecarga, un terremoto, un huracán, las estructuras pueden quedar dañadas y es necesario evaluar su integridad. Todas estas tareas ingenieriles se conocen como *Structural Health Monitoring* (SHM) en la literatura. En las últimas décadas, se desarrollaron numerosas

técnicas de SHM basadas en el análisis de vibraciones estructurales. La referencia [17] incluye una completa revisión de estas técnicas. En esta revisión, se concluye que aunque la mayoría de las técnicas de identificación de daño están basadas en modelos lineales ajustados a los datos medidos, las técnicas de identificación no lineal son potencialmente interesantes debido a la propia naturaleza no lineal del daño. Brandon [18] establece que la identificación no linear proporciona información válida en SHM. El autor aboga por el uso de técnicas de identificación en el dominio del tiempo para así conservar toda la información no lineal, que se pierde al realizar procesos de linealización de series temporales. Modena et al. [19] proponen el uso del amortiguamiento y respuestas no lineales como parámetros sensibles al daño.

La teoría de sistemas no lineales es muy extensa y en la actualidad hay disponible numerosa literatura. Las primeras contribuciones en la identificación de modelos estructurales no lineales comenzaron en la década de los 70 [82], [83]. Desde entonces se han desarrollado numerosos métodos debido a la naturaleza altamente particular de los sistemas no lineales. Al contrario que en los sistemas lineales, no existen funcionales universales que describan el comportamiento no lineal; cada caso debe formularse individualmente. El primer libro de texto en este campo fue escrito por Worden y Tolimson [13]. También se han publicado varias revisiones bibliográficas que sintetizan las metodologías de identificación de sistemas no lineales en dinámica estructural [80], [84], [81], [85]. Pese a la abundante literatura disponible sobre identificación de estructuras no lineales, solamente unos pocos métodos prácticos de ensayo modal han sido establecidos hasta ahora. Algunas publicaciones recientes en esta área se exponen en los siguientes párrafos.

Atkins et al. [20] propusieron una extensión del método lineal de apropiación de fuerza para la identificación de estructuras débilmente no lineales. Mediante una adecuada elección de la fuerza, que incluye los términos armónicos altos, se consigue que la estructura responda en un modo simple correspondiente a la estructura lineal subyacente. Para determinar las componentes multi armónicas del vector de fuerza, se elige una técnica de optimización. Los términos lineales y no lineales en la ecuación de movimiento de cada modo individual se identifican mediante el *Restoring Force Surface Method* (RFSM). Los términos no lineales acoplados se identifican aparte. Platten et al. [21] desarrollaron un método para la identificación de estructuras complejas predominantemente lineales y que presentan un pequeño número de modos

no lineales. Utilizaron una extensión del *Resonant Decay Method* en el que se aplican fuerzas sinusoidales adecuadas para excitar modos simples o pequeños grupos de modos acoplados. Finalmente se usa el RFSM para ajustar los resultados en el espacio modal obteniendo así los parámetros modales de cada modo.

Peeters et al. [22], [23] extendieron el ensayo de resonancia en fase a sistemas no lineales utilizando la teoría de *Nonlinear Normal Modes* (NNMs). En este método, se excitan individualmente NNMs en vez de los modos lineales. Esto se consigue ajustando la excitación multi armónica de tal forma que la respuesta esté en cuadratura con la excitación. Después de esta apropiación, se corta la excitación y aparece la susbsecuente vibración libre, en la que solamente aparece el modo excitado debido a su invarianza. Ésta se utiliza para extraer las curvas modales y las correspondientes frecuencias mediante el análisis en el espacio del tiempo y frecuencia.

La apropiación multi armónica y multi puntual establecida en [20], [21], [22], [23] se utiliza mucho en la industria aeroespacial. Sin embargo no resulta práctica para las aplicaciones de ingeniería civil de estructuras en servicio. En estos casos se puede elegir una apropiación imperfecta consistente en una excitación mono armónica localizada en un solo punto. En [23] se establece que esta excitación aísla satisfactoriamente un modo no lineal si la estructura posee modos bien separados.

Los métodos mencionados anteriormente se aplicaron a simulaciones numéricas o pequeños dispositivos experimentales. En estos casos, el tipo de no linealidad presente en la estructura, que constituye el problema esencial que debe resolver el procedimiento de identificación, se conoce de antemano. Las aplicaciones de la identificación modal no lineal a estructuras reales de ingeniería civil con múltiples componentes son muy escasas en la literatura, pese a su potencial utilidad.

4. Estrategias adoptadas

La finalidad última de este estudio es eminentemente práctica. No se trata de una mera especulación teórica desligada de la realidad, sino todo lo contrario. No se sigue la estrategia muy extendida en los ámbitos académicos consistente en el diseño ad hoc de un modelo experimental que valide cierto modelo teórico previamente establecido. Lo que se pretende es la inferencia de modelos teóricos avanzados a partir de observaciones del comportamiento dinámico de modelos experimentales.

Para que los modelos teóricos extraídos sean extrapolables a la práctica de la ingeniería estructural, los modelos experimentales deben tener una configuración lo más próxima posible a la de las estructuras reales. Por otra parte, para hacer posible la calibración práctica de los modelos propuestos, las técnicas experimentales de excitación y captura de datos deben ser aplicables a las estructuras reales en condiciones de servicio. Es muy común el empleo en laboratorio de técnicas experimentales conteniendo múltiples puntos de excitación y medida, que resultan inviables en estructuras reales, tanto desde el punto de vista práctico como económico. Así pues, el diseño de los experimentos se adaptará a estas limitaciones.

Siendo la base del estudio los modelos experimentales, estos se conducirán de forma progresiva. Se comenzará con modelos a pequeña escala. Posteriormente, se aumentará tanto la escala como la complejidad de los modelos hasta niveles próximos a los de las estructuras reales. La experiencia adquirida en cada estadio permitirá un mejor diseño de los siguientes experimentos, rentabilizando de esta forma los siempre escasos recursos disponibles.

El tratamiento de las señales es otro de los aspectos clave para la posterior modelización. Este tratamiento permite eliminar los errores presentes en las señales y reducir la dimensionalidad de los datos. Estas prácticas no afectan significativamente a la identificación de sistemas lineales. No obstante, se puede perder mucha información relevante en este proceso cuando se aplica a sistemas débilmente no lineales. Ante este panorama, se propone un estudio en detalle de la influencia de los tratamientos al uso de las señales y el desarrollo de técnicas alternativas que preserven el máximo de información.

Las estrategias adoptadas en la calibración de parámetros de los modelos fueron las siguientes. Empleo de datos en el dominio del tiempo que contengan el máximo de información disponible. Desarrollo de un procedimiento estocástico de calibración especialmente adaptado a la respuesta dinámica de las estructuras comunes y que supere los problemas de convergencia que aparecen con los procedimientos convencionales.

5. Descripción de los estudios y discusión de resultados

5.1. Publicación 1

El estudio del pórtico de acero a pequeña escala fue muy instructivo como primer acercamiento al campo del modelizado por elementos finitos y su posterior readaptación. Permitió al equipo de investigación familiarizarse con la técnica experimental dinámica basada en movimiento impuesto de la base. El pequeño tamaño del espécimen hizo posible la realización de numerosos ensayos con diferentes configuraciones de masa y de daño impuesto así como con diferentes excitaciones. De las mediciones se extrajeron los datos modales de las diferentes configuraciones. En la readaptación sólo se utilizaron las tres primeras frecuencias naturales por ser los datos modales más precisos, con unos coeficientes de variación inferiores al 0,5 %. Los modos aportaban más confusión que información dada su gran variabilidad de ensayo a ensayo, por esta razón no se tuvieron en cuenta durante el proceso de readaptación. Aún en este modelo tan sencillo, las definiciones de la geometría y de la rigidez de las uniones resultaron definitivas para un adecuado modelizado del pórtico. Esto es, un modelizado con sentido físico. Como era de esperar se puso de manifiesto que la selección de parámetros es un aspecto clave para evitar un mal condicionamiento en el proceso de readaptación. Los intentos con varios modelos dejaron patente que un buen ajuste a los datos experimentales no garantiza el sentido físico del modelo, sino que éste debe buscarse en otras consideraciones. El bajo número de parámetros seleccionado permitió el uso de una red neuronal para su calibración. El procedimiento iterativo propuesto para la calibración resultó muy efectivo en las diferentes configuraciones consideradas aunando rapidez de ejecución y precisión de los resultados, incluso partiendo de valores de los parámetros muy alejados de los finales. Otra de las ventajas del uso de redes neuronales fue el estudio de la transmisión de errores de los datos de entrada hacia los parámetros. Conocida la distribución de probabilidad de las variables de entrada, la red neuronal ya entrenada permite obtener rápidamente la distribución de los parámetros mediante técnicas de muestreo como el Hipercubo Latino.

5.2. Publicación 2

En el segundo artículo se estudió un puente de tablero continuo con cuatro vanos y distribución irregular de los pilares. La escala geométrica de este puente era de 1:50. El puente se diseñó por varios miembros integrantes del equipo, fue fabricado y ensayado en el *Earthquake Engineering Research Center, University of Bristol*. Los ensayos se realizaron en mesa vibrante y consistieron en una vibración aleatoria de baja intensidad, que se usó para caracterizar modalmente a la estructura, y ensayos sísmicos de diferentes intensidades en dirección transversal a la directriz del tablero. En un trabajo previo [5] se desarrolló un modelo de elementos finitos del puente, y posteriormente se readaptó en base a las frecuencias naturales identificadas para diferentes configuraciones. El presente trabajo es más ambicioso y pretende una identificación no lineal ante la sospecha de que la fricción en las uniones tiene una gran repercusión en la respuesta dinámica. Para este fin se desarrolló un método específico no solamente aplicable a este caso particular, sino de carácter general. Este método trata de salvar los inconvenientes de los métodos iterativos al uso. Estos métodos tienden a diverger o converger a soluciones sin sentido físico cuando los valores de partida de los parámetros están alejados de los finales. El método consiste en la minimización de una función de error que emplea variables físicas en el dominio del tiempo, véase (1).

$$\varphi = \frac{1}{N}\sum_{\mathrm{i=1}}^{\mathrm{N}} \frac{\sum_{\mathrm{j=1}}^{\mathrm{M}} \left(\hat{\mathrm{y}}_{\mathrm{ij}} - \mathrm{y}_{\mathrm{ij}}\right)^2}{\sum_{\mathrm{j=1}}^{\mathrm{M}} \left(\mathrm{y}_{\mathrm{ij}}\right)^2} \tag{1}$$

Donde $\hat{y}_{ij}, y_{ij}$ representan respectivamente la respuesta del modelo y la medida experimentalmente. Los subíndices i y j se refieren a los sensores y al instante de medida, *N* es el número de sensores y *M* es el número de medidas. Se puede establecer una versión ponderada cuando las medidas tengan una diferente precisión.

La ventaja de este enfoque es que se puede aplicar tanto a sistemas lineales como no lineales. Además, se pueden usar señales originales preservando de este modo toda la información subyacente en ellas y evitando los errores sistemáticos de identificación. Otra ventaja de esta formulación es que en la optimización se utilizan las series temporales correspondientes a las respuestas dinámicas estimadas a través del modelo, siendo estas mismas series temporales las que se emplean para el diseño en dinámica estructural.

Es interesante estudiar las características de la función de error definida para adaptar el algoritmo posterior de minimización a ellas. Una propiedad de esta función de error es que el mínimo global es idealmente cero, representando un ajuste perfecto del modelo a los experimentos. No obstante, en la práctica el error es siempre mayor de cero debido a las limitaciones del modelo y a los errores de medida. En este trabajo se ha encontrado que la superficie de error es altamente multimodal en el espacio de los parámetros. Sin embargo la mayoría de los mínimos corresponde a soluciones sin sentido físico, por ejemplo, valores negativos de la rigidez o del amortiguamiento. Además la superficie de error contiene zonas muy planas en las que hay pequeñas variaciones de la función. Los métodos determinísticos quedan atrapados en estas zonas planas. Las mesetas están separadas por valles angostos interconectados donde la función de error disminuye y alcanza sus mínimos. A lo largo de los valles también hay zonas planas. Una característica interesante de los valles es que son aproximadamente paralelos a las direcciones de los ejes en el espacio de los parámetros.

Con objeto de dar generalidad al método y evitar la falta de convergencia propia de los métodos determinísticos, se decidió adoptar una estrategia estocástica en la minimización de la función de error. Además, se ha optado por una esquema de búsqueda acotada, reduciendo el espacio de búsqueda a unos intervalos con sentido físico y lo más próximos posibles a la solución. De esta forma se garantiza la convergencia al mínimo global. Un posible inconveniente cuando se adoptan espacios de búsqueda muy amplios, debido a la gran incertidumbre del valor de un parámetro, es la aparición de mínimos impropios en los bordes del intervalo (véase Figura 2).

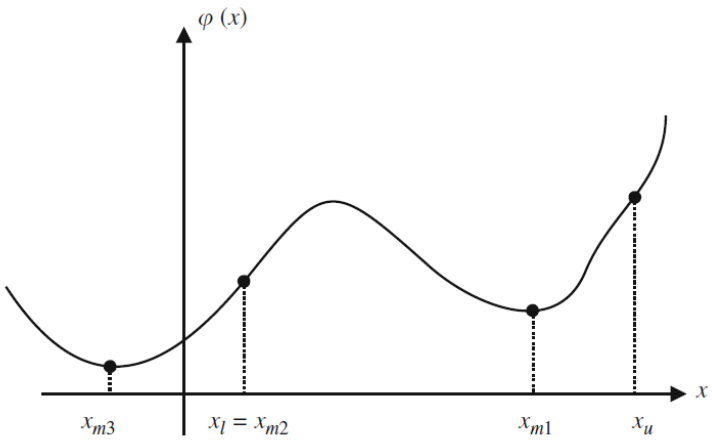

Figura 2. Representación unidimensional de la función de error $\boldsymbol{\varphi(x)}$.

Resumiendo, el método de readaptación propuesto se expresa matemáticamente del siguiente modo:

$$\begin{gathered}\min\{\varphi(\mathbf{x})\};\ \mathbf{x} \in \mathbb{R}^n \\ \ell_i \leq x_i \leq u_i \quad i = 1, \ldots, n\end{gathered} \tag{2}$$

En las que $\varphi(\mathbf{x})$ representa la función de error definida en (2), $\mathbf{x}$ es el vector de parámetros a calibrar, ℓ_i y u_i son los límites inferior y superior que se seleccionan para acotar cada parámetro.

Una característica de los métodos estocásticos es que su funcionamiento depende mucho de cada caso particular. No hay garantía de que un algoritmo capaz de proporcionar una solución a un problema sea efectivo para otro diferente. Por eso en este estudio se ha hecho un esfuerzo para adaptar el algoritmo de minimización a las características del problema establecido en vez de emplear un algoritmo de propósito general. Así, se busca la solución de forma iterativa mediante un muestreo aleatorio dentro del espacio de búsqueda. Teniendo en cuenta la condición acotada del espacio de búsqueda, se eligió la función de distribución beta como más apropiada para el muestreo. Los parámetros de la distribución de muestreo se cambian en cada paso de la iteración en base a los resultados de las anteriores. La moda de la distribución se hace coincidir con el valor del parámetro que proporcionó el mínimo error. Si la función de error correspondiente a una iteración es menor que la previa, entonces la varianza de la distribución utilizada en la iteración siguiente se incrementa; al contrario, si es mayor, la varianza se reduce. La función de muetreo está extendida siempre a todo el espacio de búsqueda, pero evoluciona desde una distribución uniforme hasta una puntiaguda concentrada en un estrecho margen alrededor del mínimo de la función de error. El método por tanto integra las fases de búsqueda global y la local. El proceso se detiene cuando se alcanza un criterio de convergencia dado. Éste puede ser un umbral dado de la función de error o un número límite de iteraciones. Se probaron dos algoritmos diferentes. Uno de ellos corresponde a una distribución isótropa de las varianzas de las distribuciones de muestreo, mientras que en el otro se considera una distribución anisótropa. La estrategia adoptada en este último caso consiste en ponderar la varianza de las distribuciones de muestreo de cada parámetro de acuerdo con su evolución en los pasos previos, de forma que se aumenta la varianza en aquellos parámetros que sufren mayor variación.

El funcionamiento de los algoritmos propuestos se probó en la identificación de un sistema dinámico lineal en base a simulaciones numéricas de la vibración libre en el dominio del tiempo. Los parámetros a readaptar en este caso fueron las frecuencias e índices de amortiguamiento, amplitud y fase de dos modos de vibración. También se incluyó el funcionamiento de un algoritmo de propósito general (CMA-ES) tras calibrar sus parámetros internos al caso propuesto. Cada algoritmo se ejecutó cien veces, la proporción de aciertos fue muy similar en todos los casos y cercana al 90%, esto significa que todos los procedimientos tienen una robustez alta y similar. Sin embargo, hubo diferencias muy significativas en lo que se refiere a la eficacia de cada procedimiento. El número promedio de iteraciones necesarias para alcanzar la convergencia fue de 20001 para el método beta isotrópico, mientras que el correspondiente del algoritmo anisótropo fue de 2473, esto es una diferencia de casi un orden de magnitud. En lo que respecta al algoritmo CMA-ES, su funcionamiento fue un poco peor que el anisótropo, necesitando 2993 iteraciones. A tenor de estos resultados se descartó el uso del método isotrópico en el resto del estudio. Cabe destacar una ventaja adicional del modelo propuesto respecto del CMA-ES, y es que no necesita ninguna calibración previa de los propios parámetros. Una vez probados los algoritmos, el anisotrópico fue utilizado en la readaptación del modelo lineal del puente a escala.

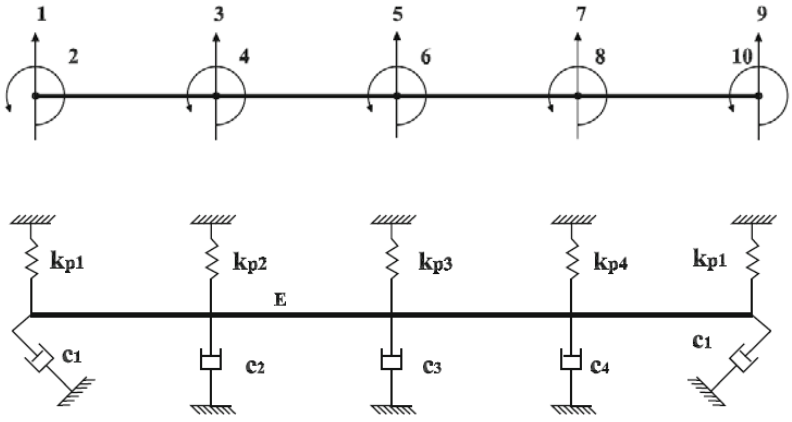

Figura 3. Esquema del modelo viscoso lineal de elementos finitos del puente a escala.

El modelo contiene diez grados de libertad correspondientes a las traslaciones transversales y giros correspondientes a los extremos del tablero y los puntos de unión con las pilas (véase Figura 3). El modelo incluye la rigidez transversal de los estribos y

el amortiguamiento rotacional. Los parámetros seleccionados para la readaptación fueron: la rigidez y coeficiente de amortiguamiento de los estribos, iguales para ambos, las rigideces y coeficientes de amortiguamiento de cada pila y un parámetro global para todos los elementos que fue el módulo de elasticidad E, sumando un total de 9 parámetros. Los desplazamientos de las cabezas de las pilas se obtuvieron mediante integración numérica de las aceleraciones medidas, mientras que la respuesta del modelo se obtuvo mediante integración numérica de la ecuación de movimiento usando el método de diferencias centrales. En una primera fase se escogieron deliberadamente unos intervalos de búsqueda exageradamente amplios para ver el funcionamiento del algoritmo anisotrópico y del CMA-ES en estas condiciones. Los valores de los parámetros obtenidos fueron muy parecidos, y presentaron un error final próximo al 9,6%. Como trabajo complementario, el algoritmo CMA-ES se probó en condiciones de búsqueda abierta en 20 intentos adicionales. En este caso los intervalos anteriores se utilizaron únicamente para la asignación de valores iniciales a los parámetros. Los resultados fueron muy concluyentes. El proceso convergió a mínimos sin sentido físico en 10 intentos y divergió en el resto. Esto demuestra que la búsqueda abierta es ineficiente cuando los valores iniciales de los parámetros están alejados de la solución.

En base a estos resultados iniciales se estableció un criterio de parada común para ambos procedimientos y cada algoritmo fue ejecutado 25 veces en estas condiciones. Como en la serie anterior, los valores obtenidos de los parámetros fueron muy similares en ambos algoritmos. En lo referente al índice de aciertos fueron muy próximos 19/25 y 20/25. Los resultados no satisfactorios correspondieron todos ellos a mínimos impropios. Sin embargo el funcionamiento del algoritmo anisotrópico fue mucho mejor que el CMA-ES siendo el número de iteraciones necesarias para alcanzar la convergencia 5 veces menor aproximadamente.

La comparación de las respuestas temporales experimentales con las predicciones del modelo viscoso lineal readaptado muestran que las predicciones del modelo son menores que las experimentales en el caso de pequeños desplazamientos y viceversa para grandes desplazamientos. Esto pone de manifiesto la existencia de no linealidades en el modelo físico. Estos resultados y la experiencia previa de los autores en modelos similares [6] indican que el comportamiento dinámico del puente podría describirse de forma más precisa utilizando disipadores friccionales en vez de viscosos lineales. Así pues en una segunda aproximación se utilizó un modelo de elementos finitos similar al

anterior pero sustituyendo los disipadores viscosos lineales por disipadores elásticos deslizantes con fricción coloumbiana. Estos disipadores se comportan de forma elástica dentro de ciertos límites de desplazamiento relativo y a partir de esos límites se produce deslizamiento y disipación de energía por fricción. Este disipador tiene un comportamiento histerético no lineal. El modelo contiene ahora trece parámetros a readaptar que se muestran en la Figura 4.

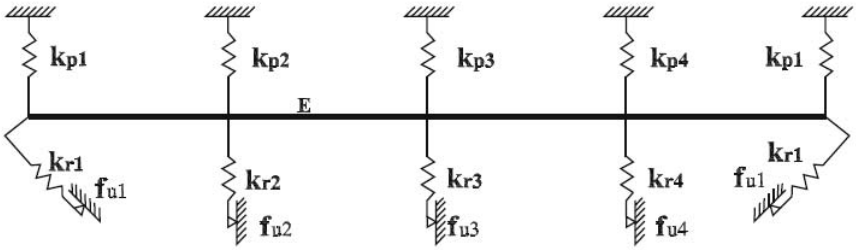

Figura 4. Esquema del modelo friccional de elementos finitos del puente a escala.

Estos parámetros se readaptaron mediante un procedimiento similar al seguido en el modelo viscoso lineal. En este caso se utilizó solamente el algoritmo anisótropo ya que demostró ser el más eficiente en el caso del modelo viscoso lineal. Se realizaron una serie de pruebas iniciales utilizando intervalos amplios hasta conseguir el orden de magnitud de los parámetros. A partir de estos resultados iniciales se fijó una banda de búsqueda estrecha y el algoritmo se ejecutó 25 veces limitado a un número máximo de 5000 iteraciones.

Todas las ejecuciones convergieron satisfactoriamente a la solución con errores muy próximos en el rango de 1,97 a 1,47%. Por tanto, el ajuste a los datos experimentales fue excelente en este caso. El error de ajuste es casi de un orden de magnitud inferior al del modelo viscoso. Queda patente, pues, que el modelo no lineal refleja mejor la respuesta sísmica que el modelo lineal. En lo que respecta a la variabilidad de los parámetros, ésta es mucho menor que en el modelo viscoso lineal. Sin embargo, la variabilidad es significativa en algunos parámetros. Este mal condicionamiento es debido a la falta de información en los datos experimentales. Del análisis de la respuesta a la excitación sísmica en el dominio de la frecuencia se sigue que el movimiento sísmico sólo excita significativamente los dos primeros modos, mientras que el tercero es débilmente excitado. Además, el cuarto no aparece en el espectro de la respuesta

porque los puntos de medida están próximos a puntos nodales de este modo. Cabe destacar que incluso, ante un caso tan mal condicionado, el algoritmo fue capaz de readaptar 13 parámetros incluyendo simultáneamente la rigidez y amortiguamiento.

5.3. Publicación 3

En este artículo se utilizó un pórtico de acero con cuatro plantas, dos vanos en dirección longitudinal y uno en la transversal. Los pisos se conformaron con chapas de acero soldadas con cordones discontinuos a las vigas. Las uniones de las barras fueron soldadas en dirección transversal y, atornilladas en la longitudinal. También se utilizaron bloques de hormigón como masas de piso adicionales. La escala geométrica del pórtico fue 1:2, aproximadamente. Se trata de un modelo con características muy próximas a los que se pueden encontrar en las aplicaciones industriales. Por tanto, los modelos que se puedan inferir de este caso se podrían extrapolar a casos reales similares.

Para la excitación dinámica del pórtico se utilizó un excitador de tipo pendular. Éste consiste en una masa excéntrica fijada al eje de un motor eléctrico. La excitación se consigue variando angularmente la posición de la masa. La frecuencia y amplitud de la excitación se consiguen controlando la posición angular del eje mediante un regulador electrónico retroalimentado con un encoder. El pórtico se instrumentó con cuatro acelerómetros sísmicos de alta sensibilidad. Estos se atornillaron en el centro de las vigas extremas de cada planta orientados en dirección longitudinal.

Para la identificación no lineal del pórtico, se seleccionaron las vibraciones libres de los modos simples de flexión aislados en dirección longitudinal. De esta forma, las fuerzas exteriores no intervienen y se reducen las fuentes de error. Además, la vibración libre contiene un amplio rango de amplitudes que ponen de manifiesto las no linealidades presentes en el pórtico.

El aislamiento de cada modo simple no lineal se intentó mediante una excitación mono armónica en un solo punto. Para ello, el excitador se emplazó en el centro de la cuarta planta orientado en dirección longitudinal. Así se excitan solamente modos de flexión. Los experimentos constaron de 20 segundos de excitación armónica seguida de la vibración libre. Para cada modo, los experimentos se realizaron en dos etapas partiendo de un valor aproximado de la frecuencia natural obtenido preliminarmente. La vibración

libre se utilizó para determinar de forma más precisa la frecuencia natural asociada a un modelo lineal correspondiente. En una segunda etapa, el excitador se reajustó a la frecuencia así obtenida y la vibración libre correspondiente se utilizó para la identificación no lineal.

Este procedimiento se aplicó a los cuatro primeros modos de flexión. El análisis de los resultados en el dominio de la frecuencia reveló que con este procedimiento solamente se consiguen aislar satisfactoriamente los dos primeros modos de vibración. El tercer y cuarto modos aparecen siempre combinados con el primero y con el segundo. Consecuentemente, sólo se utilizaron los dos primeros modos de flexión para la posterior identificación no lineal. Esto no constituye una limitación, pues en la práctica sólo los modos bajos tienen una influencia significativa en la respuesta dinámica de los pórticos.

El análisis de las señales medidas de la vibración libre reveló que todas contienen un sesgo variable en el tiempo y un ruido de alta frecuencia. Estas perturbaciones contaminan la señal verdadera y afectan significativamente al posterior proceso de identificación. La supresión de estas perturbaciones de la señal es fundamental para obtener una identificación precisa. Así pues, el filtraje de las señales es una tarea tan importante como la propia identificación. Las perturbaciones presentes en las señales suelen eliminarse mediante filtros digitales lineales. Un inconveniente de estos filtros es la definición de las frecuencias de corte. Si la frecuencia está muy alejada del rango de interés, la mayor parte de las perturbaciones continúan presentes en la señal filtrada.

Al contrario, si la frecuencia de corte está próxima al rango de interés, la mayor parte de las perturbaciones se eliminarán, pero una parte significativa de la señal verdadera también se elimina. Los filtros lineales tienden a linealizar las señales eliminando las componentes no lineales.

Para superar estos inconvenientes de los filtros convencionales se propone un procedimiento novedoso de filtraje, que se llama *Moving Linear Fitting* (MLF). Con este procedimiento se pretende eliminar simultáneamente los sesgos y el ruido de alta frecuencia manteniendo al máximo la señal verdadera. La aplicación del procedimiento está restringida a estructuras débilmente y simétricamente no lineales. La base del procedimiento es la siguiente: la vibración libre de la estructura débilmente no lineal se espera que sea localmente muy próxima a una lineal pura. El término local implica que

para la comparación se toma sólo unos pocos ciclos de vibración. El MLF se desarrolla desde esta idea central.

Para cada punto discreto de la respuesta medida, se ajusta un modelo lineal a los datos experimentales en un intervalo de tiempo aproximadamente igual a un periodo y centrado en el punto considerado. El valor del modelo ajustado correspondiente a ese punto se elige como el valor filtrado correspondiente. El ruido, debido a su naturaleza aleatoria, se cancela por compensación en el intervalo de ajuste. Por otra parte, como la función ajustada está centrada respecto de la aceleración, el sesgo se elimina. Además como el procedimiento se aplica individualmente a todos los puntos de la señal, se espera que la mayor parte de la información no lineal se mantenga en la señal filtrada.

Para comprobar la bondad del procedimiento MLF, se generaron dos tipos de señales una correspondiente a un sistema lineal puro y otra correspondiente a un sistema no lineal con ablandamiento cúbico. Después las señales se contaminaron con sesgos variables y ruido blanco. Las señales generadas fueron muy próximas a las medidas experimentalmente.

La posterior comparación de las diferencias de las señales filtradas respecto de las verdaderas, que en este caso son conocidas, reveló que el MLF proporciona resultados con un error un orden de magnitud inferior al mínimo que se puede conseguir con el filtro lineal de banda. Cabe destacar que en el MLF no es necesario establecer ninguna frecuencia de corte. En el caso de una señal real, la señal verdadera es desconocida y el error de filtraje lineal es generalmente mayor que el mínimo.

A partir de las señales filtradas con el MLF se realizó una identificación no paramétrica del pórtico. Para ello, se estudió la evolución de las propiedades dinámicas del pórtico como una función de la amplitud de la respuesta. El estudio se realizó con procedimientos expeditivos y resultó fundamental para la posterior inducción de los modelos parámetricos y su calibración.

El movimiento correspondiente a la vibración libre en el espacio de configuración correspondiente a las series temporales de aceleración filtradas está representado en las Figura 5 yFigura **6**.

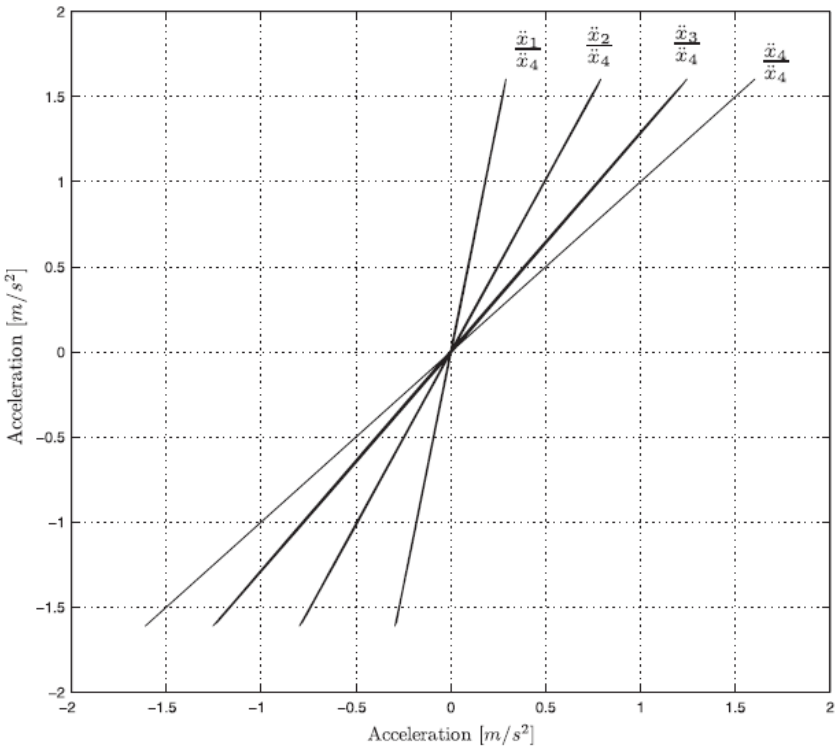

Figura 5. Movimientos del primer modo en la configuración espacial.

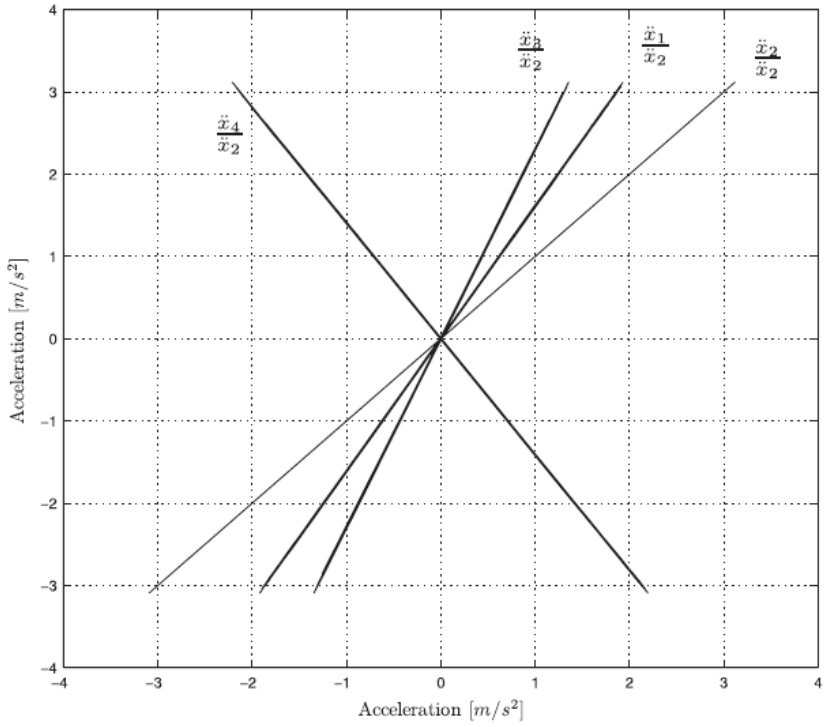

Figura 6. Movimientos del segundo modo en la configuración espacial.

Como puede verse los movimientos tienen una tendencia lineal muy marcada en todos los casos con coeficientes de correlación casi iguales a 1. Esto significa que los modos no dependen de la magnitud del desplazamiento. Por tanto las formas modales pueden considerarse lineales dentro del rango de los experimentos, que son compatibles con la serviciabilidad de la estructura.

Como la frecuencia instantánea varía en el tiempo en un sistema no lineal, se utiliza en su lugar la frecuencia aparente, que representa el promedio de la frecuencia instantánea en un ciclo de oscilación. La evolución de la frecuencia aparente como una función de la amplitud de la aceleración se analizó ciclo a ciclo de la siguiente forma. Los pasos por cero de la respuesta se obtienen por interpolación lineal de puntos consecutivos de diferente signo. Desde estos se calcula el periodo y la frecuencia aparentes de cada ciclo. La amplitud correspondiente a cada ciclo se aproxima por el valor máximo absoluto de la aceleración que haya en ese ciclo. Los resultados se muestran en la Figura 7.

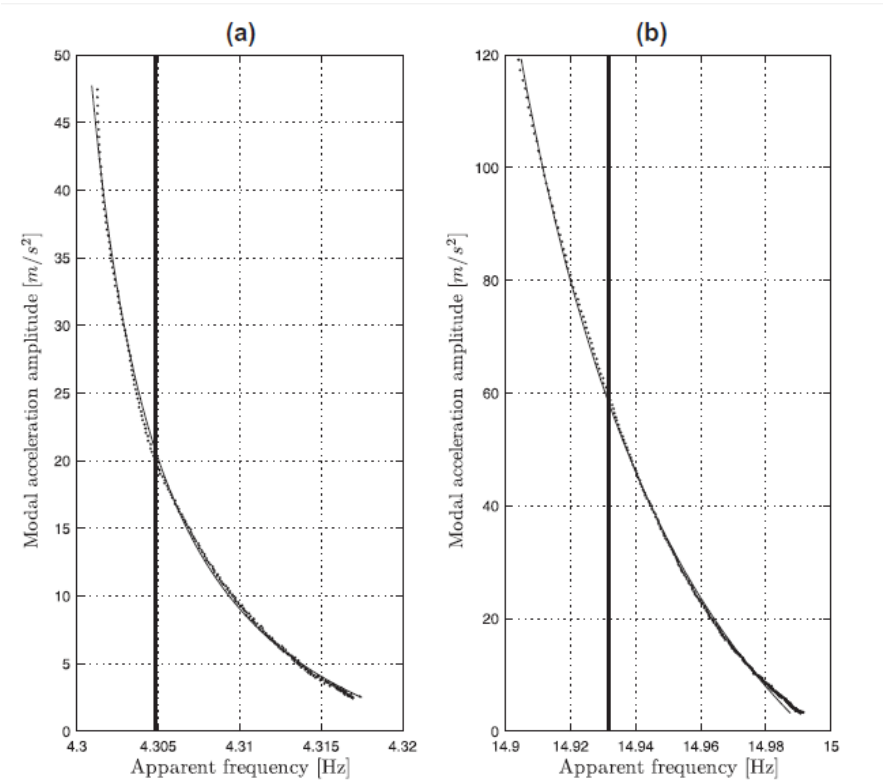

Figura 7. Curvas amplitud aceleración modal-frecuencia aparente. (a) Primer modo. (b) Segundo modo. Puntos: Resultados experimentales. Línea gruesa: Modelo lineal. Línea fina: Modelo no lineal.

Como puede apreciarse la frecuencia no es constante, como correspondería a un sistema lineal, sino que varía con la amplitud. La máxima frecuencia aparente se da para los ciclos con amplitud mínima y desde este punto la frecuencia aparente disminuye gradualmente como una función de la amplitud. La caída total de frecuencia en el rango de los experimentos son del 0,35% y 0,55% para el primero y segundo modo respectivamente. La frecuencia disminuye y tiende a estabilizarse a medida que la amplitud aumenta.

Las curvas de amortiguamiento están basadas en el coeficiente de amortiguamiento viscoso equivalente. Éste se define como el coeficiente de amortiguamiento de un modelo lineal que provee un decremento logarítmico por ciclo igual al de los experimentos. Los resultados de la identificación se muestran en la Figura 8. Ambas curvas tienen una forma similar a la de la frecuencia aparente pero en sentido inverso.

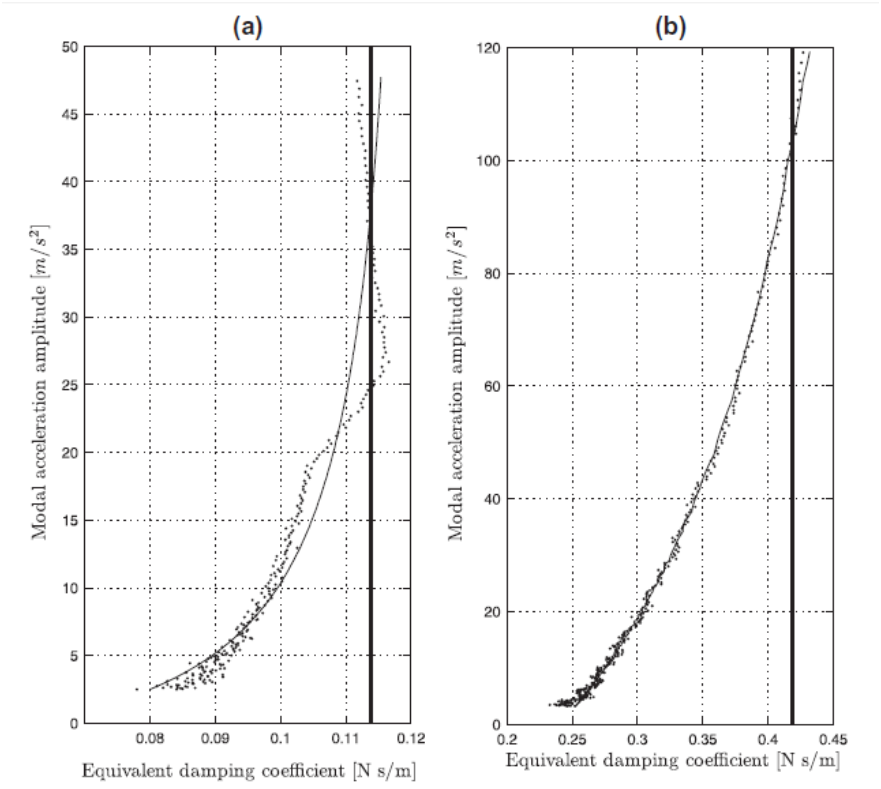

Figura 8. Curva de amplitud de aceleración modal-amortiguamiento equivalente. (a) Primer modo. (b) Segundo modo. Puntos: Resultados experimentales. Línea gruesa: Modelo lineal. Línea fina: Modelo no lineal.

Hay un valor mínimo del amortiguamiento equivalente para la amplitud más baja. Desde este mínimo el amortiguamiento aumenta gradualmente y tiende a estabilizarse.

Los incrementos totales de amortiguamiento son sobre el 45% y el 70 % para el primero y segundo modo respectivamente.

La alta linealidad encontrada en los modos permite expresar las variables espaciales en el espacio modal mediante una transformación lineal y formular independientemente las vibraciones libres a través de las variables modales correspondientes.

La frecuencia aparente definida está gobernada principalmente por la rigidez estructural. De las curvas obtenidas se puede inducir que la rigidez de la estructura analizada es débilmente no lineal. Además, la no linealidad de la rigidez es muy notable para pequeños desplazamientos y disminuye gradualmente cuando el desplazamiento aumenta. Esta tendencia indica claramente una rigidez no lineal debida a precargas. La estructura ensayada tiene numerosas uniones atornilladas y soldadas en las que están presentes las precargas. Estas precargas hacen que las interfaces de la unión estén inicialmente en contacto. Cuando la deformación estructural genera deformaciones del mismo orden que las generadas por las precargas, las interfaces de la unión se abren y hacen que la rigidez de la unión disminuya progresivamente como una función del desplazamiento modal. Éste es el mecanismo físico que produce la no linealidad observada.

El elevado número de ciclos necesario para atenuar la vibración libre indica que la estructura es débilmente amortiguada. Además, el perfil de la curva de amortiguamiento muestra que el amortiguamiento es fuertemente no lineal. La disipación de energía en esta estructura se espera que esté también concentrada en los componentes de las uniones, porque el amortiguamiento material es muy pequeño para estructuras de acero y la interacción con el medioambiente, conocida como radiación, tiene un orden de magnitud muy pequeño cuando se compara con la componente disipativa.

La energía se disipa en las uniones por deslizamientos en las interfaces. Los efectos del deslizamiento podrían reproducirse con un modelo friccional coulombiano. Sin embargo, este mecanismo no concuerda con los resultados experimentales, ya que es conocido que el coeficiente de amortiguamiento viscoso equivalente a la fricción coulombiana es una función hiperbólica asintótica a cero cuando la amplitud tiende a infinito. Las curvas experimentales muestran la tendencia opuesta. Una posible explicación a este comportamiento es que el área de deslizamiento varía también con la amplitud. Un amortiguamiento viscoso no lineal sería una solución apropiada para describir el mecanismo de amortiguamiento de esta estructura.

Como resumen puede decirse que dentro del rango de desplazamientos de los experimentos, el comportamiento global de la estructura es no lineal para pequeños desplazamientos y tiende hacia la linealidad a medida que los desplazamientos aumentan.

En este trabajo se ha deducido que si la matriz de rigidez instantánea es proporcional a una matriz de rigidez de referencia constante para un modo simple de vibración entonces la forma modal correspondiente es invariante respecto de la amplitud de la vibración, mientras que la frecuencia aparente depende de la amplitud. Estas deducciones son coherentes con los resultados experimentales y prueban la hipótesis establecida de proporcionalidad de la matriz de rigidez.

Otra ventaja de esta propiedad de comportamiento es que la no linealidad de la rigidez puede formularse en el espacio modal en vez de en el espacio físico. Después de varios intentos se adoptó la siguiente función asintótica para modelizar la rigidez (3).

$$k_r(z_r) = \frac{k_{ir}\alpha_{kr} + k_{ur}|z_r(t)|}{\alpha_{kr} + |z_r(t)|} \tag{3}$$

En la que z_r indica la coordenada modal y k_{ir} y k_{ur} son los límites de la rigidez y α_{kr} es el parámetro de forma de la rigidez. La función es simétrica respecto de la coordenada modal. La función evoluciona progresivamente desde su valor inicial k_{ir} para $z_r = 0$ y es asintótica al valor extremo superior k_{ur} cuando z_r tiende a infinito. La curvatura de la curva fuerza desplazamiento aumenta como una función del parámetro de forma α_{kr}. En la Figura 9 se representa la ley propuesta junto con la rigidez inicial y la final.

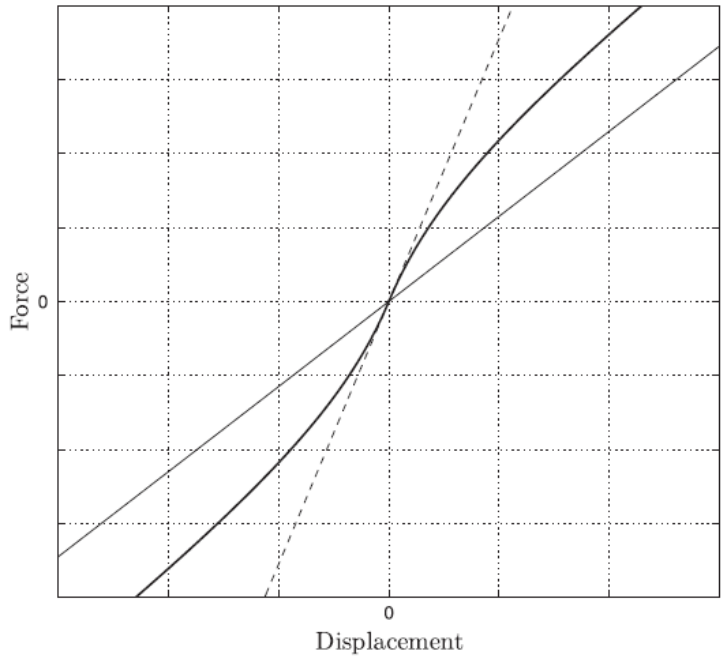

Figura 9. Ley asintótica. Línea gruesa: Curva fuerza-desplazamiento, Línea fina: Rigidez última. Línea de puntos: Rigidez inicial.

El gráfico no corresponde a ninguno de los experimentos, sino que los parámetros modales han sido exagerados deliberadamente por razones ilustrativas.

Como las curvas de amortiguamiento muestran un perfil similar a las de rigidez también se adoptó una ley asintótica para el amortiguamiento c_r como función de la velocidad modal $\dot{z}_r$.

$$c_r(\dot{z}_r) = \frac{c_{ir}\alpha_{cr} + c_{ur}|\dot{z}_r(t)|}{\alpha_{cr} + |\dot{z}_r(t)|} \qquad (4)$$

En la que c_{ir} y c_{ur} son los límites del coeficiente de amortiguamiento inferior y superior, y α_{cr} es el parámetro de forma del amortiguamiento.

Adoptando formas modales normalizadas a la masa, la ecuación no lineal del movimiento correspondiente al modo r-ésimo sería:

$$\ddot{z}_r(t) + \left(\frac{c_{ri}\alpha_{cr} + c_{ru}|\dot{z}_r(t)|}{\alpha_{cr} + |\dot{z}_r(t)|}\right)\dot{z}_r(t) + \left(\frac{k_{ri}\alpha_{kr} + k_{ru}|z_r(t)|}{\alpha_{kr} + |z_r(t)|}\right)z_r(t) = 0 \qquad (5)$$

Como la formulación de las formas modales es lineal en los parámetros, existe una solución analítica y se puede obtener de los datos experimentales aplicando mínimos cuadrados. Sin embargo la formulación modal propuesta para reproducir el comportamiento dinámico de la estructura es no lineal en los parámetros de

amortiguamiento y rigidez. En estas circunstancias, los parámetros no se pueden obtener analíticamente y es necesario adoptar un esquema iterativo para encontrar la solución. El cálculo de estos parámetros se propone como la minimización de una función de error que tiene en cuenta la diferencia entre las respuestas numéricas y las experimentales. La función de error está definida en el dominio del tiempo a través de las series temporales de aceleraciones modales correspondientes a las vibraciones libres. Se elige el error medio cuadrático normalizado como función de error. La minimización se lleva a cabo usando el método beta previamente desarrollado. La respuesta prevista por el modelo necesaria para la minimización se calculó numéricamente de la ecuación del movimiento (5) mediante un esquema de diferencias finitas. Este enfoque da lugar a una formulación explícita de la respuesta. Esta formulación explícita sería muy útil para algunas aplicaciones prácticas futuras tales como control de vibraciones. El número total de parámetros desconocidos es de 8 para cada modo. Están compuestos de tres parámetros de rigidez, tres de amortiguamiento y dos correspondientes a las condiciones iniciales. Los resultados de la calibración no lineal se indican en la Tabla 1.

Mode	k_{ir} (N/m)	k_{ur} (N/m)	α_{kr} (m)	c_{ir} (N s/m)	c_{ur} (N s/m)	α_{cr} (m/s)	ε (%)
1	737.9413	728.6962	0.0089	0.0616	0.1226	0.1572	0.0039
2	8874.5	8686.3	0.0075	0.2409	0.5935	0.7313	0.0032

Tabla 1. Resultados del modelo no lineal.

Los errores de ajuste son muy similares en ambos modos y tienen un valor muy bajo, alrededor de 0,035%, lo que representa un ajuste excelente. En la Figura 10 se muestran los ciclos iniciales y finales de la respuesta prevista por el modelo junto con los resultados experimentales.

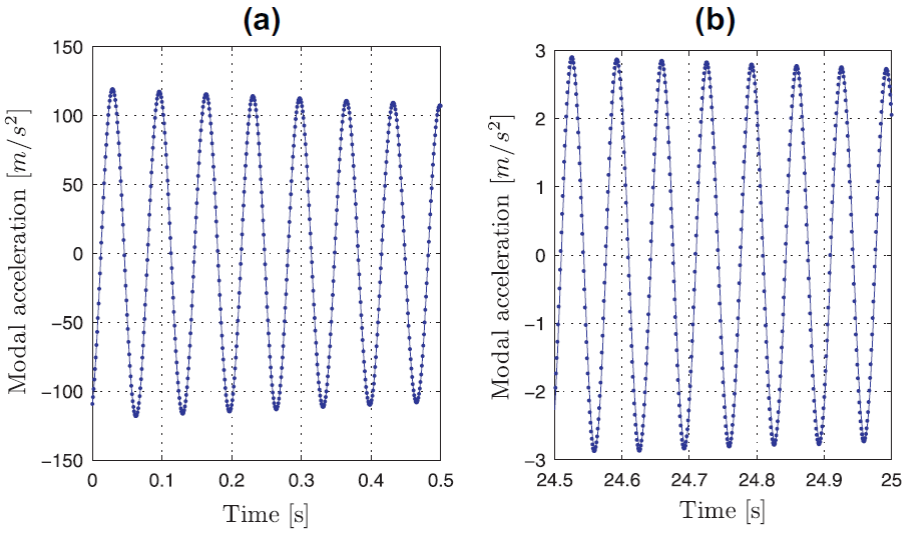

Figura 10. Vibración libre del segundo modo. Línea de puntos: Resultados experimentales. Líneas: Predicciones del modelo no lineal. (a) Ciclos iniciales. (b) Ciclos finales.

Como puede verse, hay un ajuste excelente de los resultados tanto en amplitud como en fase.

Las señales experimentales también fueron ajustadas a un modelo lineal puro, para así obtener una referencia de comparación. En este caso solamente hay cuatro parámetros desconocidos que se identificaron siguiendo un procedimiento similar al del caso no lineal. Los valores de los parámetros identificados se muestran en la Tabla 2 junto con los errores de ajuste.

Mode	k_r (N/m)	c_r (N s/m)	ε (%)
1	731.5933	0.1138	1.8081
2	8802.0	0.4184	4.9881

Tabla 2. Resultados del modelo lineal.

Como se puede apreciar, ahora los errores de ajuste son 3 órdenes de magnitud mayores que los del modelo no lineal. La Figura 11 muestra la respuesta numérica lineal y la experimental.

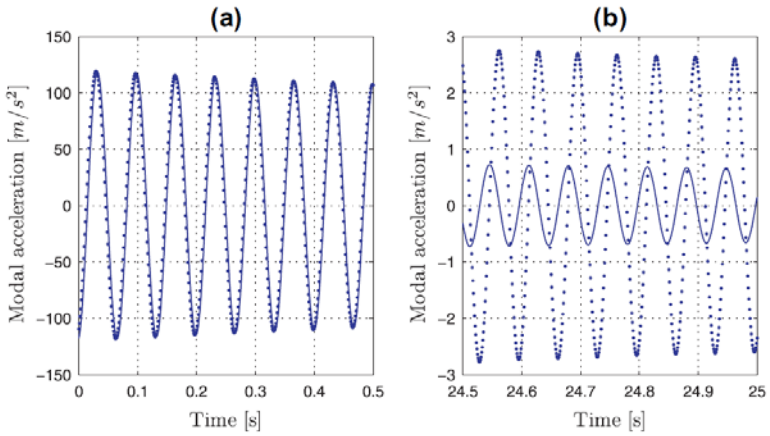

Figura 11. Vibración libre del segundo modo. Línea de puntos: Resultados experimentales. Líneas: Predicciones del modelo lineal. (a) Ciclos iniciales. (b) Ciclos finales.

En este caso se aprecia una diferencia notable tanto en la amplitud como en la fase. Queda así patente que el modelo no lineal supera claramente al modelo lineal.

6. Conclusiones y trabajo futuro

Los tres modelos experimentales estudiados en esta tesis permiten establecer varias conclusiones. En el enfoque por elementos finitos se ha encontrado que:

- El modelizado de las uniones incluyendo geometría, rigidez y amortiguamiento es fundamental para una adecuada descripción del comportamiento dinámico de los pórticos.
- El ajuste de un modelo a los datos modales experimentales no garantiza su sentido físico. Éste debe fundamentarse en otras consideraciones.
- El procedimiento iterativo de calibración de parámetros propuesto, basado en redes neuronales y frecuencias naturales, resultó muy robusto y preciso en todas las configuraciones estudiadas, aun partiendo de valores iniciales de los parámetros muy alejados de la solución.
- Así mismo, este procedimiento resultó muy apropiado para el cálculo de la transmisión de errores de los datos de los parámetros estimados, permitiendo así una visión probabilística de los resultados.
- En los modelos experimentales estudiados, se ha descubierto que su respuesta dinámica se describe de forma más precisa cuando se adoptan modelos de comportamiento no lineales en las uniones.

Se ha desarrollado un método novedoso para la calibración de modelos en el campo de la dinámica estructural. El método está basado en una función de error cuyas variables son las respuestas dinámicas en el dominio del tiempo. Ésta se minimiza mediante un algoritmo estocástico adaptado específicamente a las características de la función de error definida. El algoritmo consiste en un muestreo iterativo en el que las características de las funciones de distribución varían a tenor de los resultados de las iteraciones anteriores. Las principales ventajas del algoritmo propuesto son:

- La fase global y la local de la minimización están integradas.
- El algoritmo se aplica directamente, no necesita ninguna calibración previa de sus propios parámetros.

- Puede aplicarse tanto a sistemas lineales como no lineales.
- Las series temporales que definen la función de error pueden expresarse mediante variables espaciales o modales.

La aplicación del método a simulaciones numéricas y a los casos experimentales estudiados permite establecer las siguientes conclusiones:

- La minimización en un espacio acotado propuesta en el método es imprescindible para encontrar soluciones en los casos en que exista gran incertidumbre en el valor de los parámetros. Los métodos de minimización que contienen búsquedas abiertas son totalmente ineficientes en estos casos.
- La versión anisótropa del algoritmo resultó mucho más efectiva que la isótropa y se adoptó para la versión final del método.
- El algoritmo de minimización propuesto resultó más eficiente que otros algoritmos de propósito general muy utilizados en diferentes ámbitos.
- El método fue capaz de calibrar simultáneamente parámetros de rigidez y amortiguamiento en casos muy mal condicionados.

El estudio del pórtico a media escala fue muy instructivo y las conclusiones a las que se han llegado se podrían extrapolar a estructuras reales similares. En la parte experimental se probó una excitación mono armónica simple localizada en la última planta del pórtico con una intensidad compatible con la serviciabilidad de la estructura como medio para aislar los modos de vibración a flexión. Además, se desarrolló un método novedoso para el filtraje de la vibración libre que es aplicable tanto a sistemas lineales como a no lineales simétricos. La identificación modal del pórtico se basó en la vibración libre posterior a la excitación. Las principales conclusiones en esta parte experimental y de preprocesado de la señal son:

- Con el procedimiento de excitación elegido solo se pudieron aislar los dos primeros modos de vibración. El tercer y cuarto modo aparecieron siempre mezclados con el primero y con el segundo.
- El procedimiento de filtraje propuesto elimina más perturbaciones y mantiene más información de la señal que los filtros digitales de paso banda. Además el procedimiento se aplica directamente sin fijar ninguna frecuencia de corte.

El posterior análisis de la vibración libre correspondiente a cada planta del pórtico reveló que:

- Los modos de vibración son totalmente lineales en el rango de amplitud de los experimentos.
- Esta evidencia empírica permite expresar la respuesta en el espacio modal.

La identificación no paramétrica en el espacio modal puso de manifiesto que:

- El pórtico es débilmente no lineal en la rigidez con no linealidad del tipo de precarga.
- El amortiguamiento es muy no lineal y puede describirse con un modelo viscoso no lineal.
- El comportamiento global del pórtico es no lineal para pequeños desplazamientos modales y va paulatinamente linealizándose a medida que la amplitud aumenta.
- Se dedujo que los modos lineales de vibración son compatibles con una rigidez no lineal siempre que la no linealidad esté distribuida en toda la estructura de forma tal que la matriz de rigidez global para un desplazamiento modal cualquiera pueda expresarse como el producto de una matriz de rigidez invariante por una función escalar del desplazamiento.

De los resultados de la identificación no paramétrica y tras varios intentos, la rigidez y el amortiguamiento modales se modelizaron finalmente mediante leyes asintóticas del desplazamiento y velocidad modales, respectivamente. Los parámetros de estos modelos se calibraron simultáneamente minimizando la diferencia cuadrática entre la respuesta modal obtenida del modelo por diferencias finitas y la experimental. Para la minimización se utilizó el método estocástico previamente establecido. El modelo no lineal supera claramente al lineal puro con errores de ajuste 3 órdenes de magnitud inferiores.

La robustez de minimización podría mejorarse en futuros trabajos. Concretamente, podría establecerse algún procedimiento para salvar los mínimos impropios locales de la función de error. Éste constituye un punto débil del algoritmo propuesto.

El modelo no lineal establecido para el pórtico está destinado a vibraciones según un solo modo. Para dar generalidad al modelo éste debería ampliarse identificando los términos no lineales cruzados.

Por último el modelo debería estudiarse la aplicabilidad del modelo a estructuras reales en servicio.

7. Copia completa de los trabajos

Smart Mater. Struct. **17** (2008) 045016 (11pp) doi:10.1088/0964-1726/17/4/045016

Finite element model updating of a small steel frame using neural networks

J L Zapico[1], A González-Buelga[2], M P González[1] and R Alonso[1]

[1] Department of Construction and Manufacturing Engineering, University of Oviedo, Campus de Gijón, 33203 Gijón, Spain
[2] Department of Engineering Construction, Universitat Politecnica de Catalunya, Edificio C1, Campus Norte, c/Jordi Girona 1-3. E-08034 Barcelona, Spain

E-mail: jzapico@uniovi.es

Received 22 December 2007, in final form 13 April 2008
Published 13 June 2008
Online at stacks.iop.org/SMS/17/045016

Abstract

This paper presents an experimental and analytical dynamic study of a small-scale steel frame. The experimental model was physically built and dynamically tested on a shaking table in a series of different configurations obtained from the original one by changing the mass and by causing structural damage. Finite element modelling and parameterization with physical meaning is iteratively tried for the original undamaged configuration. The finite element model is updated through a neural network, the natural frequencies of the model being the net input. The updating process is made more accurate and robust by using a regressive procedure, which constitutes an original contribution of this work. A novel simplified analytical model has been developed to evaluate the reduction of bending stiffness of the elements due to damage. The experimental results of the rest of the configurations have been used to validate both the updated finite element model and the analytical one. The statistical properties of the identified modal data are evaluated. From these, the statistical properties and a confidence interval for the estimated model parameters are obtained by using the Latin Hypercube sampling technique. The results obtained are successful: the updated model accurately reproduces the low modes identified experimentally for all configurations, and the statistical study of the transmission of errors yields a narrow confidence interval for all the identified parameters.

(Some figures in this article are in colour only in the electronic version)

1. Introduction

In the last decade, finite element (FE) model updating has been an intensive research subject, and robust methods are now available to calculate the adequate values of the selected model parameters from the experimental data. However, the appropriate modelling and selection of parameters are still keys to succeeding in model updating, and most of the actual research in this field is devoted to this topic. Chen and Ewins [1] have proposed a method based on vector projection to verify FE models, i.e. to check whether modelling errors are present in the model. The method has been used successfully to localize the modelling errors in an analytically simulated case. The localization, however, fails when it is applied to an actual industrial component due to lack of information from the experimental data. More recently, Mares *et al* [2] have developed a stochastic updating procedure that allows the cases of ill parameterization and ill modelling to be detected. Nevertheless, these methods only serve to check whether the parameterization of a given FE model is appropriate for given experimental data or not. Thereby, the selection of appropriate parameters and the location of modelling errors still remain as difficult tasks that cannot always be automated. In practice, rationale is not enough to address these issues. Each case requires a particular study and the solutions are usually obtained after a trial and error process, in which experience and structural insight are essential [3]. Under these circumstances, the experience gained in the study of a particular case can be advantageously used in further similar cases.

This paper adds to this debate by studying a small steel frame with bolted joints. It is a part of a wider research devoted to seismic damage identification, which requires precise FE models for undamaged structure configurations [4–6]. An FE

model being composed by beam elements, with emphasis on the modelling of the joints, and capable of reproducing the low modes of the experimental frame in its original configuration is sought herein. Bolted joints have been extensively studied, and it is well known that they exhibit a nonlinear dynamic behaviour [7]. In the present paper, however, the experiments have been driven under low displacements, so as to allow the dynamic response of the frame to be approximated by a linear FE model. The FE model updating is based on neural networks (NNs) and the modal properties of the frame, which were identified from dynamic tests. Previous studies by the authors [8, 9] have proved the effectiveness of the NNs in the updating process. The modal information is deliberately reduced to the first three natural frequencies of the frame, even though a large number of modes can be identified under laboratory conditions. This approach tries to simulate the limitations on actual structures, where only the low natural frequencies can be accurately identified and the mode shapes are in general less accurate and less sensitive to the parameters of the FE model [10].

Two approaches have been sequentially tried for updating the FE model in its original configuration, and they are presented in this paper. In both, the FE model was refined on the basis of the experimental data and the results of the previous one. The dynamic performance of the updated FE model was validated through six supplementary configurations, which were obtained from the original one by modifying in turn the mass and making cuts at some elements. In order to evaluate the effect of the cuts in the stiffness of the frame, an analytical model was developed.

A statistical study of the errors of the experimental data was also carried out. The transmission of these errors to the updated parameters was addressed via sampling through the Latin Hypercube method. Finally, a confidence interval for the estimated parameters was computed from the obtained frequency distribution errors.

2. Experimental details

2.1. Original configuration

The experimental model in its original configuration was a three-storey two-bay orthogonal plane frame. The inter-storey height was 150 mm, and the beam span was 100 mm. Both the beams and the columns were strips with a 1.75 mm × 45 mm cross-section made of structural steel. The columns were continuous with the bottom bent through 90° and connected to a steel channel by two bolts 6 mm in diameter. A 10 mm thick plate was added to these connections so as to increase their stiffness. The ends of the beams were also bent through 90°. All of beams were connected to the piers by combining two bolts 4 mm in diameter and two welding spots placed at the ends of each bend corner (see figures 1 and 2.).

Additional masses were attached at the middle of each beam. They consisted of parallelepiped 30 mm × 45 mm× 60 mm steel blocks, which were connected to each beam by a bolt 8 mm in diameter (figure 3). This movable connection allowed the mass to be modified during the tests.

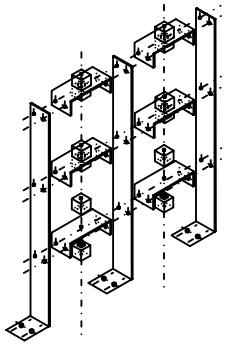

Figure 1. Experimental frame main dimensions: inter-storey height 150 mm, beam span 100 mm, strips 1.75 mm × 45 mm.

Figure 2. Detail of the bottom connections: a plate was added in order to increase their stiffness.

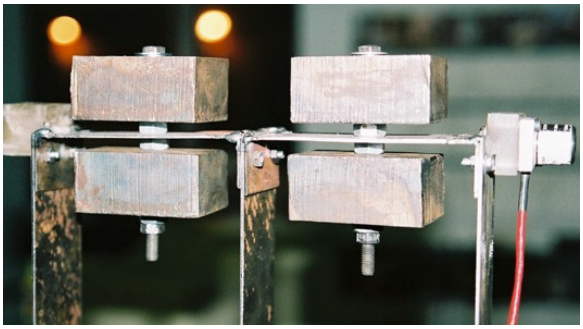

Figure 3. Detail of the attached masses.

2.2. Supplementary configurations

Six supplementary configurations, which were labelled from 1 to 6, were obtained from the original one by modifying in turn the mass and the stiffness. The mass modifications were achieved by removing and attaching some of the blocks bolted to the beams. The stiffness modifications consist of transversal cuts carried out by the ends of some beams. Two symmetric cuts were machined at each side of the beams. They were 1 mm wide, and were placed around 7 mm from the end of the beams (see figure 4). Two different cut lengths were used, namely 10 and 15 mm. These cuts try to simulate seismic damage at the frame. The distributions of the blocks and the cuts in each configuration are shown in figure 5.

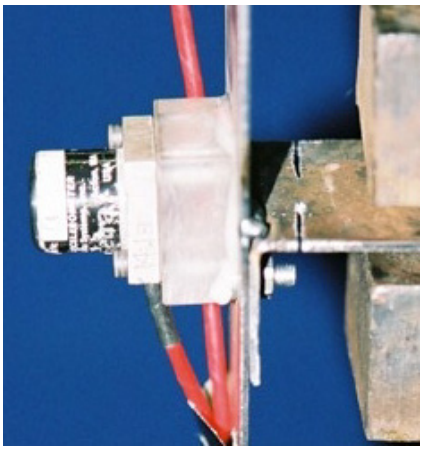

Figure 4. Detail of the simulated damage. All cuts were 1 mm wide and were placed around 7 mm from the end of the beams.

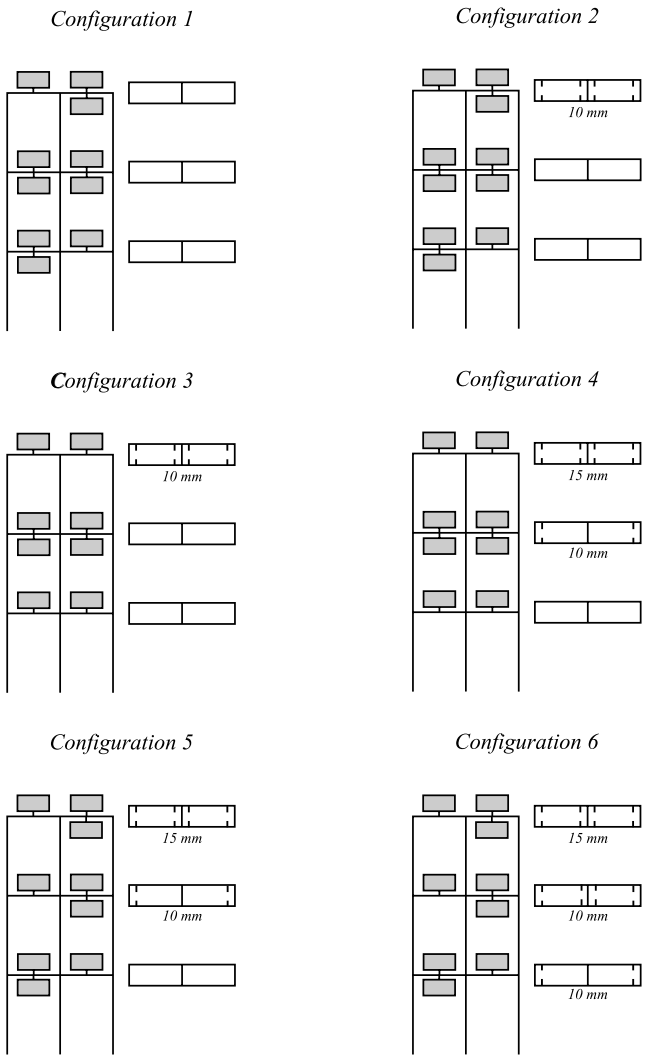

Figure 5. Distribution of the attached masses and artificial cuts in the supplementary configurations.

2.3. Dynamic testing and identification

The dynamic behaviour of the experimental structure was studied by developing shaking table testing. The single degree of freedom shaking table used, driven by an electro-mechanic actuator, is shown in figure 6. The model was bolted on the shaking table platform, the direction of movement being in the plane of the structure (see figure 2).

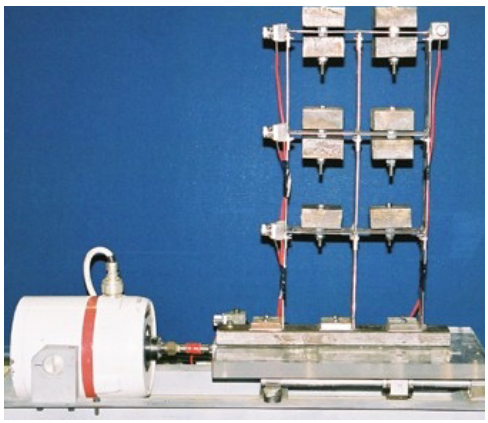

Figure 6. Photograph of the experimental model setup on the shaking table.

Both the actual shaking table movement and experimental structure response were tracked by using piezoelectric accelerometers. The distribution of the accelerometers can be seen in figure 6. The experimental structure was shaken following a broadband-testing technique: random excitation and swept sines. The time domain excitation and response signals were filtered, digitized and then passed through a Fourier analysis process to transform the time domain information to frequency domain spectra. By appropriate combination of input and output acceleration spectra, the required frequency response functions (FRFs) for the structure were derived. From the FRFs the natural frequencies were extracted, using the global rational fraction polynomial method. This method is an extension of the rational fraction polynomial method [11] to analyse globally a set of FRFs. This method is widely used and is often classified as one of the most reliable and successful [10], provided that there are not mode shapes too close in frequency.

Table 1 details the results of the modal extraction for the original configuration and for each group of tests. As was already mentioned, the characteristics of the experimental structure were changed several times, leading to different configurations. Both dynamic testing and modal identification were carried out for each configuration. Thus, at the end of the process we have a database containing mass and stiffness configurations and the corresponding experimentally extracted natural frequencies. Table 2 contains the experimental results for the supplementary configurations.

3. Finite element model updating

3.1. Choice of parameters

From a mathematical point of view, all the parameters that define the properties of each FE are candidates to be updated. Thus, FE models generally contain many potential parameters to be updated, and if all of them are considered independently,

Table 1. Modal identification for the original configuration.

Group of tests	f_1 (Hz)	f_2 (Hz)	f_3 (Hz)
Noise1	5.9914	19.2659	33.3770
Noise2	5.9677	19.2179	33.3275
Noise3	5.9413	19.2297	33.3311
Noise4	5.9654	19.2203	33.3215
Noise5	5.9560	19.2332	33.3323
Noise6	5.9266	19.2218	33.3142
Noise7	5.9218	19.1892	33.3012
Noise8	5.9299	19.2491	33.3799
Swept1	6.0068	19.3284	33.4532
Swept2	5.9912	19.3517	33.4659
Swept3	5.9878	19.3405	33.4670
Swept4	5.9813	19.3378	33.4508
Swept5	5.9959	19.3377	33.4486
Swept6	5.9827	19.3387	33.4434
Swept7	5.9904	19.3581	33.4460
Swept8	5.9850	19.3408	33.4436
Mean	5.9701	19.2850	33.3940
Std deviation	0.0271	0.0609	0.0636
Variation δ (%)	0.4544	0.3156	0.1905

Table 2. Modal identification for the supplementary configurations.

Configuration		f_1 (Hz)	f_2 (Hz)	f_3 (Hz)
1	Mean	6.3811	21.3257	35.2142
	Std deviation	0.0181	0.0193	0.0295
	Variation δ (%)	0.2844	0.0906	0.0837
2	Mean	6.3581	20.9359	35.0928
	Std deviation	0.0191	0.0257	0.0085
	Variation δ (%)	0.3002	0.1229	0.0242
3	Mean	6.9800	24.1009	38.5775
	Std deviation	0.0355	0.0686	0.0791
	Variation δ (%)	0.5084	0.2847	0.2050
4	Mean	6.8316	23.3265	38.2475
	Std deviation	0.0221	0.0335	0.0800
	Variation δ (%)	0.3238	0.1434	0.2092
5	Mean	6.5405	20.6132	36.8056
	Std deviation	0.0100	0.0262	0.0225
	Variation δ (%)	0.1522	0.1272	0.0610
6	Mean	6.3074	19.9905	36.4829
	Std deviation	0.0167	0.0268	0.0304
	Variation δ (%)	0.2643	0.1339	0.0834

the updating process becomes ill conditioned in most of the cases. This means that many different combinations of parameters lead to very close modal solutions referred to the degrees of freedom (DoFs) and modes considered in the experimental model. In practice, fortunately, the discrepancies between the modal properties of both the FE and the experimental models are mainly due to a reduced number of parameters. This is similar to the well-known Pareto's effect in economics. An alternative to obtain a well-conditioned updating process consists of selecting the significant parameters among all the possible ones.

There are some general rules for the selection of parameters. Thus, for the updating process to be well conditioned, it is necessary but not sufficient that the number of updating parameters be less than or equal to the available independent modal variables. Moreover, the modal variables should be sensitive to the selected parameters; otherwise the obtained values would be unrealistic due to the error amplification effect. Among these parameters, only those that are likely to be in error should be selected. Sometimes, similar values of the parameters are expected for several FEs. In this case, a super-element parameter should be selected for all the elements of the group.

3.2. Updating procedure

Once the parameters have been selected, the updating process can start. In this study, the parameters were computed following a forward approach. For this, a database of mapped modal properties and parameters values is generated though the FE model by varying the selected parameters at random within a given interval. Afterwards, the database is used to train a regressor, which outputs the value of the updated parameters when the identified modal properties are supplied as inputs. The regressors used in this work are NNs. The next subsection includes a more detailed description of them.

NNs have some advantages that make them suitable for updating cases with a low number of parameters [4–6, 12]. Under these conditions they are computationally effective, and the updating process can be automated. Moreover, the NN training and testing processes act as a filter against ill-conditioned cases because they are unable to generalize in these cases. Another advantage of the NNs is that once trained they are capable of giving the solution almost instantaneously. This enables us to estimate a confidence interval of the updated parameters from a given probability distribution of the inputs errors by numerical simulation through the Latin Hypercube method [5, 6].

In order to improve the accuracy of the NNs predictions, the data used for training is extracted from a narrow interval around the reference values of the parameters. Thus, it may happen that the predictions for some parameters fall outside the selected interval. What the NN does in these cases is to extrapolate, and the accuracy of its predictions is very poor under these conditions. To solve this issue, the following regressive procedure is proposed.

Step 1: set a reference value for the selected parameters, θ_i.

Step 2: set a factor ρ that defines the search intervals around the reference values, $\theta_i \pm \rho\,\theta_i$.

Step 3: generate a set of parameters by random uniform sampling within the search interval.

Step 4: compute the natural frequencies corresponding to the set of parameters through the FE model.

Step 5: train the NN mapping the data obtained in *step 3* and *step 4*.

Step 6: compute the parameters by feeding the trained NN with the experimental natural frequencies of the frame.

Step 7: if some of the computed parameters are outside the intervals defined in *step 2*, then set the reference parameters equal to the computed ones and go to *step 3*.

3.3. Neural networks

The configuration of the neural networks used was a two-layer feed-forward multi-layer perceptron (MLP). The inputs (x_i) of the MLP were the natural frequencies of the frame and

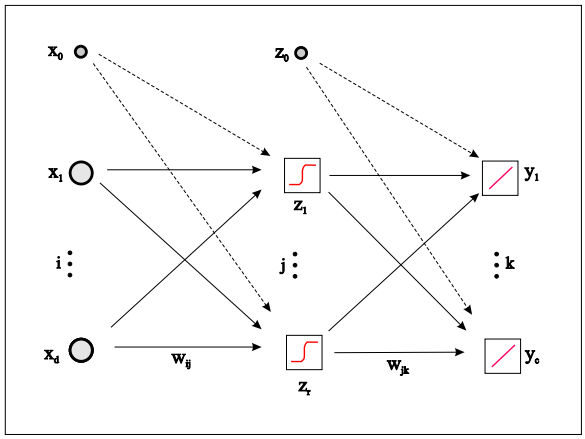

Figure 7. Configuration of a multi-layer perceptron.

the output variables were the parameters to be updated (y_i). Output variables are obtained from the input in a concatenated way, through linear combinations of previous layer values and weights (w) transformed by activation functions. A tangent hyperbolic activation function was used for the hidden layer (g) and a linear one for the output layer ($\tilde{g}$) (see figure 7).

$$y_k = \tilde{g}\left[\sum_{j=0}^{r} w_{kj}^{(2)}\, g\left(\sum_{i=0}^{d} w_{ji}^{(1)} x_i\right)\right]. \tag{1}$$

This constitutes a black-box model based on mother basis functions of a single variable. It can approximate any continuous nonlinear multivariate function within a given finite domain by adjusting its weights. The accuracy of the approximation increases with the number of hidden units [13].

In the literature, the process of fitting an MLP to a given function is known as *learning* or *training*. The learning is based on a set of patterns of mapped input and output vectors, which is called learning data, which is obtained analytically in this case. The process consists of minimizing a quadratic error function, which represents the discrepancies between the predictions of the MLP corresponding of the input data and the target ones, with respect to the MLP weights. The optimization process is divided in two steps, namely, computation of the derivatives of the error function with respect to the parameters of the net and optimization of the parameters. An error back propagation algorithm with batch strategy was used for the first step and scaled conjugate gradients for the second one. This is an efficient algorithm of optimization that takes the minimum number of cycles to minimize the error function.

After training, the *testing* process is developed by comparing the predictions of the trained MLP with the reference ones contained in a data set. This measures the capacity of generalization of the MLP. The reference data set is similar to that used for training but containing different patterns. More details about MLPs can be found in [13].

The Netlab package was used to compute the MLP, which is implemented as a set of functions written in the MATLAB language using only core functions. This is a library freely offered by its authors from Aston University [14].

4. Approach A

4.1. Finite element model

The components of the experimental frame are steel strips. The shear deformations of this type of section are negligible when compared with the flexural ones. Hence, they are modelled as standard Euler–Bernoulli beam elements, with cubic interpolation functions and without consideration of the shear deformations. On the other hand, the elements bend around the minor axis of their cross-sections, whose width is nearly 26 times greater than their height. Under these conditions, a plane strain state is expected for the bending elements. This is taken into account in the FE model by using the following equivalent Young's modulus:

$$E' = \frac{E}{1-\nu^2} \tag{2}$$

in which E is the Young's modulus and ν is the Poisson ratio.

The Bernoulli hypothesis, which states that the cross-sections remain plane after the deformation, is only valid in the zones of the beams with uniform geometry. Near the connections, however, there are usually significant geometrical discontinuities, which make the aforementioned hypothesis fail. In the bolted connections, there are stress concentrations around the bolts. The closer the cross-section to the bolts, the lower the uniformity of the stress distribution is. This results in a higher flexibility of the beams in the zones close to the connections. In order to take into account this effect in the FE model, small length (10 mm) elements were considered for modelling the beam–column and the column–support connections. They were oriented in the direction of the beams and the columns, respectively. Similar beam elements were added to simulate the connection from the centre of the additional masses to the frame.

The mass of the frame pieces was modelled as a consistent uniformly distributed one, considering the nominal density of the steel and the cross-section of the elements. The bolts, nuts, washes, beam overlaps used in the connections and the accelerometers and their bases were modelled as translational masses lumped to the corresponding model nodes. The additional masses were also modelled as lumped ones, but taking into account both translation and moment of inertia.

The model was coded in MATLAB [15] using The Structural Dynamics Toolbox [16], and it is illustrated in figure 8.

4.2. Choice of parameters and initial values

As only the first three natural frequencies of the model are available, the number of independent updating parameters should be reduced to three or less so as to guarantee a well-conditioned formulation.

The masses of the FE model are set to their nominal values, and they are not updated because there is a low uncertainty in their values. The stiffness of the bars is initially set to their nominal values, and then they are updated. As all the piers and beams are made from the same strip, all

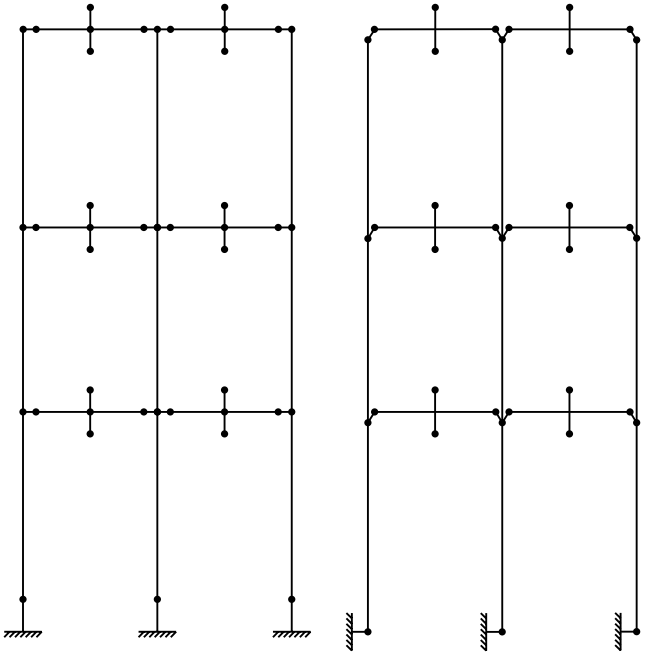

Figure 8. FE models. Left, approach A. Right, approach B.

the pieces are likely to have similar stiffness. So, one super-element parameter has been selected for updating the stiffness of the bars, namely, the second moment of area of their cross-section. Another important source of error arises from the boundary conditions [17]. In this case, it is taken into account through the stiffness of the connection elements. As for the bars, the second moment of area of the connection elements is selected as an updating parameter. To this end, two different super-element parameters have been selected: one corresponding to beam–column connections and the other for the column–support connections because they have a rather different configuration. As a previous calibration of this kind of connection is not available, the initial value selected for the pieces is also adopted for the connection elements. It should be pointed out that the adopted value constitutes an upper limit for the parameter because the connections always add some flexibility, as has been explained in the previous section.

It was found that the modal response of the FE model was quite insensitive to the stiffness of the elements connecting the additional masses, for a large range of values. Thereby, this variable was set to the value corresponding to a 200 mm^4 second moment of area. The selected parameters and their initial values are shown in table 3.

4.3. Results of updating and discussion

The initial errors of the FE model frequencies relative to the experimental ones are shown in table 4. As can be seen, all the errors are positive, and the lower the frequency the higher the error is. The initial root-mean-square (RMS) error is 9.32%. This means that the initial stiffness of the FE model is higher than that of the actual frame.

The updated values of the parameters were obtained following the procedure outlined in section 3.2. It was established that $\rho = 0.1$, and a database containing 600 datasets was generated in each iteration. The first 400 datasets were used for training, and the remaining ones for testing. After some trials, a 3:12:3 architecture was selected for the MLP, i.e. 3 inputs, a 12-node hidden layer and 3 outputs. This constitutes a trade-off between the duration of training and the precision of testing.

Table 3. Updating parameters for approach A.

Parameter	Description	Initial value
θ_1	Second moment of area of the beams and columns	20 mm^4
θ_2	Second moment of area of the beam–column connections	20 mm^4
θ_3	Second moment of area of the column–support connections	20 mm^4

The convergence to the training interval took three iterations, and the frequency RMS error corresponding to the updated model was 0.0015%. Table 4 shows the results of updating. There is a small reduction of about 2% in the stiffness of the beams and columns. As was expected, the stiffness of the beam–column connection has a higher reduction 66%. The stiffness of the column–support connection, however, increases by 74%.

Even though this model reproduces the first three natural frequencies of the frame precisely, the value of the column–support connection stiffness is 77% higher than that of the updated columns. As has been previously stated, the value of the column stiffness constitutes an upper bound of the solution. Therefore, this approach is not physically meaningful; the solution is a mere mathematical solution. Consequently, it is rejected, and a more adequate one is sought in the next section.

5. Approach B

5.1. Finite element model

A likely explanation of the physical incoherence found in the previous approach might be the absence of some geometrical feature in the modelling of the connections. In [18], it is established that geometry is essential for an adequate modelling of a connection. Thereby, the eccentricity from the centre of the connections to the centre of the elements is considered in this new model.

Thus, the beam–column connection is now modelled with two elements connected in series (see figure 8). The vertical one tries to reproduce properly the geometry of the ends of the beams by adding the eccentricity of the point of transmission of efforts between the beam and the column. This element also includes the flexibility of the connection due to its discontinuities. The horizontal one is similar to that of approach A, but in this case it is only intended to reproduce the effects of damage. The column–support connection is modelled with one horizontal element trying to reproduce adequately the geometry of the joint.

Table 4. Results of updating for approach A.

	Parameter			Relative frequency error (%)			
Iteration	θ_1	θ_2	θ_3	e_1	e_2	e_3	RMS error
Initial	20.0000	20.0000	20.0000	13.6477	8.2827	2.4251	9.3228
1	19.5582	8.3182	21.6747	1.9325	0.7229	−0.3442	1.2077
2	19.6320	6.8891	32.4221	0.0216	−0.0328	−0.0442	0.0341
3	19.6197	6.8281	34.8094	− 0.0023	−0.0010	0.0008	0.0015

Table 5. Updating parameters for approach B.

Parameter	Description	Initial value
θ_1	Offset of the vertical beam–columns connections	10 mm
θ_2	Second moment of area of the beams, columns, horizontal beam–column connections and column–support connections	20 mm^4
θ_3	Second moment of area of the vertical beam–column connections	20 mm^4

5.2. Choice of parameters and initial values

As in the previous model, the second moment of area of the cross-section has been selected as a super-element parameter to update the stiffness of the beams, the columns and the horizontal beam–column connection elements, the nominal value of the parameter being selected as the initial one.

With regard to the vertical beam–column connection elements, the second moment of area of the cross-section has also been selected as a super-element parameter, so as to take into account the unknown stiffness reduction due to the geometrical discontinuities of the cross-section in the connection zone. This parameter was initially set equal to the nominal value of the second moment of area of the beams. The vertical offset of these connections has also been selected as a super-element updating parameter because the response of the model is quite sensitive to this parameter. A 10 mm initial value was adopted for the offset, which corresponds to the nominal one.

The column–support connection has a rather different configuration. The stiff plate added to the connection guaranties a uniform stress distribution in the horizontal part of the pier and the absence of stiffness reduction in this zone (see figure 2). Consequently, the super-element parameter selected for the stiffness of the beams and columns has also been adopted for this connection element. From preliminary studies, it was found that the offset of this connection has a lower influence than that of the beam–column one on the dynamic response of the model. Thereby, it was decided not to update this offset, but to set it to 2 mm. This value corresponds to the average distance from the column to the edge of the connection plate, which was directly measured in the frame. The selected parameters and their initial values are shown in table 5.

5.3. Results of updating

The errors of the FE model frequencies relative to the experimental ones are shown in table 6. As in the previous model, all the errors are positive, and they decrease when the frequency increases. The corresponding RMS error, however, is 3.75%, which is rather lower than that of model A, 9.32%. This means that the geometrical offset of the connections has a significant effect on the dynamic response of the model.

The updating procedure was similar to the previous one, using the same factor ρ and net architecture. The convergence to the training interval required only two iterations in this case, the final RMS error being 0.0004% (see table 6). In the updating process, there is a small reduction of about 0.6% in the stiffness of the beams, columns and column–support connections. The updated offset of the beam–column connections is 25% greater than the nominal one. The stiffness of the vertical beam–column connection experiences a reduction around 26% with respect to the updated stiffness of the beams. In this approach, all the results are physically consistent and have reasonable values.

A new interpretation of the results of the previous model can be done from the actual one. Even though the nominal inter-storey height is the same for all the storeys, the vertical offset of the beam–column connections makes the length of the piers of the first floor in approach B shorter than those of approach A, while those of the remaining floors are equal in length (see figure 8). Thus, there is an increase in the stiffness of the piers of the first floor in approach B. This is balanced with a significant increment of the second moment of area of the column–support connection in approach A.

6. Validation

6.1. Description of the procedure

The capacity of the updated FE model to reproduce the experimental natural frequencies was assessed through the supplementary configurations, which include both mass and stiffness modifications from the original one. For this purpose, the values of the physical variables were set equal to those of the original configuration approach B. Moreover, the mass modifications were considered, and the effects of the cuts at the ends of the beams were taken into account by reducing the bending stiffness of the corresponding horizontal beam–column connection elements. A simplified procedure based on the classical bending theory, which will be explained in next subsection, has been developed for evaluating the ratio of the stiffness of a damaged connection to the stiffness of

Table 6. Results of updating for approach B.

	Parameter			Relative frequency error (%)			
Iteration	θ_1	θ_2	θ_3	e_1	e_2	e_3	RMS error
Initial	10.0000	20.0000	20.0000	5.3728	3.4461	1.1962	3.7494
1	12.0655	19.5759	15.2727	0.1856	−0.1716	−0.6039	0.3780
2	12.4663	19.8855	14.7033	0.0001	0.0004	0.0007	0.0004

the corresponding undamaged one in these supplementary FE models. It will be referred to as *stiffness ratio* in the remaining of the paper. Afterwards, the natural frequencies of these supplementary FE models were computed and compared with those identified experimentally.

6.2. Damage modelling

To evaluate the stiffness ratio, a linear stress diffusion model with 1:1 slope ($s = 1$) is assumed in the zone close to the cuts (see figure 9). Thus, the effective width of the beam in this zone can be formulated as

$$y(x) = b - 2x, \tag{3}$$

and the corresponding second moment of area

$$I(x) = I_c\left(1 - 2\frac{x}{b}\right), \tag{4}$$

in which I_c is the second moment of area of the complete cross-section of the beams. Assuming a uniform bending moment M, the total relative rotation in this zone would be

$$\varphi_d = \int_0^1 \frac{M}{EI_c\left(1-2\frac{c}{b}\right)}\,dx + 2\int_0^c \frac{M}{EI_c\left(1-2\frac{x}{b}\right)}\,dx$$
$$= \frac{M}{EI_c}\left(\frac{1}{1-2\frac{c}{b}} - b\log\left(1-2\frac{c}{b}\right)\right). \tag{5}$$

The counterpart of the undamaged zone would be

$$\varphi_u = \frac{M(2c+1)}{EI_c}. \tag{6}$$

Therefore, the increment of rotation due to the cuts is

$$\Delta\varphi = \varphi_d - \varphi_u = \frac{M}{EI_c}\left(\frac{1}{1-2\frac{c}{b}} - b\log\left(1-2\frac{c}{b}\right) - (2c+1)\right). \tag{7}$$

The counterpart in the FE would be

$$\Delta\varphi = \varphi_d - \varphi_u = \frac{ML_c}{EI_u}\left(\frac{I_u}{I_d} - 1\right), \tag{8}$$

where I_u and I_d are the undamaged and damaged second moments of area, respectively, and L_c is the length of the horizontal connector. Equating (8) and (7), the following expression of the stiffness ratio is achieved:

$$\eta = \frac{I_d}{I_u} = \frac{1}{1 + \frac{I_u}{I_c L_c}\left(\frac{1}{1-2\frac{c}{b}} - b\log\left(1-2\frac{c}{b}\right) - (2c+1)\right)}. \tag{9}$$

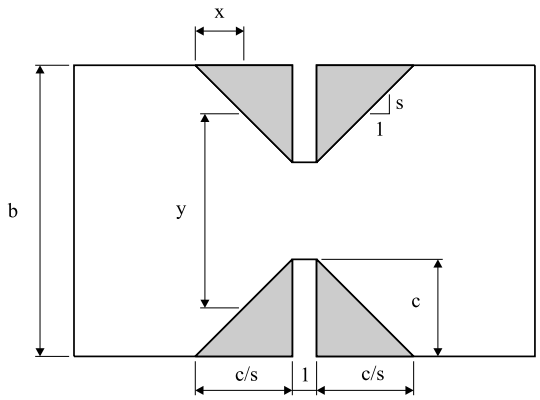

Figure 9. Damage modelling.

6.3. Results and discussion

The FE models of the supplementary configurations were obtained from that of approach B after removing the corresponding masses and multiplying the value of the stiffness of the horizontal beam–column connections by the stiffness ratio given by equation (9). Afterwards, the natural frequencies of these FE models were computed and compared with those identified experimentally.

First, the initial values of the parameters were taken into account. The relative frequency errors are shown in table 7. As can be seen, all the errors are positive. When comparing the errors of each supplementary configuration with those of the original one, a similar trend can be appreciated with slight greater values. The global RMS error is 4.86%.

Second, the updated parameters of the original configuration were adopted in the supplementary ones, and the stiffness ratios were recalculated through equation (9), adopting the updated value for the undamaged second moments of area of the beam–column connection elements, I_u. The relative errors of the updated configurations are also shown in table 7. Now there are positive and negative errors, the absolute value of the errors is less than 4%, and the global RMS error falls to 2.10%. Summing up, there is a significant improvement in the results after adopting the parameters updated in the original configuration. The remaining errors can be explained by considering the unavoidable lack of uniformity in the geometry, connection stiffness and mass distribution present in the frame. In the original FE model, however, a uniform distribution, which averages the actual values, is considered. These averages are changed in each mass and stiffness modification.

Table 7. Validation results for model B.

		Finite element model			Error (%)	
Configuration	Mode	Initial	Updated	Experimental model	Initial	Final
	1	6.80	6.46	6.38	6.56	1.17
1	2	22.00	21.20	21.33	3.16	−0.58
	3	36.37	36.01	35.21	3.27	2.26
	1	6.77	6.43	6.36	6.54	1.15
2	2	21.60	20.84	20.94	3.19	−0.44
	3	36.16	35.83	35.10	3.03	2.09
	1	7.42	7.05	6.98	6.33	1.00
3	2	24.56	23.61	24.10	1.90	−2.02
	3	40.34	40.08	38.58	4.57	3.9
	1	7.30	6.94	6.83	6.93	1.66
4	2	23.60	22.77	23.33	1.17	−2.38
	3	39.97	39.74	38.25	4.50	3.91
	1	6.95	6.60	6.54	6.22	0.86
5	2	21.46	20.82	20.61	4.11	0.99
	3	37.43	37.06	36.81	1.69	0.68
	1	6.79	6.47	6.31	7.65	2.55
6	2	21.29	20.68	19.99	6.52	3.45
	3	37.39	37.01	36.48	2.48	1.45
				RMS error	4.86	2.10

7. Study of the transmission of errors

The parameters selected in the FE model were updated by an NN from the experimental natural frequencies of the frame. Some uncertainties in the values of the parameters arise from this process. The identified natural frequencies have a stochastic nature. There are always experiment-to-experiment discrepancies even for the same physical model. These are due to measurement noise, uncontrollable excitations and identification errors. These errors in the NN input are transmitted to the updated parameters. As the relationship between the natural frequencies and the model parameters is not linear, the statistical distribution of the input errors is distorted in the updating process. On the other hand, there exist errors inherent to the NNs. Indeed, the NNs constitute a functional interpolation to discrete values of the variables. Therefore, an interpolation error is present in the updating NN, which is also transmitted to the calculated parameters. The values of the interpolation errors depend in general on the values of the variables. Considering the aforementioned advantages of the NNs, the parameter errors were computed by numerical sampling through the *Statistics Toolbox* of MATLAB [15] for approach B.

First, the mean and the variance of the identified natural frequencies were estimated from the 16 groups of different tests of the original configuration. The results are shown in table 2. The sample mean, which is the variable used as the NN input, is assumed to have a Gaussian distribution with the following mean and variance:

$$\mu \cong \bar{X}$$
$$\sigma^2 \cong S^2/n \tag{10}$$

in which $\bar{X}$ and S^2 represent respectively the sample mean and variance, and $n = 16$ is the number of samples. This is a plausible approximation according to the central limit theorem.

Then a database containing 10 000 data sets was generated at random by means of the Latin Hypercube method, assuming that the frequencies are uncorrelated and normally distributed. In fact there is some degree of correlation between the variables. However, the hypothesis of independence gives more conservative values of the further confidence intervals. The Latin Hypercube is an efficient multivariate sampling method that guaranties a uniform distribution of the samples along the probability interval.

Afterwards, this database was used to feed the updating NN, so as to obtain the random values of the parameters. The histograms corresponding to the results are shown in figure 10 along with the fitted Gaussian probability functions. As can be seen, the results are quite close to the normality. This is due to the fact that the natural frequencies identified are very precise, with a very narrow interval of variation. Under these conditions, the relationship between frequencies and parameters can be linearized, and the Gaussian input is transformed into another Gaussian distribution. On the other hand, the interpolation errors of the NN are very low when compared with those due to the frequency errors, and their effect in the distribution function of the parameters is negligible.

Finally, the parameters of the Gaussian distribution of the parameters errors were obtained by fitting the results. From these the symmetric 99% confidence intervals were calculated (see table 8). The most precise parameter is the second moment of area of the beams and columns with a relative confidence interval 0.014%, while the parameters relative to the connections have a relative confidence interval around 1%. The precision of the results, however, is excellent.

8. Conclusions

An FE model with physical meaning and an appropriate parameterization for the original undamaged configuration of

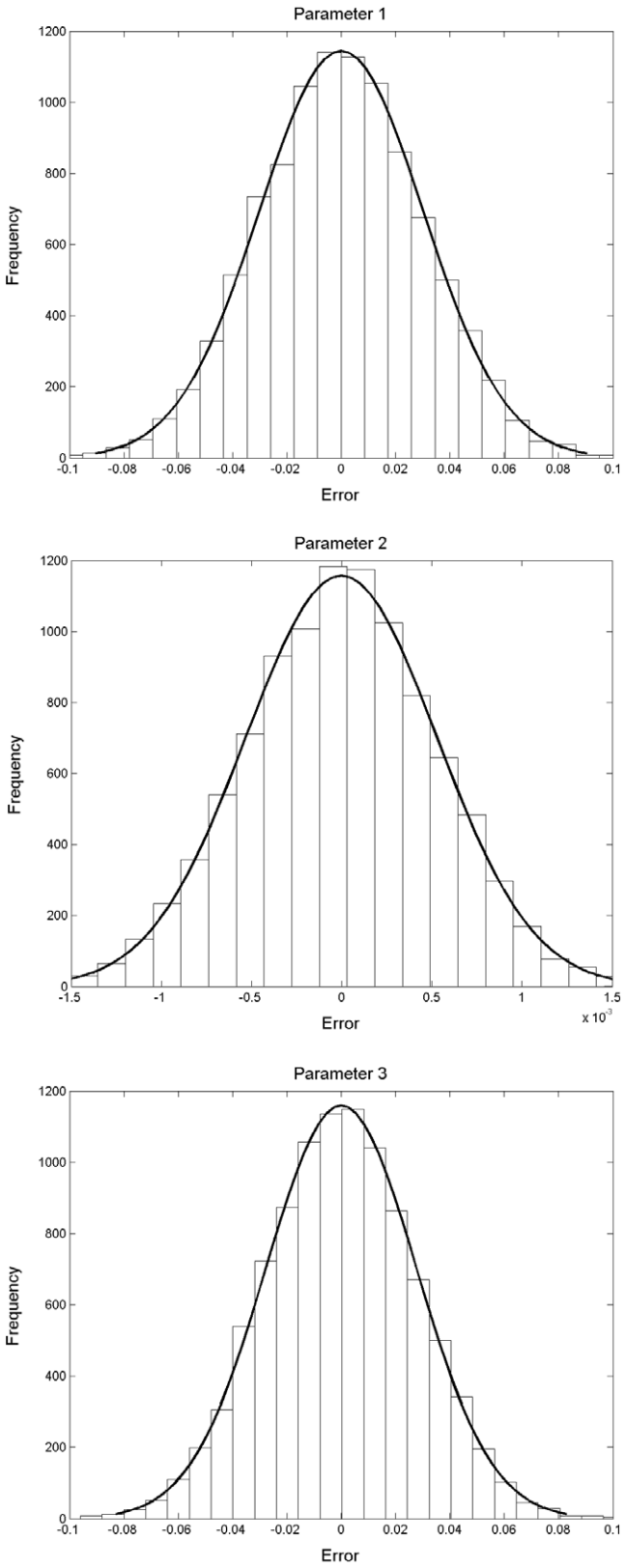

Figure 10. Histograms of the parameter errors.

the frame was achieved after some trials. It was found that geometrical offsets are essential for an adequate modelling of the bolted joints used in the frame. The proposed iterative procedure for FE model updating has been demonstrated to be effective and robust. An analytical model based on the classical bending theory has been developed to evaluate the reduction of bending stiffness of the elements due to damage. The updated FE model can reproduce the first three natural frequencies of the supplementary configurations of the frame after introducing the mass modifications and the stiffness reductions given by the analytical model. All the frequencies are obtained to within a 4% relative error, the RMS error for all the configurations being 2.10%.

From a statistical study of the procedure, it can be concluded that the coefficient of variation of the identified natural frequencies for each group of tests is less than 0.5%. With this level of precision, it is found that the relationship between the modal errors and the model parameters errors can be linearized. Under the normality hypothesis, the symmetric 99% confidence interval is within 1% for all the estimated parameters.

More generally, the procedure could be extended to full-scale frames. It would be essential to have adequate parameterization of the model by selecting groups of similar pieces and joints. These parameters could be estimated from the low frequencies of the structure, which can be precisely identified in practice.

Table 8. Confidence interval 99% for the parameters of model B.

Parameter	Upper limit	Lower limit
θ_1	12.56	12.40
θ_2	19.89	19.89
θ_3	14.78	14.64

Acknowledgments

The authors would like to knowledge the support of the European Commission and the Spanish MEC. The experimental part was performed at the Earthquake Engineering Research Centre (EERC) of the University of Bristol and funded by a Marie Curie HPMT-CT-2000-00001 grant. A González-Buelga is funded by a Juan de la Cierva MEC grant.

The collaboration of the EERC staff, particularly Professor Severn, is greatly acknowledged.

References

[1] Chen G and Ewins D J 2004 FE model verification for structural dynamics with vector projection *Mech. Syst. Signal Process.* **18** 739–57

[2] Mares C, Mottershead J E and Friswell M I 2006 Stochastic model updating: Part 1—theory and simulated example *Mech. Syst. Signal Process.* **20** 1674–95

[3] Friswell M I and Mottershead J E 1995 *Finite Element Model Updating in Structural Dynamics* (New York: Kluwer–Academic)

[4] González-Buelga A 2005 Experimental modal analysis applied to the seismic damage identification in buildings *PhD Thesis* University of Oviedo, Asturias, Spain (in Spanish)

[5] Zapico J L and González M P 2006 Numerical simulation of a method for seismic damage identification in buildings *Eng. Struct.* **28** 255–63

[6] González M P and Zapico J L 2008 Seismic damage identification in buildings using neural networks and modal data *Comput. Struct.* **86** 416–26
[7] Ibrahim R A and Pettit C L 2005 Uncertainties and dynamic problems of bolted joints and other fasteners *J. Sound Vib.* **279** 857–936
[8] Zapico J L, González M P and Worden K 2000 Damage assessment using neural networks *Mech. Syst. Signal Process.* **17** 119–25
[9] Zapico J L, Worden K and Molina F J 2001 Vibration-based damage assessment in steel frames using neural networks *Smart Mater. Struct.* **10** 553–9
[10] Peeters B and Ventura C E 2002 Comparative techniques of modal analysis techniques for bridge dynamics characteristics *Mech. Syst. Signal Process.* **17** 965–88
[11] Maia N M M and Silva J M M 2001 Modal analysis identification techniques *Phil. Trans. R. Soc. Lond.* **359** 29–40
[12] Chang C C, Chang T Y P and Xu Y G 2000 Adaptive neural networks for model updating of structures *Smart Mater. Struct.* **9** 59–68
[13] Bishop C M 1998 *Neural Networks for Pattern Recognition* (Oxford: Oxford University Press)
[14] Bishop C M and Nabney I T 1997 Netlab neural network software http://www.ncrg.aston.ac.uk
[15] MATLAB© 1998 *Users Manual Version 5.2* The Math Works, Inc.
[16] Balmès E 1997 *Structural Dynamics Toolbox* Scientific Software Group
[17] Zapico J L, González M P, Friswell M I, Taylor C A and Crewe A J 2003 Finite element model updating of a small scale bridge *J. Sound Vib.* **268** 993–1012
[18] Mottershead J E, Friswell M I, Ng G H T and Brandon J A 1996 Geometric parameters for finite element model updating of joints and constraints *Mech. Syst. Signal Process.* **10** 171–82

Mechanical Systems and Signal Processing 24 (2010) 2137–2159

Contents lists available at ScienceDirect

Mechanical Systems and Signal Processing

journal homepage: www.elsevier.com/locate/jnlabr/ymssp

A new method for finite element model updating in structural dynamics

J.L. Zapico-Valle [a,*], R. Alonso-Camblor [c], M.P. González-Martínez [b], M. García-Diéguez [c]

[a] Department of Construction and Manufacturing Engineering, University of Oviedo, Campus de Gijón 7.1.16, 33203 Gijón, Spain
[b] Department of Construction and Manufacturing Engineering, University of Oviedo, Campus de Gijón 7.1.24, 33203 Gijón, Spain
[c] Department of Construction and Manufacturing Engineering, University of Oviedo, Campus de Gijón 7.1.BC, 33203 Gijón, Spain

ARTICLE INFO

Article history:
Received 19 June 2009
Received in revised form
12 March 2010
Accepted 17 March 2010
Available online 23 March 2010

Keywords:
Model updating
Finite element model
Structural dynamics
Adaptive sampling
Stochastic method

ABSTRACT

A method is propounded in this paper to update finite element models in the field of structural dynamics. It is especially intended to solve cases for which other methods either cannot be applied or are inefficient. It is posed as the minimization of an error function defined in the time domain. The minimization is carried out by a novel adaptive sampling algorithm, which constitutes the main contribution in this work. In this algorithm, the solution is searched by sampling the parameters to be updated within a bounded space in an iterative form. The Beta distribution, which is consistent with the bounded character of the search space, is chosen for the sampling. The characteristics of the distributions are changed in each step of the process depending on the results of the previous ones. The method has been tested through a simulated dynamic model and an experimental case. In these particular cases, the performance of the proposed adaptive algorithm was better than those of other related stochastic algorithms it was compared with.

1. Introduction

Nowadays finite element (FE) models have become an essential tool in structural dynamics. They serve to reproduce numerically the dynamic behavior of actual structures and mechanical systems. In these models the continuum is divided into finite elements, and the global mechanical properties are obtained by assembling the elemental ones. The values of the physical parameters involved in the modelling are usually taken from previous experiences. In some cases, however, such information is not available or a recalibration is needed in order to improve the accuracy of the model. In certain applications such as damage and mass identification, a similar procedure, which is referred to as FE model updating in literature, is used to find the unknown parameters. Model updating consists in estimating certain parameters of the models on the basis of dynamic tests carried out on the corresponding actual structures. Physical variables are measured at several points of the structures and recorded in the time domain during the tests. These data can be subsequently transformed to the frequency and the modal domains. The parameters are then obtained in such a way that the discrepancies between the experimental data and the predictions of the model are minimized. There exist different criteria to quantify such discrepancies. If the structure of the mathematical model allows the measured variables to be formulated as an explicit function linear in the parameters to be updated, these can be analytically obtained in a least-squares sense as long as there are enough available measurements, as those reported in Ref. [1]. Nevertheless, many applications in structural dynamics lead to implicit or

* Corresponding author. Tel.: +34 985 18 19 28; fax: +34 985 18 20 55
E-mail address: jzapico@uniovi.es (J.L. Zapico-Valle).

0888-3270/$ - see front matter © 2010 Elsevier Ltd. All rights reserved.
doi:10.1016/j.ymssp.2010.03.011

non-linear-in-the-parameters formulations, for which an analytical solution is not available. In these cases, an error function of the parameters that represents the discrepancies between the experimental data and the predictions of the model is defined and minimized with respect to the parameters. For this purpose, a norm of the residuals (differences between the experimental data and the predictions of the model) and different iterative numerical methods are used. The methods normally have global and local phases. In the global phase a set of points in the neighborhood of the minima of the error function are selected by searching within the whole search space. The objective here is to increase the probability of finding a point close to the global minimum in a reduced number of iterations. From these candidate points the nearest minima are accurately found by local searches. The methods can be divided into two main categories: deterministic and stochastic [2].

According to [3], two classes can be also established for the deterministic methods: direct search and gradient-based. Direct search methods are based only on the values of the error function. The grid search is the simplest direct one. Even though it covers only the global phase, it can be very useful in structural dynamics problems to find the order of magnitude of those parameters for which there is not a prior knowledge. The nonlinear simplex methods also belong to the direct search class. They are usually adaptations of the basic Nelder–Mead method [4]. They search iteratively for a minimum from a starting point. They are very effective in the local search as long as the starting point is close to the minimum. Conversely, when it is far away from the minimum these methods tend to be unstable and do not converge to the solution. In some applications it can be advantageous to combine both the grid search and the nonlinear simplex. The former is used in the global phase, and its solution serves as the starting point for the latter in the local phase. An example of this approach can be seen in [5].

Gradient-based methods use the values of the error function and its derivatives. They are extensively used in FE model updating [6–8], the Newton-type ones being the most popular. Even though the computation of the derivatives is costly, these methods are very efficient. They are capable to approximate the solution in a few steps. A starting point is also needed, and problems arise when it is far from the solution. It can affect both the speed and the convergence of the minimization process. The so-called trust region strategy can be used to improve the robustness of these methods [9], but it slows down the process. These methods are very appropriate to cover the local phase.

Stochastic methods are an alternative to solve global optimization nonconvex problems. They search in a given space in a controlled random manner taking advantage of the information acquired in the previous iterations. They try to improve the efficiency of finding the global minimum, since the computational time is prohibitive in the pure random case, without loosening reliability [2]. These methods have been applied to FE model updating cases in the last decade. Levin and Lieven [10] applied the simulated annealing (SA) method and the genetic algorithm (GA) to update simulated and experimental cases. They tried different versions of GA, and developed a variation of the SA, which is called blended SA. They found that the latter has a better performance in several studied cases. The differential evolution algorithm, which is derived from the conventional GA, is applied in Refs. [11,12] to the identification of high nonlinear hysteretic systems. Both SA and GA are very robust methods. They can overcome local minima in high multimodal error functions. On the other hand, they are very slow when comparing with the deterministic methods. Moreover, their precision is limited. They tend to give solutions in the neighborhood of the global minimum. There are some hybrid strategies that combine GA and local search [13,3] in order to improve the results. Emerging algorithms as particle swarm optimization have been incorporated in this field. It is a very simple and robust algorithm. However, the values if its optimum parameters strongly depend on the application, and they have to be calibrated offline. Recently, a novel hybrid strategy that includes an online updating of the parameters has been tried [14].

Hansen and Ostermeier developed the evolution strategy with covariance matrix adaptation [15,16], which is denoted by the acronym CMA-ES in literature. This is a general-purpose stochastic optimization algorithm. Even though it has not been applied to FE model updating problems, it has been tested through many mathematical functions, and compared with other evolution algorithms. In most of the tests it outperforms the other algorithms, especially in the case of high multi-modal and non-separable error functions. Many successful applications to real-world minimization problems have been also reported [16]. For these reasons, it has been selected in this paper as a reference to be compared with in Sections 4 and 5.

The objective of this work is to develop a method intended to cover both the global and the local phases of the FE model updating process. In addition, it should be capable of solving in a robust and efficient manner practical cases for which other methods either cannot be applied or are inefficient. The method will be tested by means of numerically simulated and experimental data. Its performance will be compared with those of other related methods.

The results obtained are now presented in this paper, which is organized as follows. In the next section a detailed explanation of the method is given. It deals with the definition of the error function, the mathematical formulation of the problem, the details of the algorithms of minimization and their coding. Section 3 includes a brief description of CMA-ES algorithm. Finally, in Sections 4 and 5 the performance of the proposed methods is evaluated and compared with that of other methods through numerically simulated and experimental examples.

2. Description of the method

2.1. Definition and properties of the error function

Time-domain physical variables have been selected to formulate the error function. The advantage of this approach is that it can be applied to both the linear and the nonlinear systems. Moreover, it allows the raw signals to be used. Thus, all

the underlying information is preserved and the systematic identification errors are avoided. The normalized mean squared error is adopted as error function

$$\varphi = \frac{1}{N}\sum_{i=1}^{N}\frac{\sum_{j=1}^{M}(\hat{y}_{ij}-y_{ij})^2}{\sum_{j=1}^{M}(y_{ij})^2}, \tag{1}$$

where $\hat{y}_{ij}$, y_{ij} represent respectively the model-predicted output and the measured experimental one. The subscripts i and j are referred to the sensors and the instants of measurement. N is the number of sensors and M is the number of measurements. A weighted version can be established when the measurements have different accuracy. This formulation is much more restrictive than the common one-step-ahead or the model-predicted input ones but it is consistent with the usual application of the models in practice, where the model-predicted output is used. Moreover, the formulation is not linear in the parameters.

It is worthwhile to study the characteristics of the defined error function, so as to adapt the subsequent minimization algorithm to them. A quality of this error function is that their global minimum is ideally zero, which represents a perfect fit between the model and the experiment. In practice it is slightly greater than zero due to the incompleteness of the model and the measurements errors. In our experience we have found that the error surface is high multimodal in the parameters space. Most of the minima, however, correspond to solutions without physical meaning, for example, negative values of the stiffness or the damping coefficients. In addition, the error surface contains flat zones in which there is a very small variation of the function. The deterministic methods are very inefficient overcoming these zones. The plateaux are crossed by narrow interconnected valleys where the function diminishes and reaches its minima. Along them there are also flat zones. An interesting feature of the valleys is that they are roughly parallel to the direction of the axes in the parameters space.

2.2. Algorithm of minimization

2.2.1. General approach

Taking into account the aforementioned properties of the error function, it is profitable to assign an initial value of the parameters as close as possible to the solution, so as to improve the robustness and effectiveness of the minimization process. In practice, some parameters are well known beforehand, and a narrow interval for their values can be established with high confidence. A previous calibration of the parameters, however, is not always available. This is the case of some parameters of the structures such as the stiffness of the connections, boundary conditions, abrupt stiffness drops in the elements due to earthquake damage, etc. In these cases the initial values of the parameter values have to be selected within a broad band, which covers sometimes several orders of magnitude. As was pointed out in the previous section, the deterministic methods are inefficient under these circumstances. Therefore, it was decided to adopt a stochastic strategy to minimize the error function.

As will be shown later on, if an open search is adopted from the initial value of the parameters to find the global minimum, it generally tends either to diverge or to reach a minimum without physical meaning when the initial values of the parameters are far from the solution. Consequently, it is also advantageous to reduce the searching space by taking intervals of the parameters as narrow as possible within the zones with physical meaning, so as to isolate the global minimum and improve the robustness of the minimization process. Broad bands, however, have to be selected for the uncertain parameters. If the FE model does not reproduce adequately the actual structure or if it is over-parameterised or if the experimental data is not informative enough, the error surface is nearly flat in a large zone around global minimum. The measurement noise also can make additional local minima to appear [7]. These circumstances can produce large oscillations of the values of the parameters corresponding to the solution around the expected ones, and broad bands have also to be selected for the search space. A drawback of the parameter broad bands is that they can generate additional improper minima at the bounds of the search space, i.e. those having the first derivative different of zero in some directions. It is visually evident in Fig. 1. After these considerations, in the cases the method is intended for, which include parameters showing high uncertainty, it is advantageous to adopt a bounded search scheme in order to increase the robustness of the minimization process.

Summing up, the proposed FE model updating method can be mathematically expressed in the following form

$$\min\{\varphi(\mathbf{x})\}; \quad \mathbf{x}\in\mathbb{R}^n$$

$$\ell_i \le x_i \le u_i; \quad i=1,\ldots,n. \tag{2}$$

in which $\varphi(\mathbf{x})$ represents the error function defined in the Eq. (1), $\mathbf{x}$ is the vector of the parameters to be updated, ℓ_i and u_i denote respectively the lower and upper bounds selected for each parameter.

A feature of the stochastic methods is that their performance is strongly case dependent. There is no guarantee that an algorithm able to solve a given problem will be effective for another one. Hence, an effort has been made in this paper to adapt minimization algorithm to the characteristics of the established problem instead of using a general-purpose algorithm. Thus, the solution is sought by random sampling within the search space in an iterative form. Taking into account the bounded condition of the adopted search space (2), the Beta distribution, which is also defined within a

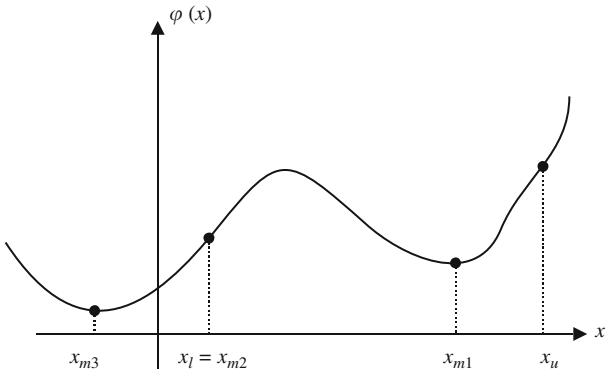

Fig. 1. Unidimensional representation of the error function $\varphi(x)$. x_u=upper bound. x_ℓ = lower bound. $x_{m\,1}$= physical meaning minimum. $x_{m\,2}$= improper minimum. $x_{m\,3}$=non physical meaning minimum.

bounded interval, has been considered suitable for this case. The parameters of the sampling distributions are changed on the basis of the previous results in every step. The algorithm evolves gradually from a global sampling within the complete bounded space to a narrow local one around a minimum of the error function. The process is stopped when a given criteria is reached. Two different algorithms have been tried. They correspond to isotropic and anisotropic variances of the sampling distributions, and they will be referred to as isotropic Beta (IB) and anisotropic Beta (AB) in the remaining of the paper. Next subsections include a detailed description of the Beta distribution and the procedures of minimization.

2.2.2. Properties of the beta distribution

The Beta distribution is continuous and defined on the interval [0,1]. Its shape depends on two non-negative parameters, which will be referred to as a, b in the remaining of the paper. The probability density function is [17]

$$f(\xi;a,b)=\frac{\xi^{a-1}(1-\xi)^{b-1}}{B(a,b)};\quad 0\le\xi\le 1. \tag{3}$$

The function B is a normalization factor that makes the total probability integrals to unit.

$$B(a,b)=\int_0^1 \xi^{a-1}(1-\xi)^{b-1}\,d\xi. \tag{4}$$

When $a>1$ and $b>1$, the distribution is unimodal and its mode as a function of the parameters is

$$mode(\xi;a,b)=\frac{a-1}{a+b-2}, \tag{5}$$

and its variance is

$$var(\xi;a,b)=\frac{ab}{(a+b)^2(a+b+1)}. \tag{6}$$

If a=b=1, the Beta distribution becomes the uniform distribution, and its variance is

$$var(\xi;1,1)=\tfrac{1}{12}. \tag{7}$$

2.2.3. Isotropic algorithm

In general, the bounds of the model parameters defined in (2) are different from those of the Beta distribution [0,1]. To overcome this, the parameters are modified by means of the following linear transformation

$$x_i=\ell_i+(u_i-\ell_i)\xi_i, \tag{8}$$

in which ξ_i is the transformed parameter.

The procedure commences with a pure random search to each variable. This is achieved by setting the two parameters of the Beta distribution equal to one, as explained in the previous section. Then, an independent set of transformed parameters is obtained at random, following the established distribution for each parameter. Afterwards, the actual values of the parameters are calculated through the transformation (8), and from these the corresponding value of the error function $\varphi(\mathbf{x})$ is evaluated.

In the subsequent steps the parameters of the sampling distribution are manipulated according to the results of the previous steps. A step is said to be successful when the value of the corresponding error function is lower than all the previous ones. If this is not the case, the step is considered unsuccessful. The first step is assumed to be successful. Thus, if a step (g) is successful, its transformed parameters are adopted as the modes of the distributions for the next one (g+1).

Otherwise, the modes are maintained.

$$mode(\xi_i^{(g+1)}) = \xi_i^{(g)} \Leftrightarrow g \equiv successful$$

$$mode(\xi_i^{(g+1)}) = mode(\xi_i^{(g)}) \Leftrightarrow g \equiv unsuccessful. \tag{9}$$

The formulation proposed by Kern et al. in Ref. [18] is adopted for the variance of the distributions

$$\sigma^{(g+1)} = \sigma^{(g)}\alpha \Leftrightarrow g \equiv successful$$

$$\sigma^{(g+1)} = \sigma^{(g)}\alpha^{-1/4} \Leftrightarrow g \equiv unsuccessful$$

$$var(\xi_i^{(g+1)}) = (\sigma^{(g+1)})^2, \tag{10}$$

with $\sigma < \sqrt{1/12}$ and $\alpha = 2^{1/n}$, in which n is the dimension of the parameters space. This constitutes a simple implementation that has a good performance on the sphere function independently of the value of n.

Identifying Eqs. (5) and (9), and (6) and (10), the following system of equations is obtained

$$\left\{ \begin{array}{l} \dfrac{a_i - 1}{a_i + b_i - 2} = mode(\xi_i^{(g+1)}) \\ \dfrac{a_i b_i}{(a_i + b_i)^2 (a_i + b_i + 1)} = var(\xi^{(g+1)}) \end{array} \right\}, \tag{11}$$

which allows the new two parameters of the sampling distributions (a_i, b_i) to be computed. As the system (11) is not linear in the parameters, the Newton–Raphson method is used to compute the value of the parameters.

The process continues until a given stopping threshold of the error function φ_s is reached, $\varphi < \varphi_s$. This criterion is valid for simulated cases, for which the minimum of the error function is zero. When dealing with experimental cases, the minimum is greater than zero and its value is not known beforehand. Therefore, this criterion is not applicable. Alternate criteria may be the standard deviation of the distributions $\sigma < \sigma_s$, or the difference of the error function between two successive successful steps $\Delta\varphi < \varphi_s$. In order to avoid the process to be running indefinitely when it is trapped into a local minimum, it is also stopped when the number of steps is greater than a given limit N_s.

The following sketch summarizes the algorithm:

- Step 1: Set a_i=b_i=1, $\varphi_m = \infty$ and N=0.
- Step 2: Set N=N+1. Generate a random set of transformed parameters ξ_i from the beta distribution (3). Compute the parameters x_i by Eq. (8) and the error function φ.
- Step 3: If $\varphi < \varphi_m$, then $\varphi_m = \varphi$, mode $(\xi_i) = \xi_i$, $\sigma = \sigma\alpha$; otherwise, $\sigma = \sigma\alpha^{-1/4}$.
- Step 4: Compute $var(\xi_i)$ by (10) and update a_i and b_i solving the system (11).
- Step 5: If $\varphi < \varphi_s$ or $\sigma < \sigma_s$ or $\Delta\varphi < \varphi_s$ or $N < N_s$, stop; otherwise, go to step 2.

The algorithm was coded in MATLAB [19], the random sampling being carried out thanks to the Statistics Toolbox.

2.2.4. Anisotropic algorithm

This approach is basically similar to the previous one, but adopting a variable sampling distribution to speed up the minimization process. This is especially important in the progress along the valleys of the error function. There are two possibilities to adapt the sampling distribution to the topography of the error function in a given point. First, to use a different variance for each parameter. Second, to rotate the principal axes of the sampling distribution in the parameters space. As pointed out in Section 2.1, generally, the valleys of the objective function (1) are roughly parallel to the direction of the axes in the parameters space. Under these circumstances, the second option is pointless, and consequently, it is rejected. Only the first option is considered. Thus, the strategy adopted here consists in weighting the variance of the sampling distribution of each parameter accordingly to its evolution in the last n successful steps, n being the dimension of the search space.

For this purpose, the increments of the transformed parameters in the last n successful steps are recorded

$$\Delta\xi_i^{(j)} = \xi_i^{(h)} - mode(\xi_i^{(h)}) \Leftrightarrow h \equiv successful, \tag{12}$$

and used to compute their dynamic variances

$$v_i^{(g+1)} = \frac{1}{n}\sum_{j=1}^{n} (\Delta\xi_i^{(j)})^2. \tag{13}$$

The weights are taken proportional to them and transformed with respect to the maximum component

$$w_i^{(g+1)} = \frac{v_i^{(g+1)}}{\max(v_i^{(g+1)})}. \tag{14}$$

Finally, the variance of the distributions is computed as follows

$$var(\xi_i^{(g+1)}) = w_i^{(g+1)}(\sigma_i^{(g+1)})^2. \tag{15}$$

The increments of the transformed parameters are initially set equal to one. The corresponding pseudo-code is given below.

- Step 1: Set a_i=b_i=1, $\Delta\xi_i^{(j)} = 1$, $\varphi_m = \infty$, N=0.
- Step 2: Set N=N+1. Generate a random set of transformed parameters ξ_i from the beta distribution (3). Compute the parameters x_i by Eq. (8) and the error function φ.
- Step 3: If $\varphi < \varphi_m$, then $\varphi_m = \varphi$, mode $(\xi_i) = \xi_i$, $\sigma = \sigma\alpha$; compute $\Delta\xi_i$ (12), v_i (13) and w_i (14); otherwise, $(\sigma = \sigma\alpha^{-1/4})$.
- Step 4: Compute $var(\xi_i)$ by (15) and update a_i and b_i solving the system (11).
- Step 5: If $\varphi < \varphi_s$ or $\sigma < \sigma_s$ or $\Delta\varphi < \varphi_s$ or $N < N_s$, stop; otherwise, go to step 2.

3. The evolution strategy with covariance matrix adaptation

CMA-ES is a more complete and sophisticated algorithm than those proposed herein, because it is intended as a general-purpose stochastic optimization algorithm. It generates, by mutation, successive populations. Each population represents a set of λ individuals, which correspond to points in the search space. The mutation consists in generating a set of offsprings by sampling from a Gaussian distribution

$$\mathbf{x}_k^{(g+1)} \sim N(\langle \mathbf{x} \rangle_\mu^{(g)}, (\sigma^{(g)})^2 \mathbf{C}^{(g)}). \tag{16}$$

The mean of this distribution is a recombination of the μ best individuals of the previous generation, so-called parents, with $\mu < \lambda$. The principal components of the distribution can have different variances, as those proposed in this paper, and they can be oriented to any direction in the search space. The distribution is dynamically adapted to the shape of the error function, so as to improve the efficiency of the process. For this purpose, the evolution of the previous generations is considered.

The matrix $\mathbf{C}^{(g+1)}$ is adapted by the so-called evolution path and the μ difference values between the recent parents and the mean value of the previous ones. The adaptation of the global step size $\sigma^{(g+1)}$ is based on a different conjugated evolution path, which is obtained by principal component analysis of the previous matrix $\mathbf{C}^{(g)}$.

A Matlab implementation of this algorithm, which is freely offered by the authors in Ref. [20], is used in this paper. A more detailed description of the algorithm can be found in Refs. [15,16].

The efficiency and robustness of both the IB and the AB algorithms was tested through two cases. The first one corresponds to a numerical simulation of a dynamic system, and the second one deals with an experimental dynamic test on a small-scale bridge. The results are compared with those of the CMA-ES. Both benchmarks are outlined in the next sections.

4. Dynamic system identification

In this case the modal properties and initial conditions of a linear viscous dynamic system are updated on the basis of a numerically simulated free vibration. For such a system, the displacements corresponding to a given co-ordinate can be formulated as follows

$$y = A_1 e^{-\zeta_1 w_1 t}\sin(w_1\sqrt{1-\zeta_1^2}t+\theta_1) + A_2 e^{-\zeta_2 w_2 t}\sin(w_2\sqrt{1-\zeta_2^2}t+\theta_2), \tag{17}$$

in which w and ζ represent the natural frequency and the damping ratio, A and θ denote the initial amplitude and the phase, respectively, and t is the time. The subscripts 1 and 2 refer to the first and the second modes of vibration of the system. This model, therefore, contains eight different parameters to be updated. The target values of the parameters are shown in Table 1. Even though the system is linear, the formulation of the response (17) is not linear in the parameters. Consequently, it does not allow a direct analytical updating. The iterative updating is based on discrete values of the response picked at regular periods of 0.01 s in the interval from 0 to 5 s at a single coordinate. The error function is computed accordingly to Eq. (1), in which y_j denotes the j discrete value of the target response, and $\hat{y}_j$ is the corresponding approximate one.

An interval between 0 and 1 has been selected for the damping ratios, which corresponds to the physical limits of these parameters. In the same sense, the phases have been bounded between $-\pi$ and π. The bounds for the rest of the variables in the updating process are shown in the Table 1. The stopping thresholds adopted in this case were $\varphi_s = 10^{-10}$ and N_s=50,000.

With regard to the CMA-ES algorithm, in the initial distribution the mean was uniformly sampled from the selected intervals and the standard deviation of each parameter equalled to half of the corresponding interval size. In order to make this algorithm to be comparable with the proposed ones, in each generation the sampling was repeated until all the sampled parameters were within the adopted intervals. This means that a truncated Gaussian distribution was used for the sampling instead of the complete one. The effect of the population size was preliminary studied for $\lambda = 2$, 5, 10 and 20. It

Table 1
Parameters of the dynamic model.

Parameter	w_1	ζ_1	A_1	φ_1	w_2	ζ_2	A_2	φ_2
Upper bound	5	1	10	π	20	1	10	π
Target	4	0.1	5	-2	12	0.15	2	1.5
Lower bound	0.1	0	1	$-\pi$	5	0	1	$-\pi$

Table 2
Results of the dynamic model.

Algorithm	No function evaluations			Success ratio
	Minimum	Average	Maximum	
IB	8914	20,001	45,914	90
AB	1323	2473	7823	91
CMA-ES	1821	2993	6681	89

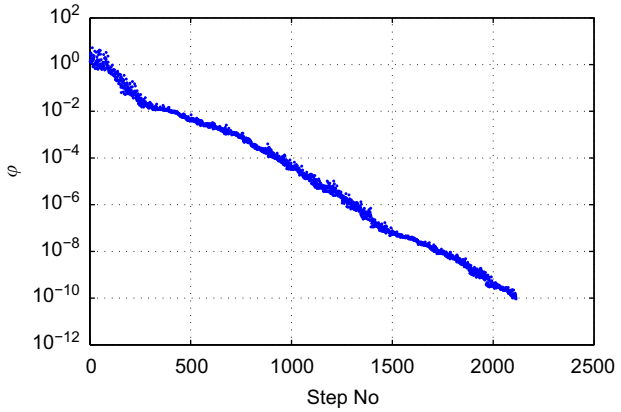

Fig. 2. Evolution of the error function of the dynamic model.

was found that the higher the population size, the higher the success ratio and the number of required error function evaluations. Eventually, a population size $\lambda = 5$ was adopted, which is a trade-off between robustness and efficiency. The default settings were selected for the rest of strategy parameters of the algorithm.

Each algorithm was run 100 times. Results are shown in Table 2. All the algorithms have a success ratio around 90%. This means that they have similar behavior from a robustness point of view. In all the unsuccessful runs, the algorithms were trapped into improper local minima. As concerns the efficiency, there are significant differences between the algorithms. The best results correspond to the AB algorithm. In average, it requires 2473 evaluations of the error function to reach the stopping threshold. The CMA-ES performs slightly worse. It needs 2993 evaluations of the error function. The worst results were those of the IB algorithm. The required number of evaluations of the error function (20,001) is almost one order of magnitude greater than those of the other algorithms.

Figs. 2–4 show respectively the evolution of the error function during a run, the corresponding parameters a and b of the Beta distribution and the parameters of the dynamic model. The time-history response of the simulated model is depicted along with the prediction of the updated model in Fig. 5. As can be seen, they are almost coincident.

5. Finite element model updating of a small-scale bridge

5.1. Experimental model and testing

The corresponding prototype of the experimental model was a typical multi-span continuous-deck motorway bridge with four identical spans and irregular distribution of the piers. From this, an experimental model was designed, manufactured and tested dynamically on a shaking table. A geometric scale 1:50 was adapted in the design, so as not to exceed the capability of the shaking table.

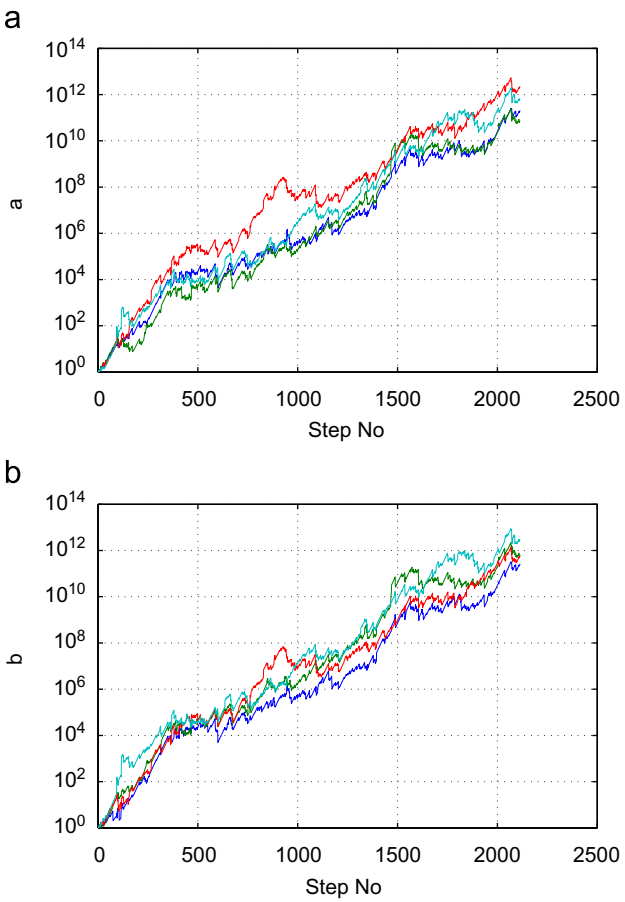

Fig. 3. (a) Evolution of the parameter a of the Beta distribution of the dynamic model. (b) Evolution of the parameter b of the Beta distribution of the dynamic model.

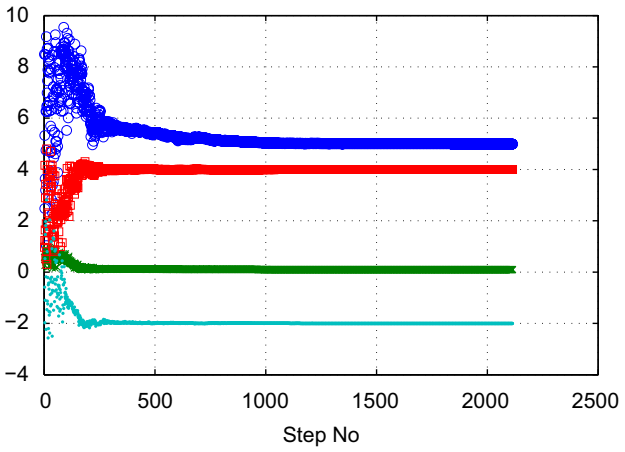

Fig. 4. Evolution of the parameters of the dynamic model. Legend: □ ω_1, ◦ A_1, ∗ ζ_1 and • φ_1.

The model deck was designed with a continuous square hollow section. Additional masses where uniformly bolted along the deck in order to attain mass similarity. Articulated parallelograms were attached to the deck at the piers locations, so as to transmit the weight of the additional masses and to constrain the deck to translate only in the horizontal direction. The deck ends hinged on the abutments that were bolted to the support (see Fig. 6). The piers were designed

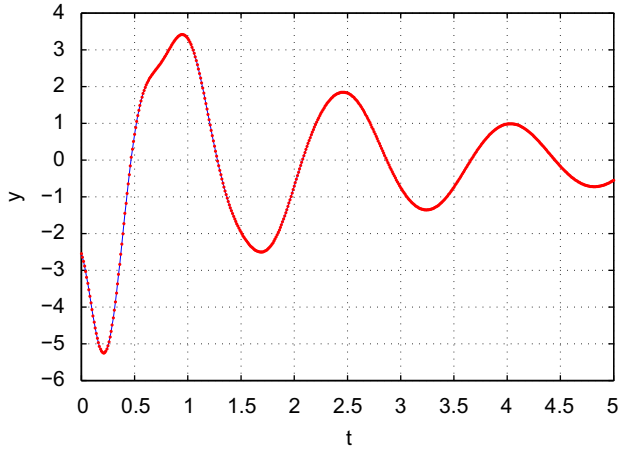

Fig. 5. Time-history response of the dynamic model. Line: simulated experiment. Dots: prediction of the updated model.

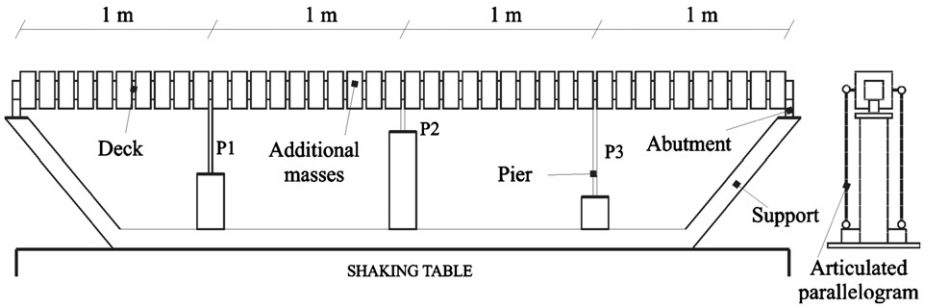

Fig. 6. Elevation of the experimental model.

with and I-beam section at the bottom, and a rectangular section for the remainder. They were bolted to the abutments at the bottom and connected through keys to the deck at the top.

An initial modal test followed by several seismic tests was carried out. In all these tests, the model was shaken in the horizontal transverse direction. In the seismic tests the experimental model was excited by a series of similar earthquakes with 0.5, 0.8, 1.0, 1.2 and 2.0 times the design intensity. The reference earthquake was an artificial one fitting Eurocode eight elastic response spectrum for medium soil conditions. Only the results of the first earthquake, in which an elastic response of the model is expected, are used in this paper. The absolute acceleration of the deck at the connections to the piers and the absolute acceleration of the table were measured by means of linear accelerometers during the test. More details of the experimental model and testing can be found in [5]. The analogue signals were converted into digital ones at a sampling frequency of 1035 Hz. As the signals contain offsets variable in the time, it was decided to use a high-pass filter to remove the offsets. It was a four order Butterworth filter with a cut-off frequency of 5 Hz. In order to avoid further divergence problems in the numerical integration, each time interval was divided into ten uniform subintervals and the corresponding filtered signals were linearly interpolated.

The objective in this case is to develop a FE model capable to reproduce accurately the seismic response of the bridge. Therefore, the modelling should include the physical aspects having relevant influence in the response, and the further updating should minimize the discrepancies between the measured response and the predictions of the model.

5.2. Linear viscous approach

5.2.1. FE model

The deck of the bridge has been divided into four finite elements, which are connected in series to five nodes. The nodes represent geometrically the locations of the abutments and connections to the piers. The degrees of freedom considered in these nodes where the horizontal transversal translation and the rotation around the vertical axis of the deck, as is depicted in Fig. 7.

The finite elements have been modelled as Timoshenko beams, i.e., considering both bending and shear deformations in the formulation of the corresponding elemental stiffness matrix. A consistent-mass matrix was obtained for the beams assuming cubic displacement shape functions, and considering both translational mass and moment of inertia. In this

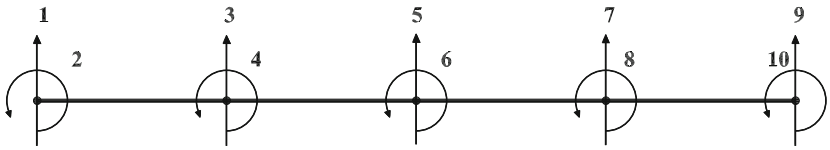

Fig. 7. Degrees of freedom of the FE model.

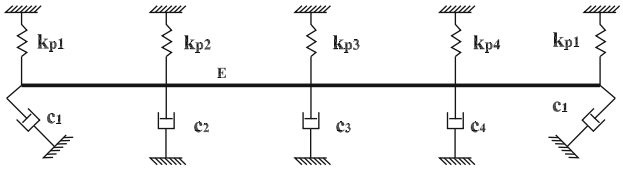

Fig. 8. Sketch of the viscous FE model.

formulation, the deck itself was assumed to have uniform mass distribution, while the additional masses were considered as lumped ones. A similar scheme was established in the formulation of the equivalent seismic force vector. The piers and the abutments were modelled as linear elastic springs. The corresponding stiffness accounts for both the element and the connection stiffnesses. The dynamic dissipative forces are mainly localized at the connections of the deck to the abutments, the connections of the piers to the deck and the abutments and the articulated parallelograms. Moreover, it is known from previous studies [5] that the rotational dissipative forces at the hinges of the abutments have a significant effect in the dynamic response of the bridge. Accordingly to this, the dissipative forces were modelled by means of linear viscous dampers lumped to the nodes of the model (see Fig. 8).

The global properties of the model are obtained by assembling the elemental ones. From this, the equation of movement of the system can be established

$$\mathbf{M}\ddot{\mathbf{y}}(t)+\mathbf{C}\dot{\mathbf{y}}(t)+\mathbf{K}\mathbf{y}(t)=\mathbf{f}_s a_g(t), \tag{18}$$

where $\mathbf{M}$, $\mathbf{C}$ and $\mathbf{K}$ represent respectively the mass, damping and stiffness matrices, $\ddot{\mathbf{y}},\dot{\mathbf{y}},\mathbf{y}$ are the acceleration, velocity and displacement vectors relative to the table, $\mathbf{f}_s$ denotes the unitary nodal seismic forces and $a_g(t)$ is the table acceleration.

5.2.2. Parameter selection and updating

It is assumed that all the finite elements of the deck have the same mechanical properties and they are uniformly distributed. The geometrical properties of the cross-section of the deck are set equal to their nominal values. The Young's modulus E, however, is considered as a global parameter to be estimated. Both abutments are assumed to have the same stiffness and damping parameters. As the piers have different lengths and cross-sections, independent parameters are considered and estimated for each.

If the mass of the model is considered in the identification process, too, it becomes undetermined for the proposed linear model. This is due to the fact that the excitation is induced by the table motion. Under this condition, the equivalent seismic forces are proportional to the mass of the model. Hence, if the mass, stiffness and damping are varied by the same ratio, the response of the model does not vary in a linear model. To circumvent this problem, the mass was not considered as an unknown parameter, but fixed to the value corresponding to the nominal geometry of the elements and the nominal density of the structural steel ($\delta = 7850\,\mathrm{kg/m^3}$). Thus the model contains nine unknown parameters, which are shown in Fig. 8. Once the structure and the parameters of the model have been established, the parameters are estimated from the measured data. The procedure used to do this will be outlined in the following paragraphs.

The available experimental data are the shaking table time-history acceleration and the absolute acceleration of the deck at the nodes corresponding to the connections to the piers, which correspond to the degrees of freedom 3, 5 and 7 (see Fig. 7). The table acceleration is selected as model input and the displacements of the deck relative to the table, as model-predicted output. The model output is obtained by numerical integration of the Eq. (18) using the central differences method.

The experimental relative displacements are obtained from the measured accelerations by numerical integration through the trapezoidal rule. This operation has the advantage of smoothing the data because it acts as a high frequency filter [3,21]. On the other hand, it gives rise to two unknown constants for each measured variable, which are considered as additional parameters in the minimization process and they will be referred to as experimental parameters in the remainder of the paper. It should be pointed out that the experimental relative displacements are a linear function of these experimental parameters.

A hybrid strategy has been selected to search for the solution. The proposed iterative algorithms are in turn applied to minimize the error function and to obtain the corresponding parameters. In each step of these algorithms, the experimental parameters are calculated through the least squares method since the experimental displacements are a linear function of them.

The error function was built on the basis of the displacements at the degrees of freedom 3, 5 and 7 (see Fig. 7). In each, 47,680 time steps were considered with a period of 96.60 μs.

5.2.3. Results and discussion

In this case only the AB and CMA-ES algorithms are used and compared. Even though the values of some parameters of the model are well known and a narrow confidence interval is expected, a broad band is deliberately selected for all the parameters to study the performance and the solutions given by both algorithms under these conditions. The lower bound is set to zero for all the parameters. The upper bound of the stiffnesses is limited, so as to prevent instability of the numerical integration of the equation of movement. In the damping coefficients, which are the more undefined parameters, the upper bound is set equal to 1000 and 10,000. These bands cover up to 11 orders of magnitude of the parameters.

A different stopping threshold was added to the AB algorithm in this case. The difference of the error function between two successive successful steps, which was set $\Delta\varphi = 10^{-8}$. In the CMA-ES algorithm, it was used the same truncated Gaussian distribution and strategy parameters of the previous case. Another stopping criterion is adopted for this algorithm. Namely, the range of the error function between two successive populations, which is limited to $\Delta\varphi = 10^{-7}$.

Results of 10 successful runs are shown in Table 3 and 4. As can be seen, the final error is around 9.6%, and the obtained values of the parameters are similar in both algorithms. It was found that the final error does not diminish significantly after additional steps.

In order to know the behavior of the algorithm in an open search, the CMA-ES was run again 20 times. In this case the parameters were not bounded, the previous bounds being used only for initialisation purposes. Results were conclusive. The process converged to minima without physical meaning in ten runs, and it diverged in the rest. Therefore, it demonstrates the need of bounding the parameters in the minimization process when a broad initialisation band is used.

Based on those initial results, a common stopping criterion is established and a new set of comparable results is obtained from both algorithms. Thus, the stopping thresholds are set $\varphi_s = 9.7\%$, N_s=10,000 for the CMA-ES and N_s=5000 for the AB. In addition, the parameter bounds are reduced to a most narrow band. Each algorithm was run 25 times under these conditions. Results are shown in Table 5 and 6, the unsuccessful ones being highlighted. As in the previous set, the obtained values of the parameters are similar in both algorithms. As concerns to the success ratios, they are very close, 19/25 and 20/25. As can be seen, all the unsuccessful results correspond to improper minima. Nevertheless, the performance of the AB algorithm is much better than the CMA-ES; it is around 5 times faster.

Even though all the success results have similar final error, there are significant variations in the values of the parameters from a run to other. Rather different combinations of the parameters lead to similar responses. The origin of these results can be in either the FE model or the data. This is the case of inadequate or overparameterized models, or non informative enough data [7].

Figs. 9–12 show respectively the evolution of the error function during a run, the corresponding parameters *a* and *b* of the Beta distribution and parameters *kp* and *c* of the FE model. The time-history response of the experimental model is depicted along with the prediction of the updated model in Fig. 13.

Table 3
Results of the viscous model with the CEMA-ES algorithm and broad band.

Case	No[a]	NMSE (%)	$\frac{E}{10^{11}}$	$\frac{k_{p1}}{10^8}$	$\frac{k_{p2}}{10^5}$	$\frac{k_{p3}}{10^6}$	$\frac{k_{p4}}{10^5}$	c_1	$\frac{c_2}{10^2}$	$\frac{c_3}{10^3}$	c_4
1	16116	9.66	2.28	2.39	3.41	1.45	1.15	0.31	3.52	2.01	0.035
2	9471	9.66	1.30	2.80	5.34	1.15	3.05	8.65	3.42	1.89	0.001
3	14046	9.67	2.59	1.52	2.83	1.54	0.57	0.04	3.52	2.01	0.003
4	5961	9.65	1.40	1.24	5.18	1.17	2.89	7.27	3.45	1.93	0.008
5	12526	9.68	1.25	3.39	5.54	1.13	3.16	9.63	3.42	1.88	0.004
6	9091	9.59	1.54	2.14	4.81	1.23	2.57	3.27	3.47	1.98	0.054
7	11421	9.60	1.69	0.54	4.58	1.27	2.30	2.56	3.47	1.99	0.069
8	15666	9.66	1.29	1.46	5.36	1.15	3.08	8.54	3.42	1.90	0.013
9	19001	9.66	2.09	2.26	3.79	1.39	1.53	1.11	3.53	2.00	0.530
10	13496	9.66	2.29	3.99	3.40	1.45	1.15	0.10	3.53	2.31	$1e^{-4}$
min	**5961**	**9.59**	**1.25**	**0.54**	**2.83**	**1.13**	**0.57**	**0.04**	**3.42**	**1.88**	$\mathbf{1}e^{-4}$
max	**19001**	**9.68**	**2.59**	**3.99**	**5.54**	**1.54**	**3.16**	**9.63**	**3.53**	**2.31**	**0.530**
Lower bound			0	0	0	0	0	0	0	0	0
Upper bound			3	5	10	10	10	1000	10	10	1000

[a] No function evaluations.

Table 4
Results of the viscous model with the AB algorithm and broad band.

Case	No[a]	NMSE (%)	$\frac{E}{10^{11}}$	$\frac{k_{p1}}{10^8}$	$\frac{k_{p2}}{10^5}$	$\frac{k_{p3}}{10^6}$	$\frac{k_{p4}}{10^5}$	c_1	$\frac{c_2}{10^2}$	$\frac{c_3}{10^3}$	c_4
1	2020	9.59	1.63	2.94	4.68	1.25	2.41	2.51	3.47	1.99	0.101
2	2349	9.95	1.06	4.69	5.81	1.08	3.52	18.81	3.36	1.73	0.434
3	1252	9.60	1.73	1.24	4.49	1.28	2.22	1.65	3.50	2.00	0.643
4	1366	9.82	1.12	3.25	5.70	1.10	3.40	14.77	3.41	1.77	1.272
5	777	9.62	1.85	2.80	4.26	1.32	1.99	4.08	3.41	1.97	0.641
6	1392	9.61	1.81	3.23	4.34	1.31	2.07	1.16	3.52	1.98	5.827
7	1091	9.65	2.25	3.87	3.48	1.44	1.22	0.59	3.52	2.01	0.018
8	801	9.80	1.67	2.12	4.63	1.26	2.34	0.23	4.06	1.54	99.544
9	1263	9.68	2.67	3.14	2.53	1.59	0.57	4.16	3.49	1.95	0.027
10	1138	9.61	1.51	2.22	4.92	1.22	2.65	0.01	3.82	1.87	20.107
min	**777**	**9.59**	**1.06**	**1.24**	**2.53**	**1.08**	**0.27**	**0.01**	**3.36**	**1.54**	0.018
max	**2349**	**9.95**	**2.76**	**4.69**	**5.81**	**1.59**	**3.52**	**18.81**	**4.06**	**2.01**	**99.544**
Lower bound			0	0	0	0	0	0	0	0	0
Upper bound			3	5	10	10	10	1000	10	10	1000

[a] No function evaluations.

Table 5
Results of the viscous model with the CEMA-ES algorithm and narrow band.

Case	No[a]	NMSE (%)	$\frac{E}{10^{11}}$	$\frac{k_{p1}}{10^8}$	$\frac{k_{p2}}{10^5}$	$\frac{k_{p3}}{10^6}$	$\frac{k_{p4}}{10^5}$	c_1	$\frac{c_2}{10^2}$	$\frac{c_3}{10^3}$	c_4
1	3291	9.69	1.34	2.02	5.19	1.18	2.91	2.21	3.44	1.97	5.35
2	2386	9.67	1.97	2.14	4.02	1.36	1.75	1.99	3.30	2.05	0.44
3	2791	9.70	2.37	4.08	3.26	1.46	1.01	1.96	3.50	2.02	7.37
4	**10001**	**111.53**	**3.00**	**4.85**	**9.99**	**9.99**	**9.99**	**9.96**	**9.82**	**9.93**	**6.59**
5	2251	9.67	1.34	0.12	5.28	1.16	3.01	6.36	3.52	1.86	9.24
6	**10001**	**111.5**	**3.00**	3.30	**9.99**	**9.96**	**9.99**	**9.95**	**9.99**	**9.96**	**9.89**
7	4126	9.70	2.01	1.03	3.95	1.37	1.68	2.29	3.28	2.08	7.13
8	**10001**	**111.6**	**2.99**	2.48	**9.98**	**9.96**	**9.99**	**9.91**	**9.95**	**9.77**	6.46
9	5491	9.68	2.01	4.42	3.95	1.36	1.69	2.76	3.40	2.00	6.36
10	6151	9.69	1.24	3.49	5.44	1.13	3.16	4.85	3.49	1.90	7.83
11	**10001**	9.86	1.10	3.94	5.73	1.09	3.44	9.44	3.51	1.82	2.55
12	1466	9.64	1.64	1.66	4.68	1.23	2.41	9.29	3.49	1.81	1.50
13	6091	9.68	2.36	4.14	3.26	1.48	1.01	2.83	3.50	2.01	2.58
14	3161	9.70	2.05	3.10	3.84	1.38	1.59	0.16	3.36	2.00	4.19
15	**10001**	**111.6**	**2.99**	3.24	**9.99**	**9.95**	**9.98**	**9.69**	**9.81**	**9.88**	8.98
16	**10001**	**111.6**	**2.99**	3.28	**9.99**	**9.98**	**9.98**	**9.86**	**9.77**	**9.99**	9.26
17	4096	9.66	1.85	2.74	4.28	1.31	1.98	4.46	3.48	1.98	4.63
18	2691	9.70	1.79	2.55	4.32	1.33	2.06	3.15	3.41	2.10	7.22
19	4286	9.69	1.25	1.91	5.41	1.14	3.14	6.48	3.49	1.92	4.29
20	2776	9.69	1.31	1.72	5.32	1.16	3.01	9.19	3.53	1.92	4.72
21	7921	9.67	1.81	0.75	4.32	1.30	2.07	6.88	3.06	2.03	2.94
22	2546	9.69	1.36	2.37	5.25	1.15	2.95	6.02	3.46	1.93	6.17
23	**9911**	**62.57**	2.24	3.64	3.91	1.26	4.04	**9.99**	**0.00**	5.75	**9.99**
24	3086	9.68	1.86	0.97	4.27	1.30	1.98	5.61	3.32	1.90	6.38
25	3501	9.67	1.40	4.37	5.15	1.17	2.86	8.46	3.10	1.95	8.88
min	**1466**	**9.64**	**1.10**	**0.12**	**3.26**	**1.09**	**1.01**	**0.16**	**3.05**	**1.81**	**0.44**
max	**7921**	**9.70**	**2.37**	**4.41**	**5.73**	**1.48**	**4.04**	**9.44**	**3.52**	**2.10**	**9.24**
Lower bound			1	0.1	1	1	1	0	0	1	0
Upper bound			3	5	10	10	10	10	10	10	10

[a] No function evaluations.

As has been commented in Section 5.1, Ref. [5] contains a previous author's work on the same experimental model. In this case a different undamped linear FE model was used, which will be referred to as undamped model hereafter. This model was sequentially updated through different configurations on the basis of its first four natural frequencies. The

Table 6
Results of the viscous model with the AB algorithm and narrow band.

Case	No[a]	NMSE (%)	$\frac{E}{10^{11}}$	$\frac{k_{p1}}{10^8}$	$\frac{k_{p2}}{10^5}$	$\frac{k_{p3}}{10^6}$	$\frac{k_{p4}}{10^5}$	c_1	$\frac{c_2}{10^2}$	$\frac{c_3}{10^3}$	c_4
1	481	9.70	1.75	2.24	4.42	1.32	2.17	7.77	3.70	1.87	7.92
2	805	9.70	1.71	3.36	4.51	1.28	2.25	0.77	2.97	2.20	6.17
3	788	9.70	1.63	4.42	4.64	1.29	2.38	4.16	3.39	2.03	4.21
4	426	9.69	1.54	2.63	4.83	1.23	2.59	7.33	3.39	2.01	9.44
5	**3445**	**73.44**	**3.00**	**5.00**	4.05	1.00	**10.00**	**10.00**	4.03	5.17	**10.00**
6	**5001**	**58.60**	1.59	4.33	4.52	1.26	4.85	0.01	**0.00**	5.42	**9.99**
7	547	9.70	1.74	3.77	4.41	1.31	2.18	5.18	3.39	2.01	4.00
8	399	9.69	2.07	3.46	3.85	1.39	1.58	7.09	3.27	1.98	7.32
9	628	9.70	2.22	3.75	3.55	1.44	1.29	7.73	3.76	1.87	4.24
10	316	9.68	1.40	2.98	5.12	1.20	2.84	7.68	3.67	1.88	3.84
11	855	9.69	1.31	1.06	5.31	1.17	3.03	7.59	3.44	1.86	7.55
12	**2914**	**111.4**	**3.00**	**5.00**	**10.00**	**10.00**	**10.00**	**10.00**	**10.00**	**10.00**	**10.00**
13	403	9.69	2.11	3.59	3.75	1.41	1.50	0.93	3.28	1.98	5.98
14	501	9.69	2.17	3.49	3.66	1.41	1.40	4.24	3.25	2.07	6.27
15	1458	9.70	1.69	1.86	4.53	1.30	2.28	4.20	3.56	2.00	3.46
16	502	9.70	2.35	3.67	3.30	1.47	1.04	4.99	3.18	1.98	7.75
17	454	9.69	1.83	3.02	4.25	1.33	2.01	2.21	3.50	2.11	4.58
18	624	9.70	1.44	2.64	5.08	1.18	2.80	6.28	3.87	1.72	5.48
19	455	9.70	1.55	3.55	4.79	1.26	2.53	0.62	3.13	2.16	1.73
20	**5001**	**58.45**	1.90	2.52	3.93	1.36	4.26	**0.00**	**0.00**	5.53	**10.00**
21	**2779**	**58.41**	2.26	**5.00**	3.23	1.48	3.55	**0.00**	**0.00**	5.58	**10.00**
22	417	9.67	1.82	2.96	4.32	1.30	2.06	5.08	3.04	2.11	1.04
23	446	9.70	1.98	3.87	3.99	1.37	1.73	7.46	3.34	1.97	5.80
24	440	9.70	2.10	2.55	3.76	1.40	1.51	5.03	3.26	1.98	6.00
25	764	9.70	1.36	3.57	5.21	1.18	2.93	6.37	3.83	1.72	5.63
min	**316**	**9.67**	**1.31**	**1.06**	**3.30**	**1.17**	**1.04**	**0.62**	**2.97**	**1.72**	**1.04**
max	**1458**	**9.70**	**2.35**	**4.42**	**5.31**	**1.47**	**3.03**	**7.77**	**3.87**	**2.20**	**9.44**
Lower bound			1	0.1	1	1	1	0	0	1	0
Upper bound			3	5	10	10	10	10	10	10	10

[a] No function evaluations.

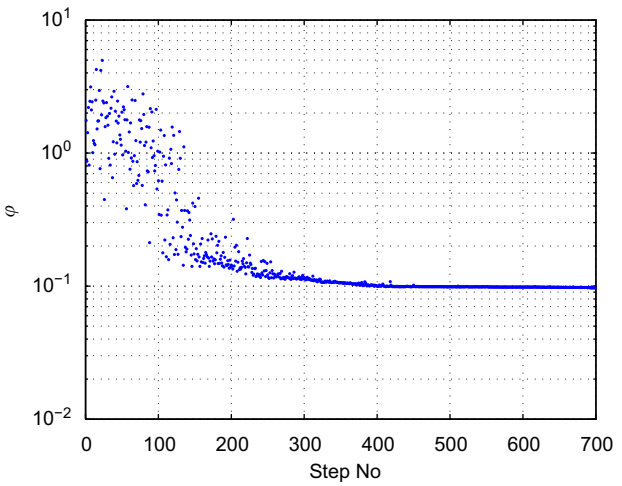

Fig. 9. Evolution of the error function of the viscous model.

modal identification was based on a different set of experimental data. Namely, the bridge was excited in the transverse direction by shaking the table with a low intensity random vibration. The response of the bridge was measured by an accelerometer that was placed at different positions of the deck using a magnetic base. These points were the connections

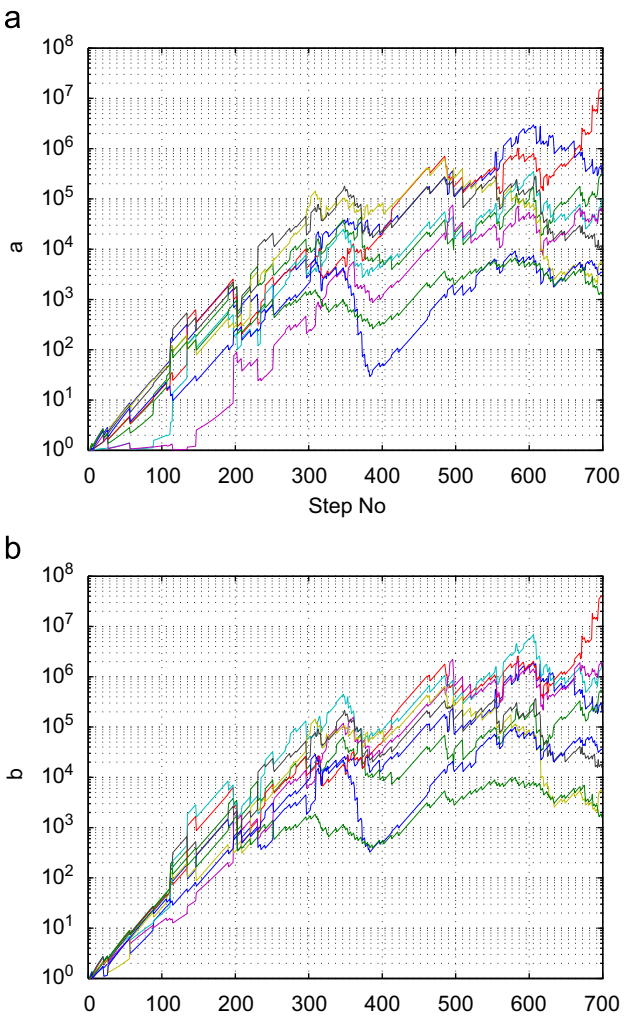

Fig. 10. (a) Evolution of the parameter a of the Beta distribution of the viscous model. (b) Evolution of the parameter b of the Beta distribution of the viscous model.

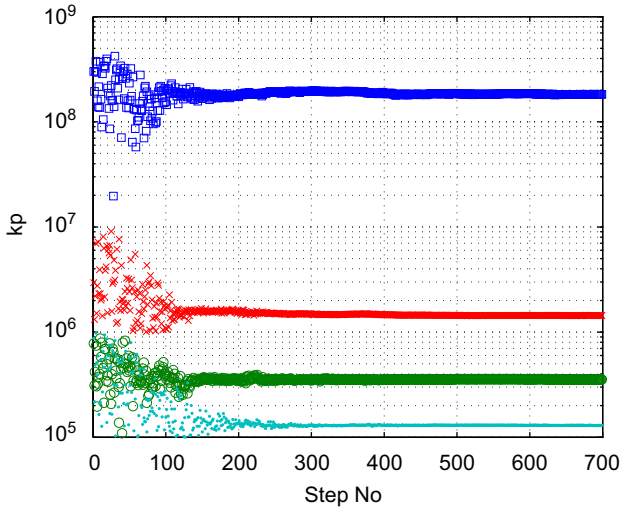

Fig. 11. Evolution of the parameters kp of the viscous model. Legend: □ kp_1, ◦ kp_2, ∗ kp_3 and • kp_4.

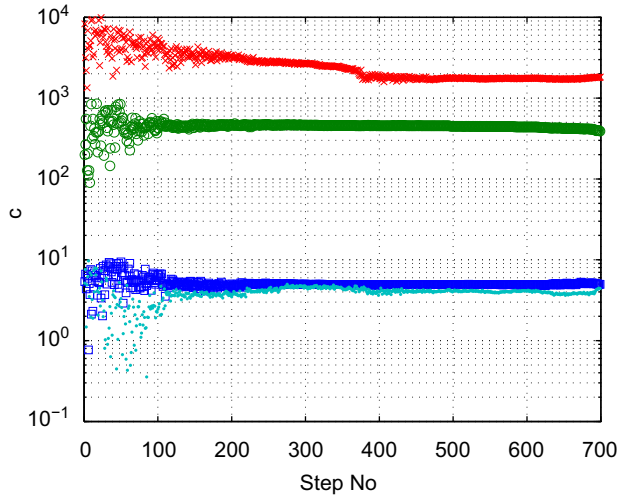

Fig. 12. Evolution of the parameters c of the viscous model. Legend: □ c_1, ◦ c_2, ∗ c_3 and • c_4.

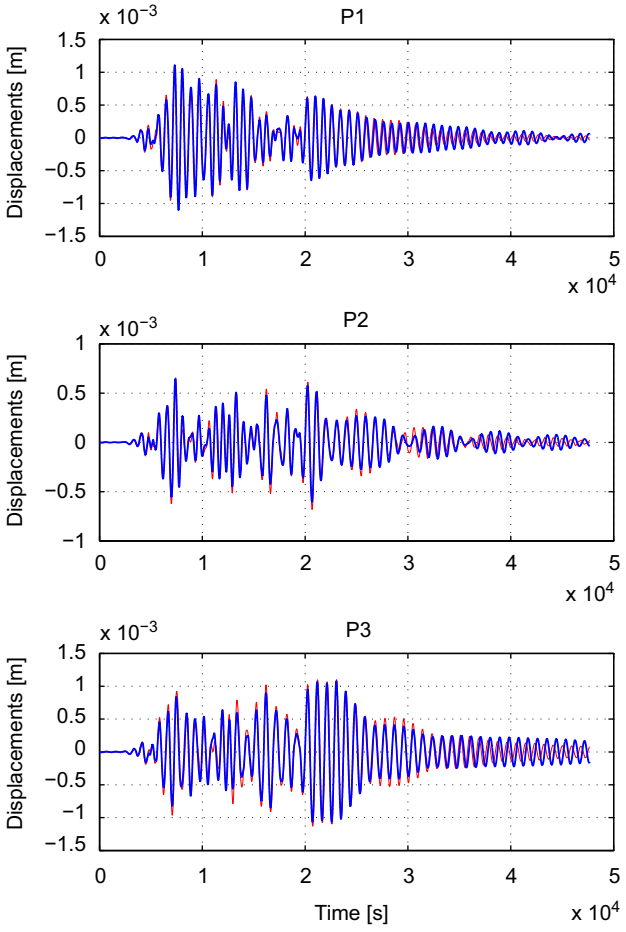

Fig. 13. Time-history response at the connections of the deck to the piers P1, P2 and P3. Bold line: experiment. Fine line: prediction of the viscous model.

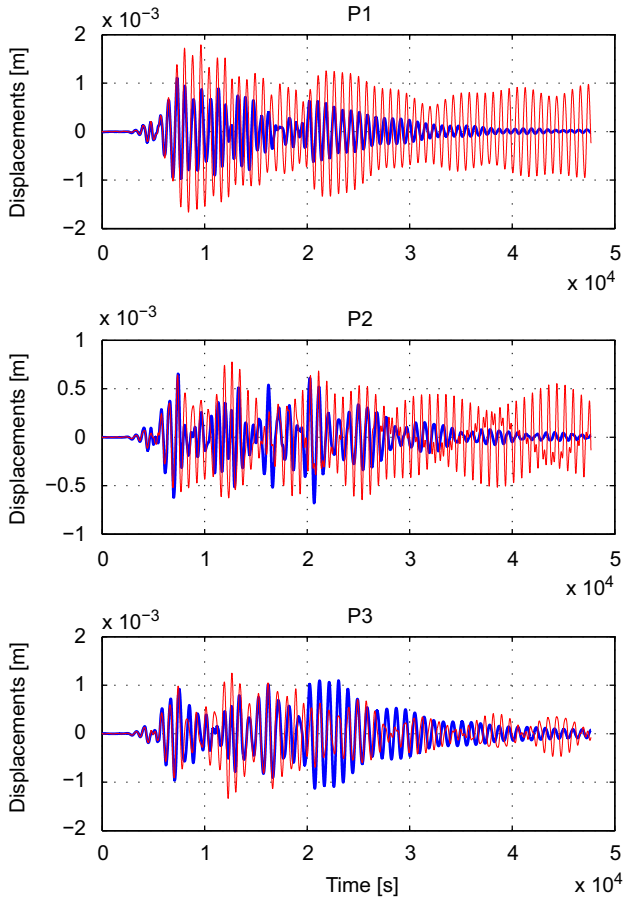

Fig. 14. Time-history response at the connections of the deck to the piers P1, P2 and P3. Bold line: experiment. Fine line: prediction of the undamped model.

of the deck to the piers and the abutments, and the middle of each span. This set-up allowed the four first natural frequencies to be accurately identified in each configuration. Some global and local stiffness parameters of this model were selected and updated until a reasonable convergence to the natural frequencies was reached. The results of this previous updated model will be used here for comparison purposes.

The first comparison is related to the response predicted by the undamped model. It was obtained as that of the viscous model by integration of the equation of motion using the central differences method. Results are depicted in Fig. 14 along with the measured response. The corresponding value of the error function was 243%, which is one order of magnitude higher than that of the viscous model. As expected, the results indicate that the undamped model gives a rough approximation of the seismic response due to the absence of damping. The comparison has also been done in the inverse sense. This is, the natural frequencies of the obtained updated viscous models are compared with the experimental ones. For this purpose, the values of the parameters corresponding to the successful cases shown in Table 6 were used to compute the global stiffness matrix, and from this and the global mass matrix the natural frequencies were computed by solving the corresponding generalized eigenvalue problem. Results are shown in Table 7 along with the experimental ones. As can be seen, all the obtained first and second natural frequencies are within a narrow interval. Nevertheless, they are approximately 3% lower than the experimental ones. The variations for the third and fourth modes are higher, and their average values are far from the experimental ones.

Table 8 shows the values of some updated parameters of both models that can be directly compared. It is found that the Young's modulus of the updated undamped model is within the interval achieved with the viscous model. However, the stiffnesses of the abutments, $k_{p\ 1}$, have a difference of two orders of magnitude.

In Ref. [22] the same experimental model was identified through a GA. An analytical linear model was used in that work, and the mass and damping matrices were directly updated using a different procedure to obtain the model response. Consequently, the results of both approaches are not quantitatively comparable. The time of computation of the GA, however, was about 120 h, while that of the AB was around 20 min. The time responses predicted by both updated models have a similar trend. The predictions of the models are lower than the experimental ones for large displacements, and vice versa in the case of small displacements (see Fig. 13).

Table 7
Natural frequencies of the updated viscous model.

Case	Natural frequencies			
	f_1	f_2	f_3	f_4
1	11.29	13.10	24.22	37.15
2	11.29	13.09	23.98	36.78
3	11.29	13.11	23.66	35.95
4	11.29	13.08	23.08	34.90
7	11.29	13.09	24.20	37.14
8	11.29	13.10	25.73	40.43
9	11.29	13.10	26.44	41.87
10	11.29	13.11	22.38	33.31
11	11.29	13.10	21.80	32.10
13	11.29	13.10	25.93	40.82
14	11.29	13.09	26.17	41.40
15	11.29	13.11	23.93	36.49
16	11.29	13.10	27.04	43.15
17	11.29	13.09	24.64	38.08
18	11.30	13.10	22.50	33.78
19	11.28	13.10	23.22	35.07
22	11.29	13.09	24.50	37.97
23	11.28	13.10	25.34	39.59
24	11.29	13.09	25.90	40.75
25	11.29	13.10	22.12	32.87
min	11.28	13.08	21.80	32.10
max	11.30	13.11	27.04	43.15
Average	11.29	13.10	24.34	37.48
Experimental	11.60	13.60	25.75	35.00
Error (%)	−2.67	−3.68	−5.48	+7.09

All these results and previous author's experience in similar models [1] indicates that the seismic response of the bridge could be more precisely described by using frictional dampers instead of the linear viscous ones. This will be the matter of the next subsection.

5.3. Nonlinear frictional approach

The FE model corresponding to this approach is the same of the viscous model as concerns the modelling of the deck, abutments and piers (see Fig. 15). For the dampers it was tried an elasto-slip model with Coulomb's friction, which has a hysteretic nonlinear behavior (see Fig. 16).

The dissipative force in a damper is now described by the following behavior law

$$f_D = \begin{cases} k_r y_n & \text{if } |y_n| \le f_u/k_r \\ f_u sign(y_n) & \text{if } |y_n| > f_u/k_r \end{cases}, \tag{19}$$

in which k_r is the stiffness of the damper, and f_u is the friction force (see Fig. 17). y_n is a transformed variable obtained from the measurable state variable y and the internal one y_r as follows

$$y_n = y - y_r. \tag{20}$$

The transformed variable is updated every time the sign of the velocity $\dot{y}$ changes. Figs. 16 and 17 clarify these concepts. Thus, when $|y_n| \le f_u/k_r$ the damper behaves elastically. If this is not the case, the damper slips and the energy is dissipated by friction.

The equation of motion now becomes

$$\mathbf{M}\ddot{\mathbf{y}}(t) + \mathbf{f}_D(t) + \mathbf{K}\mathbf{y}(t) = \mathbf{f}_s a_g(t), \tag{21}$$

where $\mathbf{f}_D$ denotes the vector of dissipative forces that are obtained from Eq. (19). The rest of variables are identical to those of the previous model, Eq. (18).

The parameters to be updated have been selected with the criteria used in the viscous model. Now there are thirteen unknown parameters, which are shown in Fig. 15. These parameters were obtained through the procedure established in the previous model (Section 5.2.1).

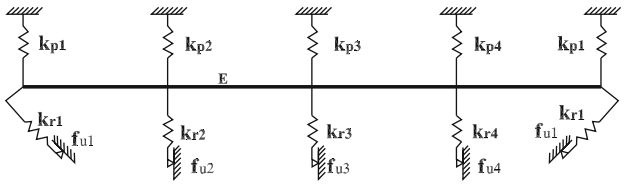

Fig. 15. Sketch of the frictional FE model.

Table 8
Comparison of the updated parameters of the undamped and viscous models.

Model	E	k_{p1}
Undamped	2.02×10^{11}	3.11×10^{6}
Viscous	2.35×10^{11}	4.48×10^{8}
	1.31×10^{11}	1.06×10^{8}

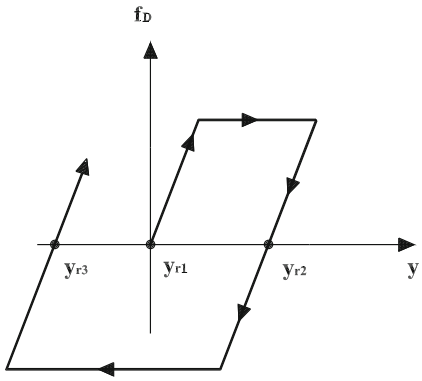

Fig. 16. Hysteretic behavior of the elasto-slip model.

5.3.1. Results and discussion

In this case only the AB algorithm, which have demonstrate to be the faster in the previous approach, is used. A first series of runs was carried out using a broad band in order to achieve the order of magnitude of the parameters. From these initial results a narrow band was established, and the algorithm was run 25 times. The stopping criterium in this case was the maximum number of iterations, which was set N_s=5000. Results are shown in Table 9.

All the runs were successful, none of them was trapped into local minima. They converge to solutions with close values of the normalized error, which ranges from 1.97% to 1.47%. Hence, the fitting to the experimental data was excellent in this case. The error is almost one order of magnitude lower than that of the viscous model, 9.6%, and two orders with respect of the undamped model, 243%. As can be seen in Fig. 18, there is a good fitting in both the amplitude and the phase. Hence, it is demonstrated that the seismic response is more accurately predicted by this nonlinear model than the previous ones.

Table 10 shows the obtained values of some parameters along with the corresponding ones of the undamped model. As can be seen, the value of the Young's modulus of the undamped model is within the interval obtained with the frictional model. The linear stiffness of the abutments, $k_{p\ 1}$, obtained with both models has now the same order of magnitude and is included within the achieved interval. This model also contains the initial angular stiffness of the abutments, which is equivalent to $k_{r\ 1}$. This parameter has the same order of magnitude in both models. Even though its value is not within the achieved interval, they are very close. All these results prove that the frictional model is quite close to the undamped one as concerns to the initial stiffness.

As the stiffness of this model is nonlinear, its natural frequencies depend on the amplitude of the displacements. Taking into account that a low amplitude was used in the modal testing, a value of the stiffness matrix consistent with these conditions was selected. Thus, it was assumed that all the dampers behave elastically under these conditions, and the corresponding initial stiffness matrix was used to compute the natural frequencies in each case. Results are shown in Table 11 along with experimental ones. As in the previous model, the results of the two first modes are within a narrow interval. In addition, the average of the results is very close to the experimental ones, with discrepancies lower than 1%.

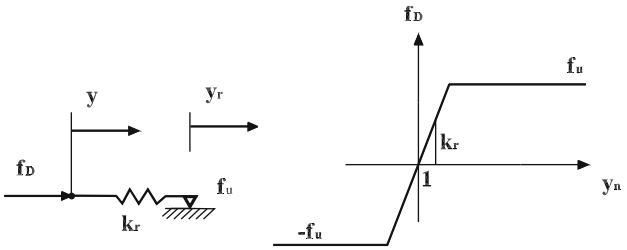

Fig. 17. Elasto-slip model. Left: scheme. Right: constitutive law.

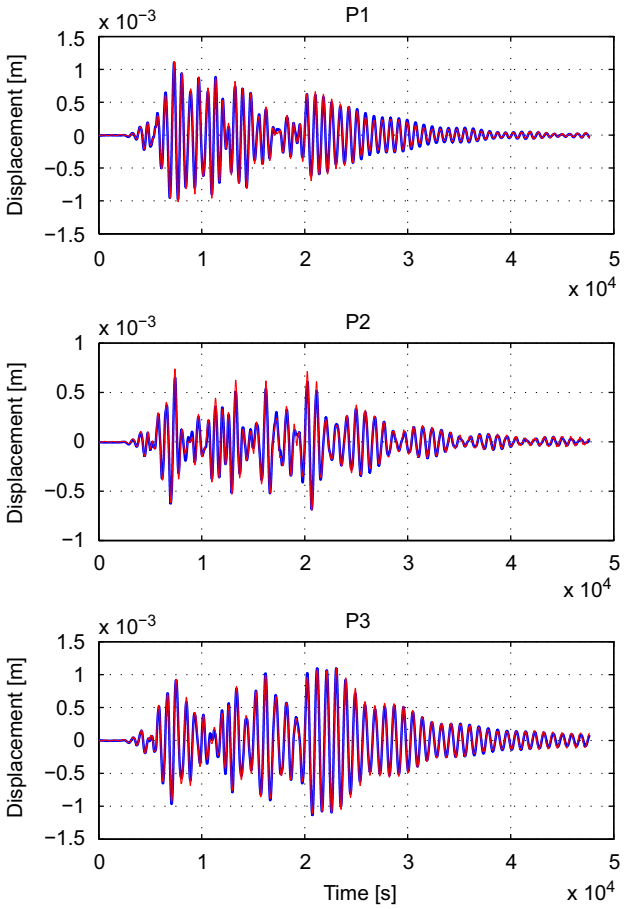

Fig. 18. Time-history response at the connections of the deck to the piers P1, P2 and P3. Bold line: experiment. Fine line: prediction of the frictional model.

These results shown that the frictional model is capable to reproduce accurately the first two experimental modes. Results of the third and fourth modes are better than those of the viscous model, but their averages are far from the experimental ones. The model does not reproduce accurately the high modes.

As concerns the variability of the obtained parameters, it is lower than that of the viscous model. Nevertheless, it remains significant in some parameters. The ill-conditioning of this case is due to lack of information in the training data. To prove this statement, the Fourier's spectra of the seismic response of the bridge, which corresponds to the accelerations of the deck relative to the table at the three measured points, was computed. They are shown in Fig. 19. As can be seen, the first two modes where clearly excited by seismic shake. The third mode, 25.75 Hz, was weakly excited. The fourth mode, 35 Hz, is not visible in the spectra. This is due to the fact that high modes are weakly excited by the table motion and, additionally, the measurement points are very close to the modal points of this mode (see Fig. 12 of Ref. [5]). This is the reason why the frictional model, only reproduces accurately the first two modes.

Table 9
Results of the frictional model with the AB algorithm and narrow band.

Case	NMSE (%)	$\frac{E}{10^{11}}$	$\frac{k_{p1}}{10^6}$	$\frac{k_{p2}}{10^6}$	$\frac{k_{p3}}{10^6}$	$\frac{k_{p4}}{10^6}$	$\frac{k_{r1}}{10^5}$	$\frac{k_{r2}}{10^5}$	$\frac{k_{r3}}{10^5}$	$\frac{k_{r4}}{10^5}$	f_{u1}	f_{u2}	f_{u3}	f_{u4}
1	1.86	1.87	3.67	0.36	0.92	0.13	0.25	0.86	4.73	0.70	6.05	55.12	138.13	74.85
2	1.52	1.94	5.00	0.33	1.01	0.09	0.22	1.02	4.49	0.94	4.73	63.28	111.59	98.45
3	1.59	1.97	4.83	0.30	0.92	0.16	0.27	1.17	5.39	0.20	5.11	80.76	161.89	138.20
4	1.51	1.88	6.58	0.31	1.04	0.13	0.20	1.29	4.33	0.60	4.77	82.71	99.04	163.60
5	1.58	1.95	6.37	0.29	0.90	0.15	0.25	1.26	5.54	0.33	5.41	87.64	172.84	102.14
6	1.76	1.81	5.35	0.32	0.96	0.16	0.26	1.27	4.40	0.47	5.75	87.70	128.11	183.04
7	1.62	2.04	5.71	0.28	1.06	0.14	0.22	1.32	4.44	0.22	4.94	87.61	110.43	135.47
8	1.81	1.83	3.79	0.33	0.90	0.15	0.27	1.22	4.82	0.61	5.70	84.04	145.21	68.42
9	1.65	2.06	5.58	0.31	1.04	0.10	0.23	0.95	4.57	0.62	5.12	59.89	118.83	177.06
10	1.97	1.94	2.96	0.34	0.94	0.17	0.30	0.99	4.73	0.24	6.13	65.66	140.56	154.01
11	1.59	1.86	5.64	0.32	1.02	0.15	0.22	1.25	4.34	0.42	4.96	81.33	104.60	99.79
12	1.69	1.99	7.43	0.29	1.06	0.13	0.21	1.23	4.32	0.39	5.83	80.79	106.17	132.75
13	1.47	1.84	7.54	0.31	0.97	0.12	0.23	1.26	4.62	0.78	5.14	85.78	126.63	98.87
14	1.60	2.00	4.01	0.29	1.07	0.11	0.22	1.39	4.27	0.70	5.10	91.13	99.43	74.32
15	1.81	1.90	5.52	0.32	1.03	0.15	0.36	1.24	4.36	0.40	4.28	80.12	106.20	128.96
16	1.73	1.87	4.50	0.31	0.88	0.18	0.23	1.27	5.58	0.20	5.37	89.37	170.78	95.53
17	1.54	1.88	7.05	0.32	1.05	0.14	0.22	1.17	4.16	0.54	5.05	74.26	96.40	102.66
18	1.64	2.04	4.52	0.30	1.07	0.08	0.22	1.13	4.32	0.81	5.37	72.47	102.61	141.96
19	1.53	1.97	4.81	0.31	1.04	0.09	0.22	1.13	4.40	0.89	4.80	71.86	107.35	93.01
20	1.52	1.94	5.63	0.31	0.95	0.11	0.25	1.11	4.99	0.72	5.40	75.71	144.11	134.65
21	1.53	1.90	8.90	0.31	0.97	0.16	0.22	1.11	4.73	0.27	5.61	74.46	132.29	151.76
22	1.56	1.93	5.03	0.32	0.94	0.14	0.26	1.05	5.02	0.42	5.75	71.41	147.95	111.81
23	1.84	2.04	3.24	0.28	0.98	0.12	0.26	1.39	4.81	0.58	5.29	96.35	134.24	62.17
24	1.61	1.92	4.33	0.31	1.05	0.10	0.22	1.27	4.29	0.92	4.83	81.13	98.99	98.09
25	1.49	1.86	6.72	0.32	0.94	0.11	0.23	1.11	4.94	0.79	5.56	75.46	140.91	119.81
min	**1.47**	**1.81**	**2.96**	**0.28**	**0.88**	**0.08**	**0.20**	**0.86**	**4.16**	**0.20**	**4.28**	**55.12**	**96.40**	**62.17**
max	**1.97**	**2.06**	**8.90**	**0.36**	**1.07**	**0.18**	**0.36**	**1.39**	**5.58**	**0.94**	**6.13**	**96.35**	**172.84**	**183.04**
Lower bound		1.80	1	0.1	0.5	0.05	0.1	0.5	1	0.1	0	50	50	50
Upper bound		2.10	10	1	5	0.5	0.5	5	10	1	10	100	200	200

Table 10
Comparison of the updated parameters of the undamped and frictional models.

Model	E	k_{p1}	k_{r1}
Undamped	2.02×10^{11}	3.11×10^{6}	1.69×10^{4}
Frictional	2.06×10^{11}	8.90×10^{6}	3.60×10^{4}
	1.81×10^{11}	2.96×10^{6}	1.97×10^{4}

From a practical point of view, the parameters of the best solution, which correspond to the case 13 in Table 9, can be adopted for the final updated model. As has been demonstrated, this model is capable of giving accurate predictions of the seismic response. The model could be used in other applications in which only the first two modes have significant influence in the response. For a more complete updating of the model, it is necessary to use other experimental data containing more information from the high modes, and to include other measurement points more sensitive to the fourth mode.

Finally, it should be pointed out that the proposed method was capable to update simultaneously the stiffness and damping parameters in such an ill-conditioned case.

6. Conclusions

A new method intended to update FE models in the field of structural dynamics has been developed. The method is based on an error function defined in the time domain. The error function is minimized through a sampling algorithm adapted specifically to its characteristics. Two different approaches have been tried. They correspond to isotropic and

Table 11
Natural frequencies of the updated frictional model.

Case	Natural frequencies			
	f_1	f_2	f_3	f_4
1	11.69	13.54	24.23	34.92
2	11.70	13.62	24.98	36.59
3	11.75	13.60	25.13	36.83
4	11.67	13.62	25.03	36.91
5	11.73	13.57	25.26	37.50
6	11.72	13.59	24.50	35.92
7	11.69	13.61	25.57	37.80
8	11.72	13.57	24.15	34.82
9	11.70	13.61	25.62	37.92
10	11.74	13.59	24.22	34.38
11	11.70	13.63	24.85	36.42
12	11.66	13.60	25.57	38.17
13	11.71	13.60	24.93	37.01
14	11.68	13.62	25.01	36.17
15	11.92	13.81	25.20	36.92
16	11.69	13.55	24.59	35.75
17	11.69	13.64	25.09	37.13
18	11.68	13.61	25.32	36.94
19	11.70	13.62	25.10	36.71
20	11.73	13.59	25.11	37.05
21	11.67	13.57	25.24	37.82
22	11.73	13.58	24.97	36.65
23	11.72	13.59	24.78	35.42
24	11.68	13.64	24.82	35.93
25	11.70	13.57	24.92	36.92
min	11.66	13.54	24.15	34.38
max	11.92	13.81	25.62	37.17
Average	11.71	13.61	24.97	36.58
Experimental	11.60	13.60	25.75	35.00
Error (%)	+0.95	+0.07	−3.03	+4.51

anisotropic sampling distributions. The minimization process has been synthesized in a simple algorithm capable of solving both the global and the local phases of the updating.

The method was tested through two different benchmarks, a numerical simulation and an experimental case. It is found that bounds are indispensable in the random search to obtain reliable results. The proposed algorithms can be directly applied; they do not need any initial calibration. They can be applied to both linear and nonlinear models. In the tested cases, the solution was attained in a robust and efficient manner even for rather uncertain values of the parameters. The efficiency of the anisotropic approach is one order of magnitude higher than the isotropic one. The proposed anisotropic algorithm outperforms both the GA and the CMA-ES. The former is a common stochastic algorithm in FE model updating, and the latter is considered the state-of-the-art of the general-purpose stochastic optimization algorithms. Hence, the proposed method in its anisotropic version is very promising in the field of structural dynamics. Future work is needed in order to overcome the improper local minima of the error function, which constitute a drawback of all the tested algorithms.

Acknowledgments

The economic support given by the Spanish Ministry of Education and Innovation trough the project BIA2006-15266-C02-01 is gratefully appreciated. The experimental part of this work was performed at the Earthquake Engineering Research Center (EERC) of the University of Bristol, under the ECOEST2 network in the Human Capital and Mobility Program of the European Commission. The collaboration of the EERC staff, particularly Professor Severn, is greatly acknowledged.

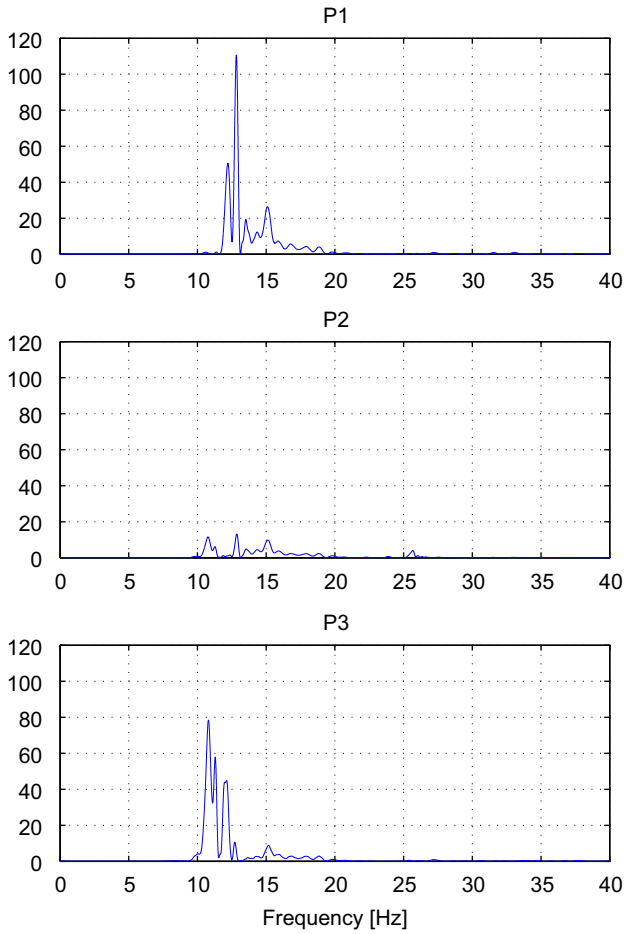

Fig. 19. Fourier's spectra of the seismic response at the connections of the deck to the piers P1, P2 and P3.

References

[1] J.L. Zapico, F.J. Molina, M.P. González, S. Montes, Identification of a composite frame from a pseudodynamic test, Mechanical Systems and Signal Processing 19 (2005) 579–595.
[2] J. Arora, Introduction to Optimum Design, second ed., Elsevier Academic Press, London, UK, 2004.
[3] G.R. Liu, X. Han, Computational Inverse Techniques in Nondestructive Evaluation, CRC Press, Boca Raton, Florida, USA, 2003.
[4] J.A. Nelder, R. Mead, A simplex method for function minimization, The Computer Journal 7 (1965) 308–313.
[5] J.L. Zapico, M.P. González, M.I. Friswell, C.A. Taylor, A.J. Crewe, Finite element model updating of a small scale bridge, Journal of Sound and Vibration 268 (2002) 993–1012.
[6] M.I. Friswell, J.E. Mottershead, Finite Element Model Updating in Structural Dynamics, Kluwer Academic Publishers, Dordrecht, the Netherlands, 1999.
[7] L. Ljung, System Identification, Prentice Hall PTR, New Jersey, USA, 1999.
[8] N.M.M. Maia, J.M.M. Silva, Theoretical and Experimental Modal Analysis, Research Studies Press Ltd., Taunton, Somerset, England, 1997.
[9] A. Teughels, G. De Roeck, Structural damage identification of the highway bridge Z24 by FE model updating, Engineering Structures 278 (2003) 589–610.
[10] R.I. Levin, N.A.J. Lieven, Dynamic finite element model updating using simulated annealing and genetic algorithms, Mechanical Systems and Signal Processing (1998) 91–120.
[11] A. Kyprianou, K. Worden, M. Panet, Identification of hysteretic systems using the differential evolution algorithm, Journal of Sound and Vibration 248 (2001) 289–314.
[12] N. Ajavakom, C.H. Ng, F. Ma, Performance of nonlinear degrading structures: identification, validation, and prediction, Computers and Structures 86 (2008) 652–662.
[13] C.G. Koh, Y.F. Chen, C.-Y. Liaw, A hybrid computational strategy for identification of structural parameters, Computers and Structures 81 (2003) 107–117.
[14] O. Begambre, J.E. Laier, A hybrid particle swarm optimization simplex algorithm (PSOS) for structural damage identification, Advances in Engineering Software, 2009, doi:10.1016/j.advengsoft.2009.01.004.
[15] N. Hansen, S.D. Müller, P. Koumoutsakos, Reducing the time complexity of the derandomized evolution strategy with covariance matrix adaptation (CMA-ES), Evolutionary Computation 8 (2003) 1–18.
[16] N. Hansen, A. Ostermeier, Completely derandomized self-adaptation in evolution strategies, Evolutionary Computation 9 (2001) 159–195.
[17] V.K. Rohatgi, A.K.M.D. Ehsanes Saleh, An Introduction to Probability and Statistics, second ed., Wiley & Sons, New York, USA, 2001.

[18] S. Kern, S.D. Müller, N. Hansen, D. Büche, J. Ocenasek, P. Koumoutsakos, Learning probability distributions in continuous evolutionary algorithms—a comparative review, Natural Computing 1 (2004) 3–52.
[19] Users Manual Version 6.5 MATLAB, The Math Works, Inc., 2002.
[20] Institute of Computational Science 〈http://www.icos.ethz.ch/software/evolutionary_computation/cmaes.m〉.
[21] K. Worden, G.R. Tomlinson, Nonlinearity in Structural Dynamics, Institute of Physics Publishing, Bristol, UK, 2001.
[22] D.H. Bassir, J.L. Zapico, M.P. González, R. Alonso, Identification of a spatial linear model based on earthquake-induced data and genetic algorithm with parallel selection, International Journal for Simulation and Multidisciplinary Design Optimization 1 (2007) 39–48.

Engineering Structures 56 (2013) 246–259

Contents lists available at SciVerse ScienceDirect

Engineering Structures

journal homepage: www.elsevier.com/locate/engstruct

Nonlinear modal identification of a steel frame

J.L. Zapico-Valle [a,*], M. García-Diéguez [b], R. Alonso-Camblor [b]

[a] Department of Construction and Manufacturing Engineering, University of Oviedo, Campus de Gijón 7.1.16, 33203 Gijón, Spain
[b] Department of Construction and Manufacturing Engineering, University of Oviedo, Campus de Gijón 7.1.BC, 33203 Gijón, Spain

ARTICLE INFO

Article history:
Received 23 April 2012
Revised 18 March 2013
Accepted 30 April 2013
Available online 6 June 2013

Keywords:
Nonparametric identification
Nonlinear modal identification
Asymptotic nonlinear law
Preloaded stiffness

ABSTRACT

The nonlinear modal identification of a four-storey steel frame is presented in this paper including both the experimental and the analytical aspects. The first two bending modes of the frame were experimentally isolated by a single-point mono-harmonic excitation. The subsequent free decay vibration was measured and used for identification purposes. An original filtering procedure was developed in order to overcome the drawbacks of the common band-pass filters and to enhance the accuracy of the signals. The nonparametric identification of the structure was carried out through an expeditious procedure based on the analysis of the evolution of the apparent frequency and equivalent viscous damping coefficient as a function of the apparent amplitude of the free decay cycles. The results of this identification reveal that the structure is weakly nonlinear in stiffness and strongly nonlinear in damping, while the mode shapes remain linear within the range of measurements. Asymptotic nonlinear laws defined in the modal space where proposed to model both the stiffness and the damping. This is another original contribution in this paper. The proposed nonlinear model was fitted to the experimental data in the time domain. Results were excellent with fitting errors three orders of magnitude lower than those of a pure linear model.

1. Introduction

Framed structures are extensively used in civil engineering applications such as buildings and industrial constructions. The design and further control and monitoring of these structures are commonly based on mathematical models, experiments and previous experiences. Linear models are usually used for analyzing these structures in the engineering applications. This approach strongly simplifies the modelling, analysis and extraction of modal properties. However, linearity seldom occurs in reality. Structures always contain some degree of nonlinearity due to material and interface behaviour, instabilities, etc. [1]. Therefore, an epistemic error is introduced by the linear modelling and a nonlinear approach should be used when more accurate predictions are required.

This is the case when evaluating the dynamic response of a structure at or near resonances. Under these conditions, the stiffness and inertial forces tend to cancel each other out and the response is governed mainly by damping. It is well known that damping is often amplitude dependent. For this reasons, damping measurements are recommended in Reference [2] as a way to achieve accurate damping models to check the vibration serviceability of footbridges. ISO code [3] also encourages the choice of a suitable damping model and its calibration through experiments to check the serviceability of buildings and walkways against vibrations. Advanced seismic design codes [4] include several performance criteria for steel framed structures. No significant damage to the structure is recommended for the immediate occupancy performance level. This means that the structure should remain in the elastic range during the seismic excitation. Under these circumstances, the structure response is also dominated by damping. Appropriate modelling and calibration of damping is thus essential for the verification of this performance level. These are just a few examples in which damping could be a significant design factor.

Due to safety as well as economic reasons, in many cases the performance of structures should be checked once they are set up. As the structures tend to degrade when aging, their integrity should also be monitored periodically or continuously. After an exceptional event such as an overload, earthquake, and hurricane structures may result damaged and an evaluation of their integrity should be carried out. All these engineering tasks are referred to as structural health monitoring (SHM) in literature. During the last decades, numerous SHM techniques based on the analysis of measured vibration response were developed. Reference [5] includes a comprehensive literature review of these techniques. In this survey it is conclude that even though the majority of the reviewed damage identification techniques rely on linear models fit to measured data, nonlinear identification techniques are potentially interesting due to the inherent nonlinear nature of the damage. More specifically, Brandon [6] states that nonlinear identification can provide

* Corresponding author. Tel.: +34 985 18 19 28; fax: +34 985 18 20 55.
E-mail address: jzapico@uniovi.es (J.L. Zapico-Valle).

0141-0296/$ - see front matter © 2013 Elsevier Ltd. All rights reserved.
http://dx.doi.org/10.1016/j.engstruct.2013.04.026

valuable information for SHM. The author advocates the use of time-domain system identification techniques to retain important nonlinear information, which is lost when linearizing time series. Modena et al. [7] claim the use of damping and nonlinear responses as damage-sensitive features.

The theory of nonlinear systems is extremely broad and a large body of literature is available, as reported in References [1,8]. Many potential applications of the nonlinear theory in structural engineering are also highlighted in these references. This field has evolved and is a mature subject nowadays. Even though the literature on testing and identification of nonlinear structures is abundant, only few practical methods of modal testing have been established so far. Some recent publications in this area are outlined in the next paragraphs. Atkins et al. [9] propose an extension of the linear force appropriation method to the identification of weakly nonlinear structures. By an appropriate force choice, which includes high harmonic terms, the structure is made to respond in a single mode corresponding to the underlying linear structure. An optimization approach is chosen to determine the multi-harmonic components of the force vector. The restoring force surface method is used to identify the linear and nonlinear terms in the equation of motion of each individual mode. The nonlinear cross-coupling terms are separately identified. Platten et al. [10] developed a method for the identification of complex structures that are predominantly linear and feature a small number of nonlinear modes. They use an extension of the resonant decay method, in which appropriate burst sine forces are applied to excite single modes or small groups of coupled modes. The restoring force surface method is finally used to curve-fit the results in modal space obtaining thus the modal parameters of each mode. Peeters et al. [11,12] extended the phase resonance testing to nonlinear systems by using the nonlinear normal modes (NNMs) theory. In this method, underlying NNMs are individually excited instead of linear modes. This is achieved by tuning a multi-harmonic excitation such as the response is in quadrature with respect to the excitation. After this NNM force appropriation, the excitation is turned off and the subsequent free decay vibration, in which only the excited mode remains due to its invariance, is used to extract the modal curves and corresponding frequencies through time-frequency analysis. The aforementioned methods were applied to numerical simulations or to small experimental rigs. In these cases, the type of nonlinearity present in the structure, which constitutes the essential issue to be addressed in the identification process, is known beforehand. The applications of nonlinear modal identification to full-scale engineering structures with multiple components is scarce in literature, despite their potential usefulness.

This paper deals with the nonlinear modal identification of an experimental four-storey medium-size steel frame. A practical identification procedure to be applied to similar structures is sought in this study. Taking into account the highly individualistic nature of nonlinear systems [8], the main goal here is to discover the nonlinear features of the frame through dynamic experiments. From this knowledge, a suitable dynamic model, that can be easily implemented in the engineering applications, will be inferred. The model will be finally calibrated by fitting experimental data. The calibrated nonlinear model will be used for future applications on SHM, finite element model updating and structural serviceability checking. To achieved the planned objectives, a two-step experimental procedure similar to those of Refs. [9–12] is proposed. The isolation of single modes by appropriate harmonic excitation is sought in the first step. The subsequent free decay vibration is used for identification purposes. The multi-point multi-harmonic appropriation established in [9–12] is very popular in the aerospace industry. However, it is not practical for in-service civil engineering applications. Instead, an imperfect appropriation consisting in a single-point mono-harmonic excitation was chosen for this case. In Ref. [12], it is stated that this excitation isolates satisfactorily a nonlinear modal mode if the structure has well-separated modes. A novel procedure is tried to filter the raw digital signals. The procedure is aimed to keep most of the original nonlinear information, which can be removed when using conventional filters. The filtered signals are used for the nonparametric identification of the structure. There are some nonparametric identification methods available in literature. The method developed by Feldman [13] based on Hilbert transform constitute a prominent example. In the present case, a more expeditious procedure is developed in order to study the evolution of both the stiffness and damping as a function of the vibration amplitude and to infer appropriate models for them. The calibration of the proposed models is posed as the minimization of an error function defined in the time domain and accounting for the discrepancies between the response predicted by the model and the experiments. The model response is computed from the initial conditions through a finite differences scheme. An adaptive stochastic algorithm developed previously by the authors [14] is adopted for the minimization. This algorithm is very effective in solving nonlinear-in-the-parameters cases.

2. Experimental part

2.1. Structure

The Uniovi Structure is a middle-size four-storey steel frame with two bays in the longitudinal direction and one bay in transversal one. The overall dimensions of the structure are 4 m length, 1.5 m width and 7.3 m height (see Fig. 1). All columns and beams are HEA-120 and IPN-100, respectively, of steel grade S-275. The floors of the frame are 4 mm thick steel sheets connected to the beams through discontinuous welding. The foundations consist of two continuous concrete beams lying on the floor of the laboratory.

Each column consists of two pieces. They are spliced through end plates connected by four bolts 12 mm in diameter. The columns are welded to 20 mm thick plates anchored to the foundation. The beams corresponding to the transversal direction are directly connected to the web of columns by a welded-all-around fillet. In the longitudinal direction, however, the beams are connected to the

Fig. 1. Uniovi structure.

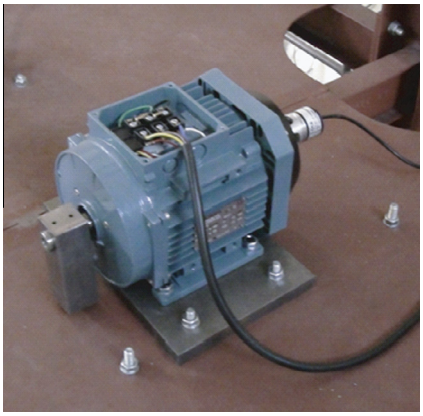

Fig. 2. Pendulum exciter.

flange of the columns. The connection was designed with a 8 mm thick end plate and four bolts 10 mm in diameter.

2.2. Excitation and measurement chain

A pendulum-like exciter was used to excite the frame only in the longitudinal direction. It consists of an eccentric mass connected to the shaft of a variable-speed electrical motor (see Fig. 2). The excitation was carried out by harmonically varying the angular position of the mass. The desired frequency and amplitude of the excitation were achieved by controlling the angular position of the shaft through an electronic regulator. The regulator is feedbacked by an encoder. The frequency range of the exciter is from 0 to 100 Hz and the angle range is from 1 to 20. The total mass of the pendulum is 1 kg.

The structure was provided with four seismic Brüel & Kjær accelerometers with a sensibility of 10 V/g. Each was screwed at the middle of the end beam on each floor pointed towards the longitudinal direction. The hardware used to record the signals was a dSPACE RTI1104 data acquisition card. The analogical signals were converted into digital ones at a sampling frequency of 1 kHz. The processing task was then carried out using MATLAB [15].

2.3. Testing

Free decay responses of isolated bending modes in the longitudinal direction are chosen as experimental references for the nonlinear modal identification. This approach is very accurate because the excitation uncertainties are avoided. Moreover, free decay vibrations contain a broad range of amplitudes that shows up the nonlinearities present in the structure. As a starting point for the nonlinear testing, a preliminary linear stochastic subspace identification was carried out through a low intensity random test. The following bending natural frequencies were identified for the longitudinal direction: 4.3, 15.0, 34.0, 61.9 Hz.

The isolation of each single nonlinear mode is tried by a single-point mono-harmonic excitation. To this end, the exciter was placed at the center of the fourth floor and pointed to the longitudinal direction of the structure. Only bending modes are thus excited. A similar case of single mode excitation in a real structure is reported in Reference [16]. In this case, the first bending modes of a 101-storey building were successfully excited by means of mono-harmonic force given by an active mass damper installed on the ninetieth floor.

For the present application, the experiments consisted of 20 s sinusoidal force followed by the free decay vibration. For each mode, a first test was performed at the frequency obtained in the preliminary identification. Then a more precise value of the natural frequency was achieved from the free response by Fourier analysis. In a second stage, a test was eventually performed by tuning the excitation to the precise natural frequency. The data of these final tests were used for the nonlinear identification.

3. Signal preprocessing

3.1. Assessment

The quality of the obtained free vibrations is assessed by visual observation of the data in both the time and frequency domains. The frequency spectra used for the latter were obtained through a Fourier transform. The results are shown in Fig. 3 for the four aforementioned excitation levels, which are labeled: *a*, *b*, *c* and *d*. It is visually evident that the responses of cases *a* and *b* are dominated by a single mode in each case: first mode and second mode, respectively. In test *c*, however, the first, second and third modes contribute with similar significance to the response. Response of test *d* is mainly composed by the first, second and fourth modes. In addition, the second mode has the highest contribution. In order to improve the results, tests *c* and *d* were repeated placing the exciter on the third floor, the mode shape ordinate of which is larger than that of the fourth floor. Even with this arrangement, the free responses showed a significant contribution of the first and second modes. What follows from these results is that only the first two bending modes can be properly isolated through the proposed single-point mono-harmonic excitation. As a consequence, only these modes will be used for identification purposes in the remainder of the paper. In practice, this is not a limitation because only the low modes have usually a significant influence in the dynamic response of structures.

Fig. 4 shows the raw data of the first mode free vibration measured at the fourth floor. As can be seen, the signal contains a time-variant offset. Moreover, a high-frequency noise is also present along all the signal. These disturbances corrupt the underlying 'true' signal and strongly affect the further identification process. Therefore, removing the disturbances from the measured signals is essential in order to achieve an accurate model identification. Signal filtering becomes thus as important as the identification. This will be the matter of next section.

3.2. Filtering

The disturbances present in the signals are usually removed by means of band-pass linear filters adjusted to the frequency range of interest. A drawback of these filters is the definition of cut-off frequencies. If the cut-off is far from the frequency range of interest, the filtered signal will remain corrupted. Conversely, if the cut-off is chosen close to the range of interest, the disturbances will be removed, but a significant part of the 'true' signal will be removed too. This is not an inconvenience for linear systems, providing the same filter is applied to the input and output [17]. In the case of nonlinear systems, however, linear filters tend to linearize the signals by removing the nonlinear components.

In order to overcome the aforementioned drawbacks of the conventional filters, a novel filtering procedure is proposed here to preprocess the free decay signals. This procedure will be referred to as moving linear fitting (MLF) in the rest of the paper. Next sections contain a detailed description of MLF and the comparison with conventional filters in simulated cases.

3.2.1. The moving linear fitting

The procedure presented here is intended to remove simultaneously both the offsets and high-frequency noise present in the

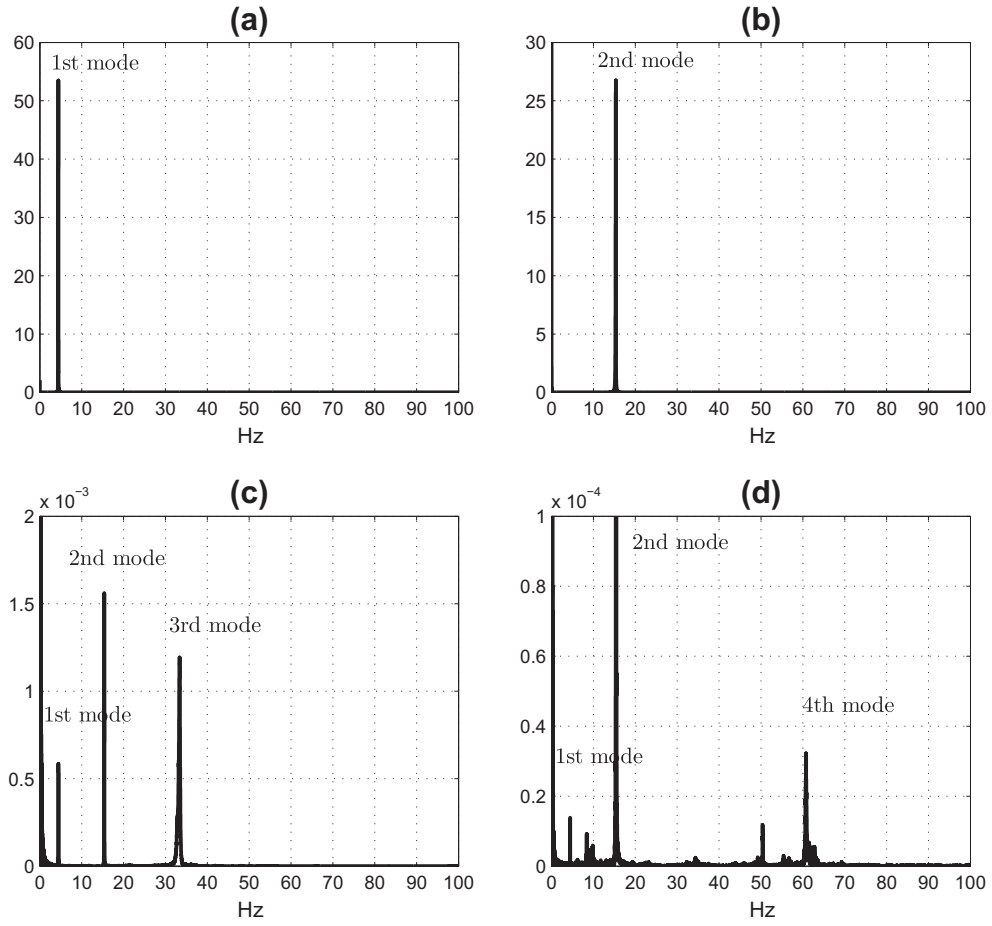

Fig. 3. Fourier spectra of free decay responses for different excitation frequencies. (a) 4.43 Hz. (b) 15.33 Hz. (c) 33.38 Hz. (d) 61.10 Hz.

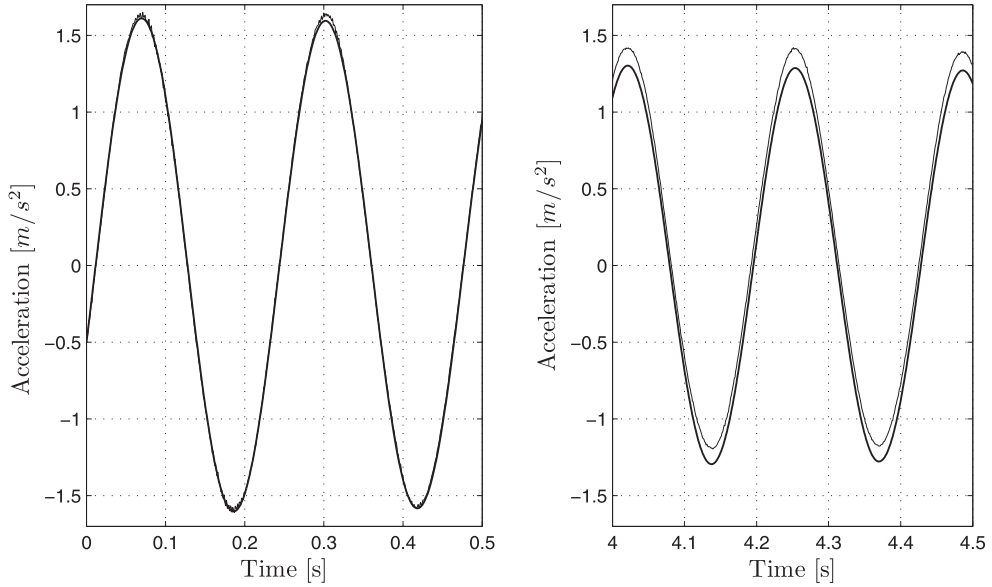

Fig. 4. Two different time-domain segments of first mode response. Fine line: Raw signal. Bolt line: Filtered signal.

free vibration signals, keeping as much as possible of the 'true' signal. The application of the proposed filter is restricted to weakly nonlinear structures showing symmetric nonlinearities. The bases of the procedure are the following. The free decay vibration of a weakly nonlinear structure is expected to be locally very close to that of a pure linear structure. The term locally implies that an interval of time that includes only a few cycles of vibration is taken for comparison. The MLF is developed from this central idea. For

each discrete point of the measured response, a linear model is fitted to the experimental data within an interval of time approximately equal to a period of vibration and centered with respect to the considered point. The value of the fitted linear model corresponding to the point is chosen as the related filtered value. The noise, due to its random nature, is canceled by averaging over the fitting interval. As the fitted function is centered with respect to the acceleration, the offset is removed. Finally, most of the linear and nonlinear information contained in the raw signal is expected to be kept in the filtering, because the procedure is applied individually to all the points of the signal. These intuitive statements will be verified through numerical simulations later. The outlined procedure is detailed in the following paragraphs.

The acceleration response of the pure linear model used for reference in the MLF can be trigonometrically formulated as

$$\ddot{x}(t) = e^{-\xi\omega t}\left[C_1 \cos\left(\omega\sqrt{1-\xi^2}t\right) + C_2 \sin\left(\omega\sqrt{1-\xi^2}t\right)\right], \tag{1}$$

in which ω and ξ stand for the natural frequency and damping ratio and C_1 and C_2 are constants of integration that depend on the initial conditions [18]. The variables ω and ξ are estimated from the raw signal by expeditious methods. ω can be approximated by peak-picking in the Fourier spectrum and ξ can be calculated from the logarithmic decrement. The estimated values of ω and ξ are used for filtering all the points of the response. The constants C_1 and C_2, however, are evaluated in each individual point by fitting the linear model to the raw data over a centered segment. For this purpose, Eq. (1) is formulated in its discrete version as follows:

$$\ddot{\mathbf{x}} = \mathbf{A}\mathbf{c}, \tag{2}$$

in which $\ddot{\mathbf{x}}$ is a $N \times 1$ vector containing the acceleration response of the model taken at a constant increment of time Δt, which is chosen equal to the experimental sampling period, $\mathbf{c}$ is a 2×1 vector including the parameters C_1 and C_2, $\mathbf{A}$ is a $N \times 2$ matrix that contains the terms of Eq. (1) that are functions of time, and N is the fitting order. N is chosen odd, and the segment including $\frac{N-1}{2}$ points before and after the analyzed point is used for fitting. N should have such a value that the length of the segment is close to the natural period of the response. Under this conditions, N turns out to be

$$N = \frac{2\pi}{\omega\Delta t} + 1. \tag{3}$$

For each point, ith, the parameters are chosen in such a way that the discrepancies between the reference model and the measurements are minimized in the selected segment. This yields the following solution in a least-squares sense:

$$\mathbf{c_i} = (\mathbf{A}^T\mathbf{A})^{-1}\mathbf{A}^T\ddot{\mathbf{x}}_e, \tag{4}$$

in which vector $\ddot{\mathbf{x}}_e$ denotes the measured acceleration. Once the parameters, $\mathbf{c_i}$, are obtained, the filtered acceleration of the analyzed point, $\ddot{x}_i$, is calculated by the following:

$$\ddot{x}_i = \mathbf{A}_{\frac{N+1}{2}}\,\mathbf{c_i}, \tag{5}$$

in which $\mathbf{A}_{\frac{N+1}{2}}$ stands for the $\frac{N+1}{2}$ row of matrix $\mathbf{A}$. This loop is repeated for all the points of the signal except for the $\frac{N-1}{2}$ initial and final ones.

3.2.2. Validation

The aim of this section is to check the quality of MLF. For this purpose, the performance of the MLF is evaluated through two numerical simulations and compared to that of a conventional filter.

The numerical simulations consist of a combination of original free vibration, time-variant offset and noise. They were selected close to those of the vibration measured at the fourth floor in Test *a* (see Fig. 3). Two different original vibrations were generated. The first one corresponds to a pure linear model

$$m\ddot{x}(t) + c\dot{x}(t) + kx(t) = 0, \tag{6}$$

in which $m = 1$ kg, $c = 0.119$ N s/m and $k = 730.975$ N/m. The response was computed analytically at a time step $\Delta t = 10^{-3}$ s (Fig. 5a). The second original vibration belongs to a nonlinear model having cubic softening stiffness

$$m\ddot{x}(t) + c\dot{x}(t) + k_1x(t) - k_2x^3(t) = 0, \tag{7}$$

in which $m = 1$ kg, $c = 0.125$ N s/m, $k_1 = 731$ N/m and $k_2 = 10^7$ N/m^3. The related response was computed by central differences using an increment of time $\Delta t = 10^{-5}$ s. In both cases the same time-variant offset was used (Fig. 5b), which was obtained by the following equation:

$$\ddot{x}_o(t) = 0.1\sin(0.044\ t - 0.1). \tag{8}$$

The amplitude, phase and frequency of this function were reckoned in such a way that the function shape in the time domain was roughly similar to that of the experiments. Finally, a random noise having a maximum amplitude of 0.01 m/s^2 was added to each discrete value of the response. The final corrupted signal is shown in Fig. 5c. As the shape of the final signal was selected close to that of the real signal that will be analyzed later, the performance of the filters in these simulated cases is therefore expected to be similar to that of the experimental cases. The advantage of the simulations is that the original vibration is known a priori and an accurate evaluation of the performance can be done. A four order Butterworth filter was additionally used. In this case different cut-off frequencies were tried in order to evaluate their influence in the results.

The filters were applied to the corrupted signals. Then, the filtered signals were compared with the original ones. As the filters introduce phase lags, the initial point of the original signal was selected in such a way that the discrepancies were minimized in the comparison. The quality of the filtering was evaluated through the normalized mean squared error, NMSE

$$\mathrm{NMSE} = \frac{\sum_{i=1}^{M}\left(\ddot{x}_i^f - \ddot{x}_i\right)^2}{\sum_{i=1}^{M}\ddot{x}_i^2}, \tag{9}$$

in which $\ddot{x}_i^f$ and $\ddot{x}_i$ represent respectively the filtered and original signals. In the Butterworth filter different values of the low cut-off frequency were tried. Results show the same trend in both the linear and nonlinear models (Table 1). There is a minimum error at 0.125 Hz. Below this frequency the error increases because a significant part of the offset remains in the filtered signal. Above this frequency the error also increases due to the fact that some original signal is removed by filtering. Keeping the best value obtained for the low cut-off, several values were tried for the high cut-off frequency (Table 1). The error trend in this case is similar to that of the low cut-off. However, the errors are higher for the nonlinear model and the best result is at 25 Hz for the linear model and at 150 Hz for the nonlinear model. A possible explanation of these results is that the response of the nonlinear models contains harmonics of the fundamental frequency that are removed by this frequency boundary.

As for the MLF, errors are one order of magnitude lower than the best results of the Butterworth filter. In addition, the parameters of the MLF are directly estimated from the raw signal. In the simulated cases, which are close to the experimental measurements that will be analyzed later, the MLF clearly outperforms the Butterworth filters.

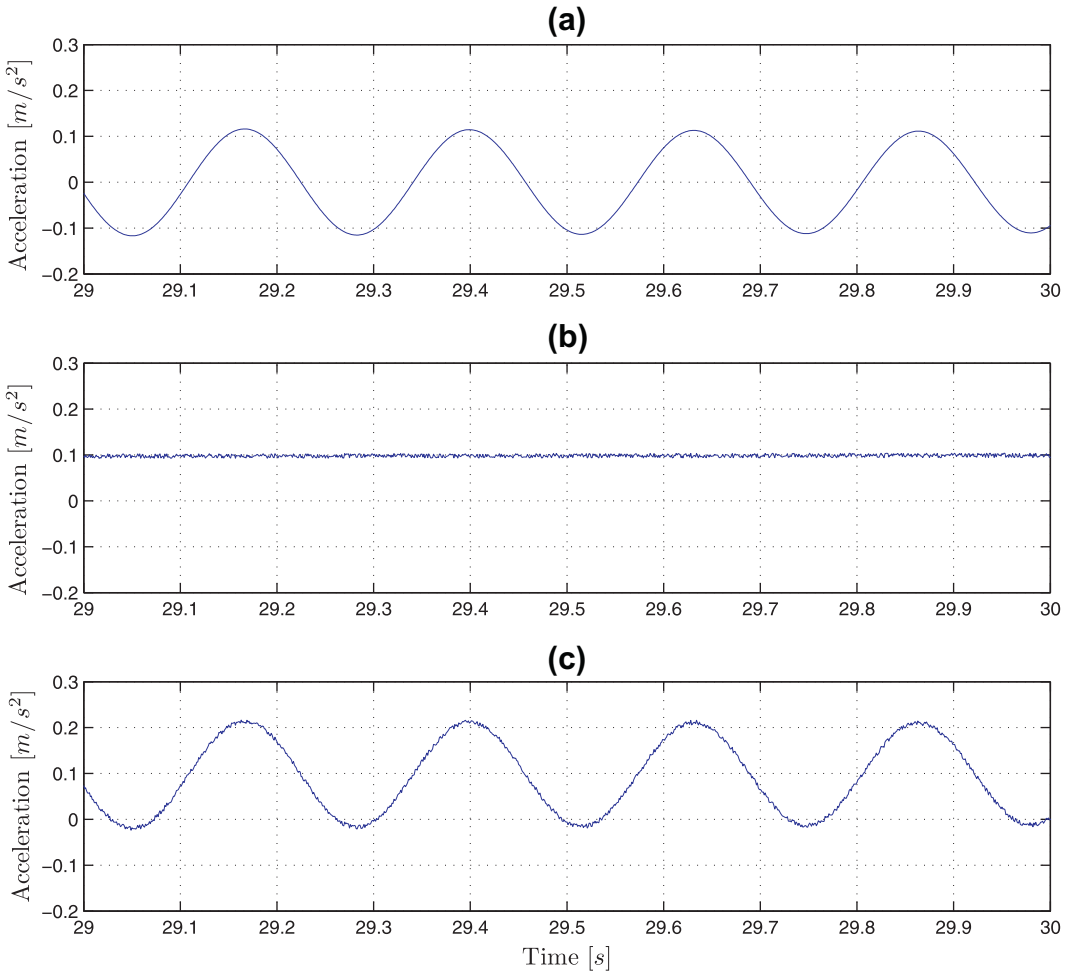

Fig. 5. Simulated response. (a) Original free vibration. (b) Disturbance. (c) Corrupted signal.

Table 1
Comparison between Butterworth filter and MLF. Best results are in bold.

Cut-off (Hz)		NMSE (%) $\times 10^{-4}$	
Low	High	Linear	Nonlinear
0.03125	–	5884	7006
0.0625	–	371	479
0.125	–	**329**	**425**
0.250	–	332	429
0.500	–	402	528
1.000	–	1057	1533
0.125	400	264	342
0.125	300	199	260
0.125	200	137	178
0.125	**150**	116	**137**
0.125	100	73	390
0.125	50	40	344
0.125	**25**	**24**	310
0.125	12.5	26	291
0.125	6.25	423	1127
MLF		**2.64**	**14.57**

4. Nonparametric identification

The evolution of the structure properties as a function of response amplitude is studied in this section by means of expeditious procedures. The study will serve to induce models describing properly the dynamic features of the structure. This is essential and should be previous to the modelling and parametric identification.

4.1. Mode shapes

The motion of the free vibration in the configuration space corresponding to the filtered time series of acceleration is depicted in Figs. 6 and 7. As can be seen, the motions exhibit a remarkable linear trend in all the cases, with correlation coefficients almost equal to one. This means that modes do not depend on the displacement magnitude. Therefore, mode shapes can be considered linear within the acceleration ranges of the experiments, which are compatible with the serviceability of the structure.

4.2. Backbone

The so-called backbone or skeleton curve [13] is obtained and analyzed in this section from the filtered free decay signals. Backbone represents the evolution of frequency as a function of acceleration amplitude. As the instantaneous frequency is time variant for nonlinear systems, the apparent frequency, i.e. the average value of the instantaneous frequency over a cycle of oscillation, is used instead. Thus, each cycle of the free response is evaluated independently as follows. The response zero-crossings are obtained by linear interpolation between consecutive points having different sign. From these, the apparent or averaged period and frequency of each cycle are computed. The amplitude related to each cycle is approximated by the maximum absolute value of the acceleration response.

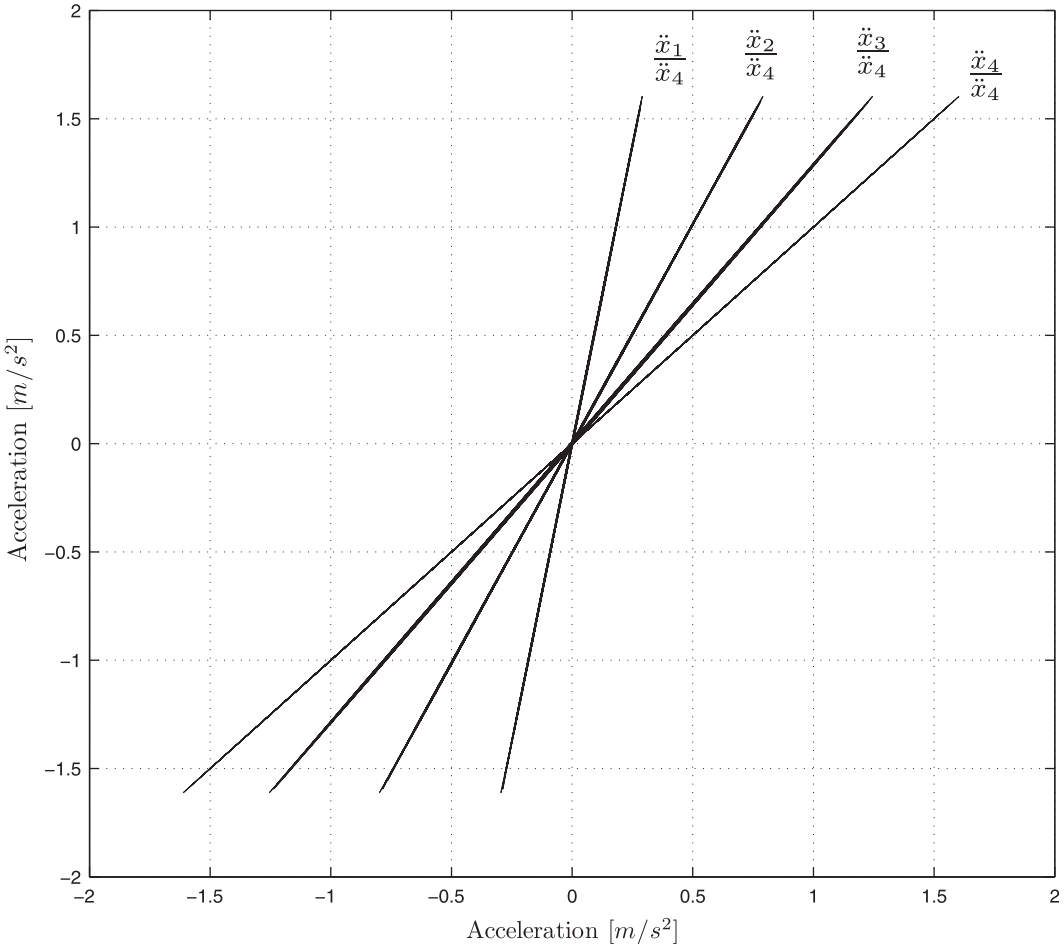

Fig. 6. First mode motions in the configuration space.

The obtained backbones are depicted in Fig. 9. As the results show a high scatter, specially for low amplitude, the graphics contain the moving average of 25 consecutive cycles in order to clarify the trend of data, which is the same for both modes. Backbones exhibit an incurvate shape. There is a maximum value of the apparent frequency for the lowest amplitude. From this point, frequency diminishes gradually as a function of amplitude. The total frequency drops in the range of experiments are around 0.35% and 0.55% for the first and second modes, respectively. Most of the frequency diminution take place for low values of the amplitude, while frequency tends to stabilize as the amplitude increases.

4.3. Damping curve

The damping curve is based on the equivalent viscous damping coefficient. This is defined as the damping coefficient of a linear model that provides a logarithmic decrement per cycle equal to that of the experiments. As in the previous section, this variable is averaged over 25 consecutive cycles in order to reduce the scatter, which is even higher for this variable. As the structure is lightly damped, the defined equivalent damping coefficient, c_i, can be approximated by the following formula:

$$c_i \cong \frac{\omega_i \delta_i}{\pi n}, \tag{10}$$

in which ω_i stands for the apparent frequency of ith cycle as evaluated in previous section, $n = 25$ is the considered number of cycles, and δ_i is the so-called logarithmic decrement [18]

$$\delta_i = \ln \frac{A_i}{A_{i+n}}, \tag{11}$$

in which A_i stands for the amplitude of ith cycle and is approximated as in the previous section.

The results of the identification are shown in Fig. 10 for both modes. As the curve of the first mode shows a little irregular shape, the related experiment was repeated and a similar shape was obtained. This odd result is therefore an inherent feature of this structure; it is not a particularity of the first experiment. Both curves show the same trend that is quite similar to those of the backbones, but in opposite direction. There is a minimum value of the damping for the lowest amplitude. From this minimum, damping increases gradually as a function of amplitude. The total damping increments in the range of experiments are around 45% and 70% for the first and second modes, respectively. Damping increases significantly for low values of the amplitude and tends to stabilize as the amplitude increases.

4.4. Discussion of results

The high linearity found for the modes can be likely due to the fact that stiffness nonlinearity is uniformly distributed across the structure. This issue will be addressed in detail in next section. This linearity allows the spatial variables to be expressed in the modal space by a linear transformation and the free decays to be independently formulated through the related modal variables.

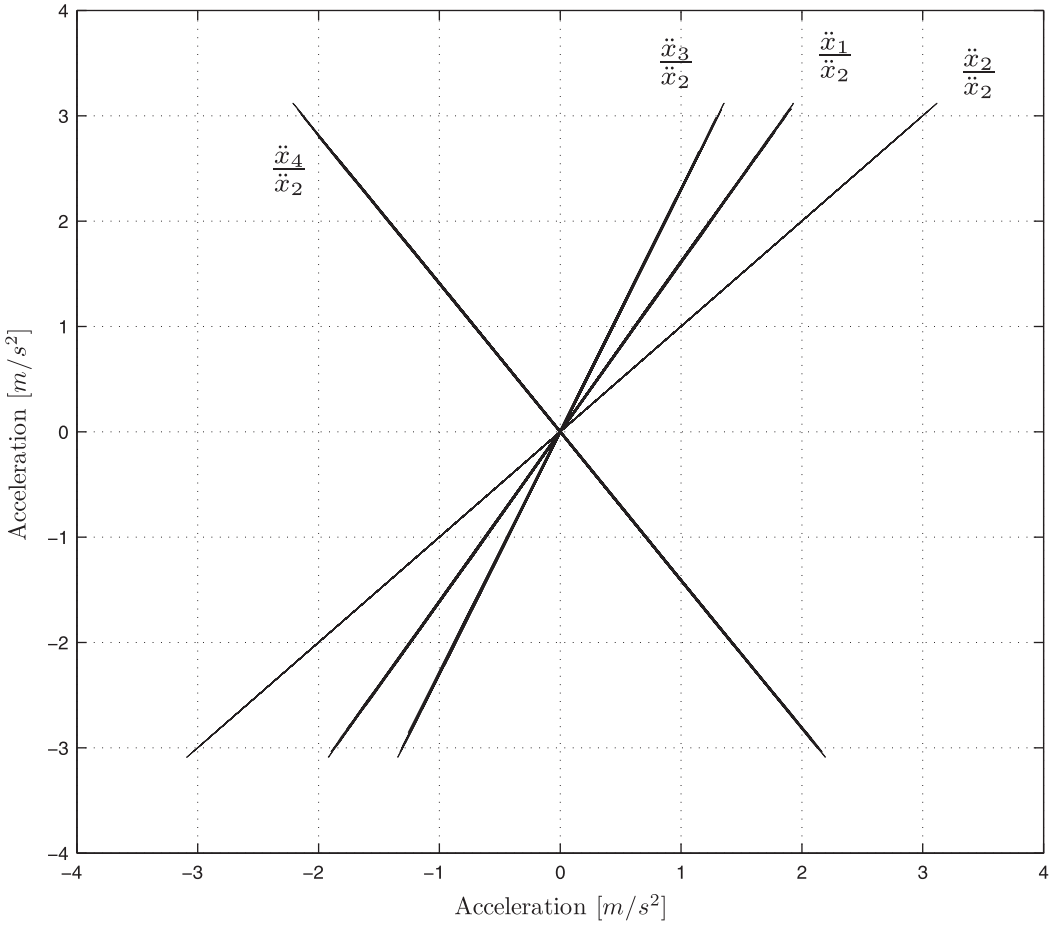

Fig. 7. Second mode motions in the configuration space.

The defined apparent frequency of the free vibration is mainly governed by the structural stiffness. From the obtained backbones can be therefore induced that the stiffness of the analyzed structure is weakly nonlinear. Moreover, the stiffness nonlinearity is notable for small displacements and diminishes gradually as the displacement increases. This trend of the backbones clearly indicates a typical preloaded nonlinear stiffness [13]. The tested structure has plenty of bolted and welded joints in which preloaded forces are present. These preloads make the joint interfaces to be initially in contact. When the structural vibration generates deformations commensurable to the pre-compressed deformations, the joints interfaces open in the related zones and this makes the structural stiffness to diminishes progressively as a function of the modal displacement. This is the physical mechanism that produces the observed nonlinearity.

The high number of cycles needed to attenuate the free response indicates that the structure is lightly damped. Moreover, the shape of the damping curve shows that damping is strongly nonlinear. The dissipation of energy in this structure is expected to be also concentrated at the component joints, because material damping is very low for steel structures and the interaction with the surrounding, which is known as radiation in literature, has an order of magnitude too small when comparing it to that of the dissipation component. The energy is dissipated in the joints by interfacial slip damping [19]. The effects of slipping could be reproduced by a Coulomb friction model. This damping mechanism does not agree with the experimental results. It is well known that the viscous damping coefficient equivalent to the Coulomb friction is a hyperbolical function that is asymptotic to zero when amplitude tends to infinity. The experimental damping curves show the opposite trend. This is due to the fact that the slipping area is not constant, but it increases progressively as a function of the shear stresses in the joints that depend on the response displacement. A linear viscous damping, which is another common mechanism adopted in practice, does not reproduce the experiments that show a strong nonlinearity. A nonlinear viscous damping would be thus an appropriate solution to describe the damping mechanism of this structure.

Within the displacement range of the experiments, the global behaviour of the structure is nonlinear for low displacements and tends to linearity for large displacements, the nonlinearities being localized at the joints of the structural components.

5. Modelling

5.1. Mode shapes

Adopting a discrete approach to globally model the free vibration of the structure and accounting for the properties induced from the experiments, the free vibration of the structure can be globally modelled by the following equation of motion:

$$\mathbf{M}\ddot{\mathbf{x}} + \mathbf{C}(\dot{\mathbf{x}}, \mathbf{x}) + \mathbf{K}(\mathbf{x})\mathbf{x} = \mathbf{0}, \tag{12}$$

in which $\mathbf{M}$, $\mathbf{C}$ and $\mathbf{K}$ stand for the mass, damping and stiffness matrices, $\ddot{\mathbf{x}}$, $\dot{\mathbf{x}}$ and $\mathbf{x}$ are the acceleration, velocity and displacement vectors. All these matrices are referred to the considered degrees of freedom (dofs), which are the floor translations in this case. As

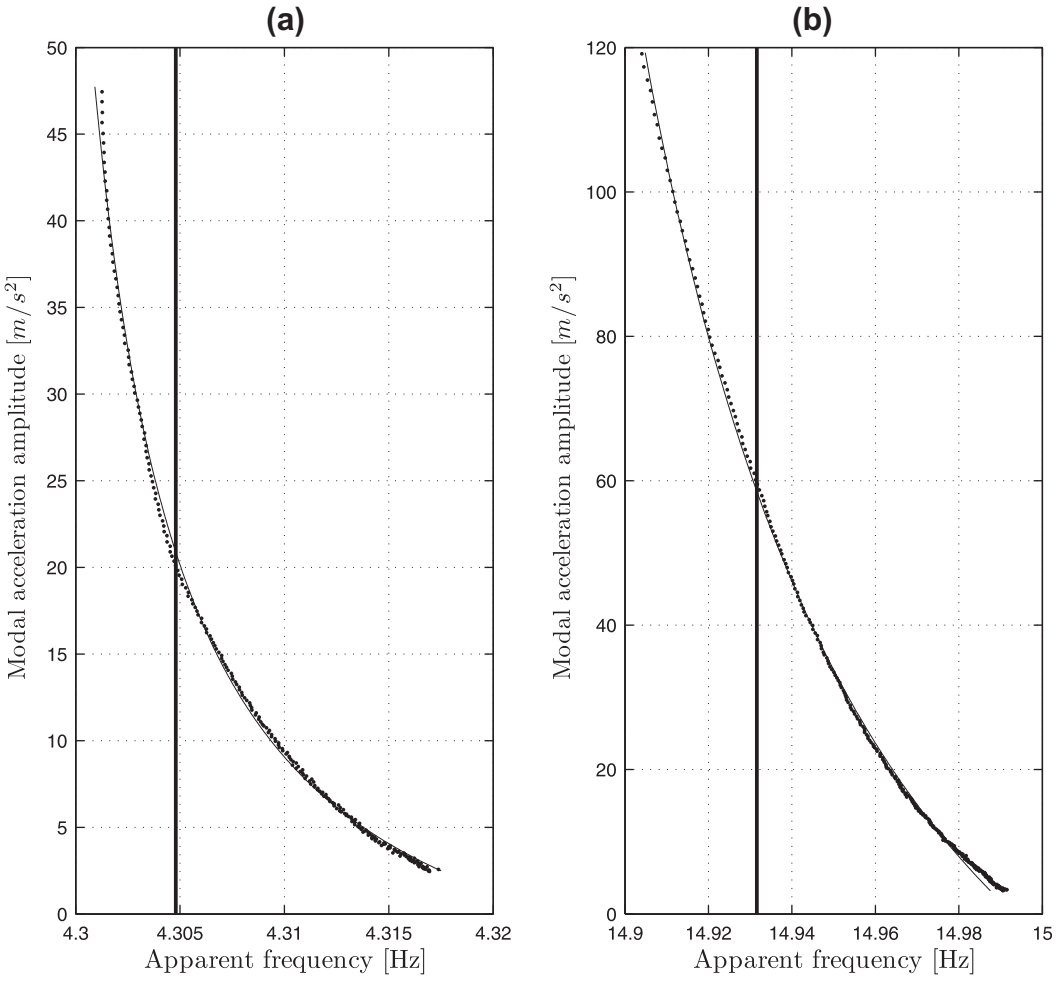

Fig. 8. Backbone. (a) First mode. (b) Second mode. Dots: Experimental results. Bold line: Linear model. Fine line: Nonlinear model.

stiffness and damping are nonlinear, the related matrices can be formulated as functions of the state variables x and $\dot{x}$ and other internal variables.

In accordance with the experimental results, mode shapes can be modelled by the following real-valued linear function:

$$x_{ir}(t) = \psi_{ir}\, x_{or}(t), \tag{13}$$

where ψ stands for the mode shape. Subscripts i, r and o indicate dof, mode and reference dof. This allows the following modal transformation to be formulated:

$$\mathbf{x_r}(t) = \psi_r z_r(t), \tag{14}$$

in which z_r denotes the rth modal coordinate.

In what follows, we are going to prove that the linear modes (13) are compatible with the nonlinear model (12) if a given hypothesis is satisfied. This hypothesis is that the nonlinearity is uniformly distributed across the structure in such a manner that the instantaneous stiffness matrix corresponding to a given modal coordinate, $z_r(t)$, is proportional to a constant reference matrix, $\mathbf{K_o}$. This is mathematically expressed in the form

$$\mathbf{K}(z_r) = \beta(z_r)\mathbf{K_o}, \tag{15}$$

in which $\beta(z_r)$ is a function of the modal coordinate, z_r, that takes the value $\beta(z_{ro}) = 1$ for the reference coordinate, z_{ro}. Indeed, taking into account that damping is very low and that the experimental modes are not complex, a proportional scheme can be adopted for damping. This means that modes can be obtained from the underlying undamped model of (12)

$$\mathbf{M}\ddot{\mathbf{x}} + \mathbf{K}(\mathbf{x})\mathbf{x} = \mathbf{0}, \tag{16}$$

substituting (14) and (15) into (16), this becomes

$$\mathbf{M}\boldsymbol{\psi_r}\ddot{z}_r(t) + \beta(z_r(t))\mathbf{K_o}\boldsymbol{\psi_r} z_r(t) = \mathbf{0}, \tag{17}$$

which describes the rth free vibration of the undamped model in the modal space. This nonlinear equation can be linearized by taking for β a constant value, β_a, given by the average over a cycle of vibration

$$\mathbf{M}\boldsymbol{\psi_r}\ddot{z}_r(t) + \beta_a\mathbf{K_o}\boldsymbol{\psi_r} z_r(t) = \mathbf{0}. \tag{18}$$

The solutions of this linear equation are [18]

$$z_r(t) = Ae^{i\omega_a t}, \tag{19}$$

in which A represents the constant vibration amplitude and ω_a is the apparent frequency, which is identical to that defined in Section 4.2 to analyze the experimental results. Both β_a and ω_a are functions of the response amplitude, A. Substituting (19) into (18) and after some mathematical manipulation, the latter becomes

$$\left(\mathbf{K_o} + \frac{\omega_a^2(A)}{\beta_a(A)}\mathbf{M}\right)\boldsymbol{\psi_r} = \mathbf{0}, \tag{20}$$

which constitutes a generalized eigenvalue problem. As matrices $\mathbf{K_o}$ and $\mathbf{M}$ are constant, the related eigenvector, $\boldsymbol{\psi_r}$, and eigenvalue, ω_o^2,

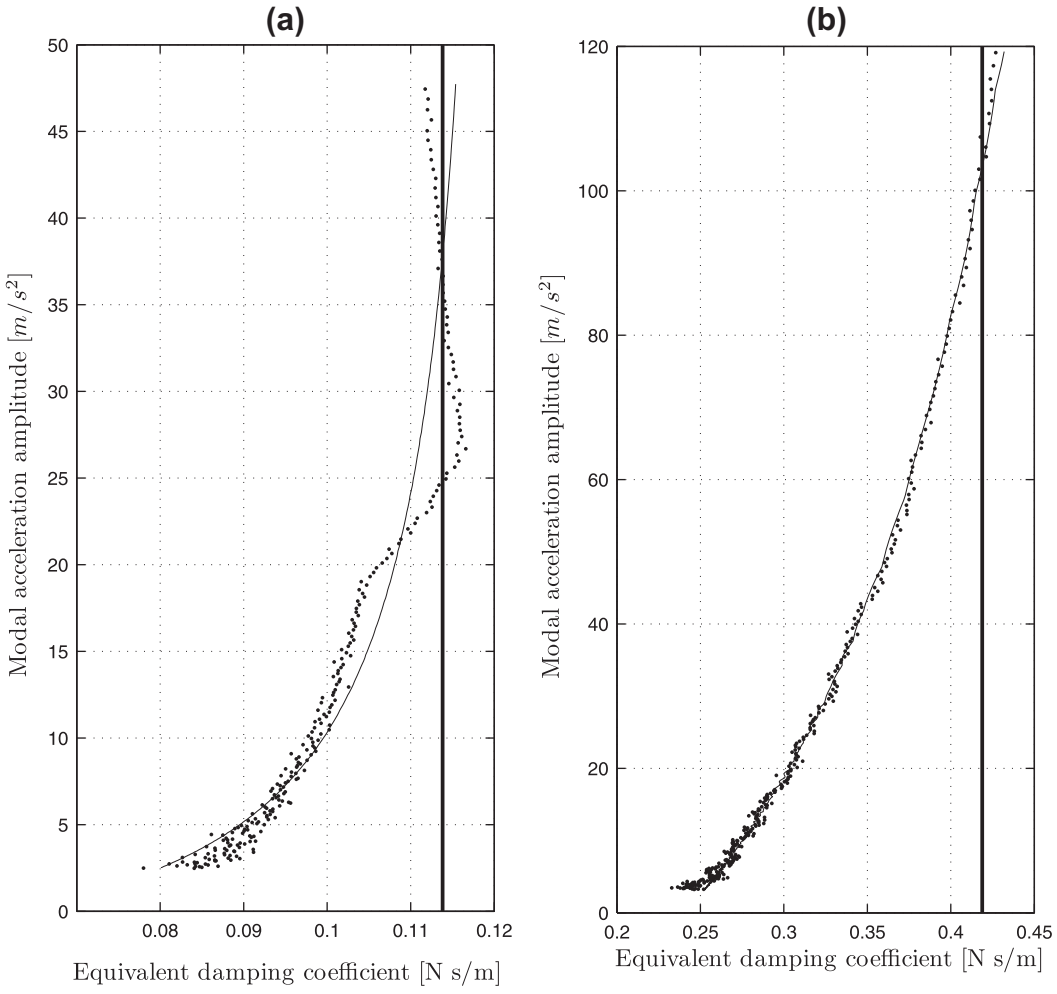

Fig. 9. Damping curve. (a) First mode. (b) Second mode. Dots: Experimental results. Bolt line: Linear model. Fine line: Nonlinear model.

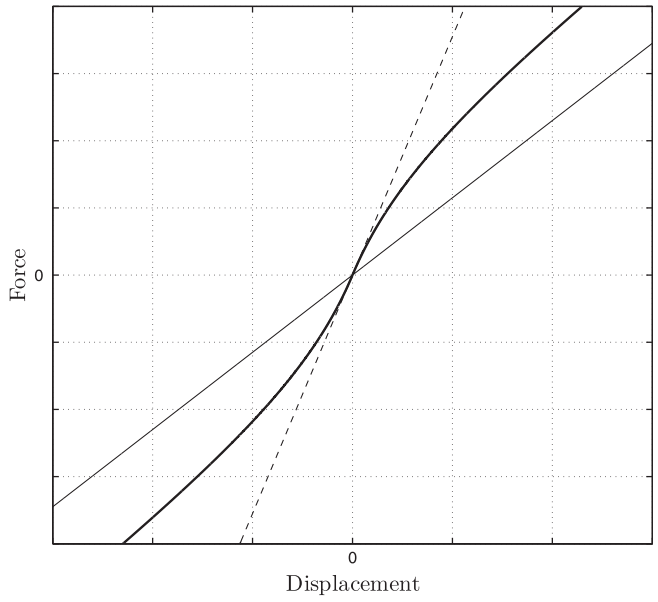

Fig. 10. Asymptotic law. Bold line: Force–displacement curve. Fine line: Ultimate stiffness. Discontinuous line: Initial stiffness.

are invariant. From the latter, the value of ω_a as a function of A can be obtained

$$\omega_a(A) = \omega_o \sqrt{\beta_a(A)}. \tag{21}$$

What we have found is that if the instantaneous stiffness matrix, **K**, is proportional to a constant reference matrix, $\mathbf{K_o}$, for a single mode free vibration, then the related mode shape, $\boldsymbol{\psi_r}$, is invariant with respect to the amplitude of vibration, A, while the apparent frequency, ω_a, is amplitude dependent. These deductions are consistent with the experimental results and prove the stated hypothesis.

5.2. Stiffness

The direct identification of the global stiffness matrix (12) is not practical, because it contains many parameters including cross-coupling terms and requires lots of experimental data. In this study, the identification is carried out in the modal space instead taking advantage of the experimental isolation of individual modes. After some trials, the following asymptotic law, which is suited to the experimental results as a function of the modal coordinate, z_r, was eventually adopted for the modal stiffness:

$$k_r(z_r) = \frac{k_{ir}\ \alpha_{kr} + k_{ur}|z_r(t)|}{\alpha_{kr} + |z_r(t)|}, \tag{22}$$

in which k_{ir} and k_{ur} are the bounds of the stiffness and α_{kr} is the stiffness shape parameter. The function is symmetric with respect to the modal coordinate. Moreover, it evolves progressively from the initial value k_{ir} for $z_r = 0$ and is asymptotic to the ultimate value k_{ur} when z_r tends to infinity. The curvature of the corresponding

force-displacement curve increases as a function of the stiffness shape parameter, α_{kr}. A force-displacement curve showing the evolution of the proposed law along with the initial and ultimate stiffnesses is depicted in Fig. 10. The graphic does not correspond to the experiments, but the model parameters have been deliberately exaggerated for illustration purposes.

5.3. Damping

As the obtained damping curves exhibit a shape similar to that of the backbones, an asymptotic law is also adopted to model the modal damping, c_r, as a function of the modal velocity, $\dot{z}_r$

$$c_r(\dot{z}_r) = \frac{c_{ir}\ \alpha_{cr} + c_{ur}|\dot{z}_r(t)|}{\alpha_{cr} + |\dot{z}_r(t)|}, \tag{23}$$

in which c_{ir} and c_{ur} are the bounds of the damping coefficient and α_{cr} is the damping shape parameter.

5.4. Modal equation of motion

Assuming mass-normalized mode shape vectors [18], the proposed nonlinear equation of motion corresponding to the rth mode would be

$$\ddot{z}_r(t) + \left(\frac{c_{ri}\alpha_{cr} + c_{ru}|\dot{z}_r(t)|}{\alpha_{cr} + |\dot{z}_r(t)|}\right)\dot{z}_r(t) + \left(\frac{k_{ri}\alpha_{kr} + k_{ru}|z_r(t)|}{\alpha_{kr} + |z_r(t)|}\right)z_r(t) = 0. \tag{24}$$

6. Calibration

In this section the parameters of the proposed models are calibrated by fitting its response to the filtered experimental data in the time domain.

6.1. Mode shapes and modal accelerations

As the adopted formulation for the mode shapes (13) is linear in the parameter and the number of available data sets is higher than the number of parameters, an analytical solution exists and can be obtained in a least-squares sense [17] as follows:

$$\psi_{ir} = \left(\ddot{\mathbf{x}}_{\mathbf{or}}^{\mathbf{T}}\ddot{\mathbf{x}}_{\mathbf{or}}\right)^{-1}\ddot{\mathbf{x}}_{\mathbf{or}}^{\mathbf{T}}\ddot{\mathbf{x}}_{\mathbf{ir}}, \tag{25}$$

in which ψ_{ir} stands for the rth mode shape coordinate related to the ith dof, $\ddot{\mathbf{x}}_{\mathbf{or}}$ and $\ddot{\mathbf{x}}_{\mathbf{ir}}$ represent the acceleration time series of rth mode for the reference and ith dofs, respectively. Results are shown in Table 2 along side the correlation coefficients, which are close to one in all the cases.

The mode shapes are mass-normalized by the following [18]:

$$\phi_{\mathbf{r}} = \frac{1}{\sqrt{\psi_{\mathbf{r}}^{\mathbf{T}}\mathbf{M}\psi_{\mathbf{r}}}}\psi_{\mathbf{r}}, \tag{26}$$

Table 2
Mode shapes.

Mode	dof	ψ	Correlation
1	1	0.1811	0.99995725
	2	0.4929	0.99999108
	3	0.7767	0.99998806
	4	1.0000	1.00000000
2	1	0.6186	0.99998222
	2	1.0000	1.00000000
	3	0.4326	0.99997735
	4	−0.7084	−0.99998769

in which $\boldsymbol{\phi}_{\mathbf{r}}$ and $\mathbf{M}$ stand for the mass-normalized rth mode shape and the mass matrix, respectively. The latter was formulated as a diagonal matrix including the total mass of each storey for each corresponding dof.

The modal accelerations are obtained from (14) through the following least-squares solution:

$$\ddot{\mathbf{z}}_{\mathbf{r}} = \left(\phi_{\mathbf{r}}^{\mathbf{T}}\phi_{\mathbf{r}}\right)^{-1}\phi_{\mathbf{r}}^{\mathbf{T}}\ddot{\mathbf{X}}_{\mathbf{r}}, \tag{27}$$

in which $\ddot{\mathbf{z}}_{\mathbf{r}}$ denotes the time series acceleration of rth mode, $\ddot{\mathbf{X}}_{\mathbf{r}}$ is a matrix containing the spatial time series of acceleration. Results are shown in Fig. 11. The obtained modal accelerations will be used hereafter to identify the rest of model parameters.

6.2. Stiffness and damping

The formulation (24) proposed to reproduce the modal dynamic behaviour of the structure is not linear in the stiffness and damping parameters. Under these circumstances, the unknown parameters cannot be analytically obtained and an iterative scheme should be adopted to find the solution [17]. Thus, the evaluation of these parameters is posed as the minimization of an error function accounting for the discrepancies between the numerical and experimental responses. The error function is defined in the time domain through time series of modal accelerations corresponding to the free decays. The normalized mean squared error is chosen as error function

$$\varepsilon = \frac{\sum_{t=0}^{(M-1)\Delta t}\left(\ddot{z}_r^{(a)}(t) - \ddot{z}_r^{(e)}(t)\right)^2}{\sum_{t=0}^{(M-1)\Delta t}\left(\ddot{z}_r^{(e)}(t)\right)^2}, \tag{28}$$

where $\ddot{z}_r^{(a)}(t)$ and $\ddot{z}_r^{(e)}(t)$ represent respectively the model-predicted and the experimental modal accelerations, the latter being evaluated through Eq. (27). M and Δt are the number of available data points and the sampling period, respectively.

The minimization is carried out by an adaptive stochastic algorithm developed previously by the authors, which will be referred to as beta algorithm for the remainder of the paper. This algorithm is described in detail and tested against numerical simulations and experiments in Ref. [14]. A brief description of the beta algorithm is given here. In this algorithm the solution is sought by sampling the parameters to be identified within a bounded space in an iterative form. The Beta distribution, which is consistent with the bounded character of the search space, is selected for sampling purposes. Initially, the parameters of the sampling distributions are set equal to one. Thus, the Beta distribution becomes the uniform distribution and an initial point is obtained by pure random sampling. In the subsequent steps, the properties of the sampling distributions are modified accordingly the results of the previous steps. A step is said to be successful when the value of the related error function (28) is lower than the previous ones. If not, the step is considered unsuccessful. If a step is successful, the modes of the distributions are set equal to the last sampled values of the parameters. Moreover, the variances of the distributions are increased multiplying the previous ones by a factor greater than one. Conversely, if a step is unsuccessful, then the modes of the distributions are not modified, while the variances are decreased multiplying the previous ones by a factor less than one. Both factors are functions of the dimension of the parameter space. The anisotropic version of the algorithm, which significantly speeds up the minimization process, was chosen in this case. This consists in adopting a different value of the variance for each distribution. To this end, the increments of the parameters in several previous successful steps are recorded and used to calculate variance weights. In each successful step the variances of the distributions are multiplied by the

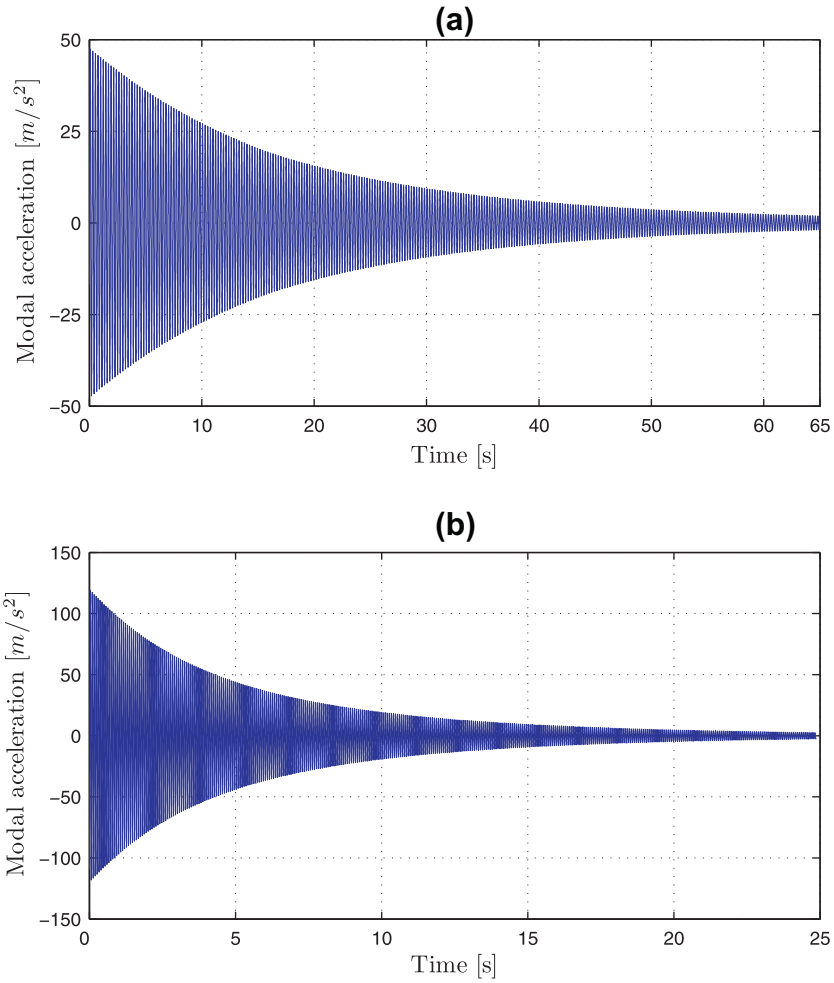

Fig. 11. Modal acceleration free vibrations. (a) First mode. (b) Second mode.

corresponding weights. The process is repeated until a given stopping criterion is reached.

The model-predicted response needed to evaluate ε in each step of the minimization was numerically computed from the equation of motion (24) adopting the following regressive differences approximation for the first derivative with respect to time:

$$\dot{z}(t) = \frac{z(t) - z(t-\Delta t)}{\Delta t}, \tag{29}$$

while a central differences scheme was chosen for the second derivative:

$$\ddot{z}(t) = \frac{z(t+\Delta t) - 2z(t) + z(t-\Delta t)}{\Delta^2 t}. \tag{30}$$

This approach gives rise to a practical explicit formulation of the response that is obtained substituting (29) and (30) into (24)

$$\begin{aligned} z_r(t) =& 2z_r(t-\Delta t) - z_r(t-2\Delta t) \\ & - \frac{(k_{ri}\alpha_{kr} + k_{ru}|z_r(t-\Delta t)|)\ \Delta^2 t}{\alpha_{kr} + |z_r(t-\Delta t)|} z_r(t-\Delta t) \\ & - \frac{\left(c_{ri}\alpha_{cr} + c_{ru}\frac{|z_r(t-\Delta t) - z_r(t-2\Delta t)|}{\Delta t}\right)\ \Delta t}{\alpha_{cr} + \frac{|z_r(t-\Delta t) - z_r(t-2\Delta t)|}{\Delta t}} \\ & \times (z_r(t-\Delta t) - z_r(t-2\Delta t)), \end{aligned} \tag{31}$$

where Δt represent in this equation the integration period. A value of $\Delta t = 5 \times 10^{-4}$ s was chosen for the integration. This value constitutes a trade-off between accuracy of results and computation cost. Besides, this explicit formulation would be useful for some future practical applications such as vibration control.

Table 3
Nonlinear model results.

Mode	k_{ir} (N/m)	k_{ur} (N/m)	α_{kr} (m)	c_{ir} (N s/m)	c_{ur} (N s/m)	α_{cr} (m/s)	ε (%)
1	737.9413	728.6962	0.0089	0.0616	0.1226	0.1572	0.0039
2	8874.5	8686.3	0.0075	0.2409	0.5935	0.7313	0.0032

The total number of unknown parameters is eight for each mode. They comprise three stiffness parameters: k_{ir}, k_{ur} and α_{kr}; three damping parameters: c_{ir}, c_{ur} and α_{cr}; and two initial conditions: $z(0)$ and $z(\Delta t)$. Calibration results are shown in Table 3. The achieved fitting errors are similar for both modes and have very low values, around 0.0035%. According to Ref. [1], the proposed model provides an excellent representation of the free response, because the fitting error is lower than 1%. Fig. 12 shows the initial and final cycles of the response predicted by the model along with the experimental results. As can be seen, there is an excellent agreement of results in both amplitude and phase. The numerical response was also used to compute the related backbones and damping curves by the same procedure as for the experimental data. Results are shown in Figs. 8 and 9 and they also indicate a very good fitting to the experiments.

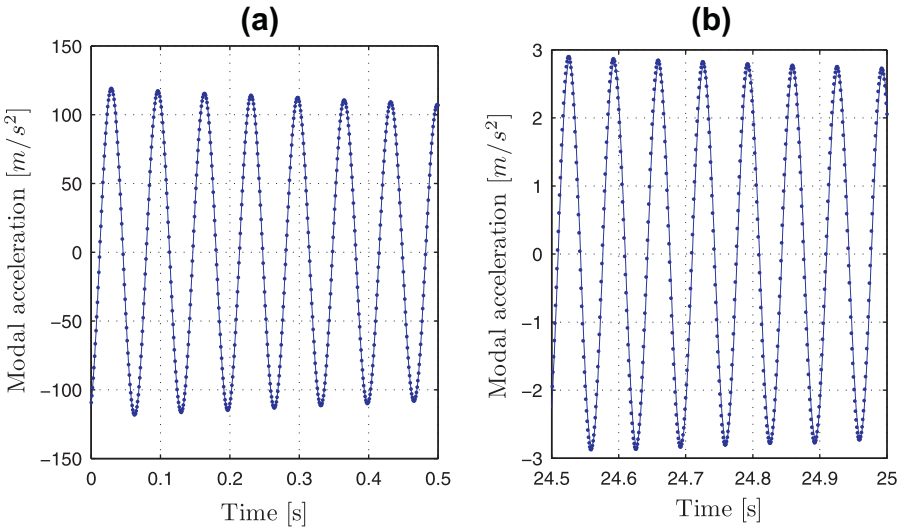

Fig. 12. Second mode free vibration. Dots: experimental results. Lines: Nonlinear model predictions. (a) Initial cycles. (b) Final cycles.

Table 4
Linear model results.

Mode	k_r (N/m)	c_r (N s/m)	ε (%)
1	731.5933	0.1138	1.8081
2	8802.0	0.4184	4.9881

6.3. Discussion of results

In order to have a reference to be compared with, the procedure used for the identification of the nonlinear model was applied to a pure linear model

$$\ddot{z}_r(t) + c_r\dot{z}_r(t) + k_r z_r(t) = 0. \tag{32}$$

This case has only four unknown parameters: c_r, k_r, $z_r(0)$ and $z_r(-\Delta t)$. The identified parameters are shown in Table 4 along side the fitting errors. As can be seen, the fitting errors are three orders of magnitude higher than those of the nonlinear model. Fig. 13 shows the numerical and experimental responses, which have a notable discrepancy in both amplitude and phase. The corresponding backbones and damping curves in Figs. 8 and 9 are now straight lines that do not reflect the reality. Thus, the nonlinear model clearly outperforms the linear one.

It has been demonstrated in the nonparametric identification that the structure behaviour tends to linearity as the displacement increases, while it turns out to be nonlinear for small displacements. The upper parameters k_{ur} and c_{ur} established for the nonlinear model represent the asymptotic values of the stiffness and damping when the modal displacement tends to infinity. Consequently, the parameters k_{ur} and c_{ur} represent respectively the stiffness and damping coefficient of the underlying linear model. It should be highlighted that a linear identification based on low response level, as that caused by ambient or operational excitation, would be far away from the 'true' underlying linear model, especially for the damping. In the studied structure, these discrepancies would be between 0.6% and 1.1% for stiffness and around 55% for damping.

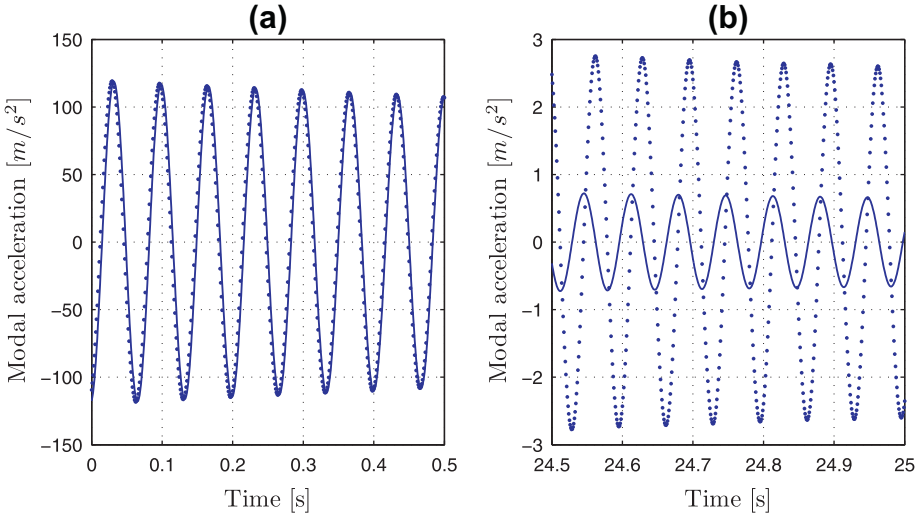

Fig. 13. Second mode free vibration. Dots: experimental results. Lines: Linear model predictions. (a) Initial cycles. (b) Final cycles.

7. Conclusions

This exercise on the UNIOVI structure has been very instructive and allows a number of conclusions. On the experimental side, it was found that the first two bending modes in the longitudinal direction of the structure can be individually isolated by means of a single-point mono-harmonic excitation placed at the top floor and they remain during the subsequent free decay vibration. The identification was based on the measured modal free decays. A novel procedure called moving linear fitting was developed to filter the raw signal, which is a prerequisite for an accurate identification. It was proved that the proposed procedure outperforms conventional band-pass filters.

The nonparametric identification reveals that the structure is weakly nonlinear in stiffness and strongly nonlinear in damping, while mode shapes remain linear within the range of experiments. It was proved that these linear mode shapes are compatible with the nonlinear stiffness as long as the nonlinearity is uniformly distributed across the structure. The global behaviour of the structure is nonlinear for low modal displacements and tends to linearity for large displacements. The shape of the backbones indicates a typical preloaded nonlinear stiffness, while a nonlinear viscous damping can describe the damping curves.

Modal modes has been linearly modelled. This allows the free responses to be expressed in the modal space by a linear transformation. Nonlinear asymptotic laws were chosen to model the modal stiffness and damping. The proposed nonlinear modal model was calibrated by minimizing the discrepancies between the model-predicted response and the experiments in the time domain. The nonlinear model clearly outperforms the pure linear model, with fitting errors three orders of magnitude lower. The ultimate stiffness and damping parameters of the nonlinear model, those corresponding to large displacements, are found to be representative of the underlying linear model instead of the initial parameters, which correspond to that of small displacements.

This accurate nonlinear model and its calibration procedure will be exploited in future applications on SHM, finite element model updating and structural serviceability checking. The cross-coupling nonlinear terms should be identified in future to complete the model.

Acknowledgements

The authors wish to thank the Science and Innovation Ministry of Spain for its financial support (Projects BIA2006-15266-C02-01 and BIA2006-15266-C02-02). The experimental part of this work has been carried out at the laboratory of Fluid Mechanics of the University of Oviedo. The collaboration of the staff of this area, particularly Professor Santolaria, is greatly acknowledged.

References

[1] Worden K, Tomlinson GR. Nonlinearity in structural dynamics: detection, identification and modelling. Taylor & Francis; 2001 [ISBN:9780750303569].
[2] Živanović S, Pavic A, Reynolds P. Vibration serviceability of footbridges under human-induced excitation: a literature review. J Sound Vib 2005;279:1–74.
[3] ISO. Basis for design of structures-serviceability of buildings and pedestrian structures against vibration. Geneva: ISO 10137 International Organization for Standardization; 2007.
[4] FEMA-350E. Recommended seismic design criteria for new steel moment-frame buildings. Washington (DC): Federal Emergency Management Agency; 2000.
[5] Sohn H, Farrar CR, Hemez FM, Shunk DD, Stinemates DW, Nadler BR. A review of structural health monitoring literature: 1996–2001. Los Alamos National Laboratory Report LA-13976-MS; 2003.
[6] Brandon JA. Towards a nonlinear identification methodology for mechanical signature analysis, damage assessment of structures. In: Proceedings of the international conference on damage assessment of structures (DAMAS 1999), Dublin, Ireland; xxxx. p. 265–72.
[7] Modena C, Sonda D, Zonta D. Damage localization in reinforced concrete structures by using damping measurements, damage assessment of structures. In: Proceedings of the international conference on damage assessment of structures (DAMAS 1999), Dublin, Ireland; xxxx. p. 132–41.
[8] Kerschen G, Worden K, Vakakis AF, Golinval J-C. Past, present and future of nonlinear system identification in structural dynamics. Mech Syst Sig Process 2006;20:505–92.
[9] Atkins PA, Wright JR, Worden K. An extension of force appropriation to the identification of non-linear multi-degree of freedom systems. J Sound Vib 2000;237:23–43.
[10] Platten ME, Wright JR, Dimitriadis G, Cooper JE. Identification of multi-degree of freedom non-linear systems using an extended modal space model. Mech Syst Sig Process 2009;23:8–29.
[11] Peeters M, Kerschen G, Golinval J-C. Dynamic testing of nonlinear vibrating structures using nonlinear normal modes. J Sound Vib 2011;330:486–509.
[12] Peeters M, Kerschen G, Golinval J-C. Modal testing of nonlinear vibrating structures based on nonlinear normal modes: experimental demonstration. Mech Syst Sig Process 2011;25:1227–47.
[13] Feldman M. Hilbert transform in vibration analysis. Mech Syst Sig Process 2011;25:735–802.
[14] Zapico-Valle JL, Alonso-Camblor R, González-Martínez MP, García-Diéguez M. A new method for finite element model updating in structural dynamics. Mech Syst Sig Process 2010;24:2137–59.
[15] Users Manual Version 6.5 MATLAB. In The Math Works, Inc.; 2002.
[16] Shi W, Shan J, Lu X. Modal identification of Shangai World Financial Center both from free and ambient vibration response. Eng Struct 2012;36:14–26.
[17] Ljung L. System identification. 2nd ed. Upper Daddle River (NJ): Prentice Hall PTR; 1999 [07458].
[18] Maia NMM, Silva JMM. Theoretical and experimental modal analysis. Research Studies Press, Ltd.; 1997 [ISBN:978-0863802089].
[19] Prandina M. Spatial damping identification. PhD thesis. University of Liverpool; 2010. <www.cfd4aircraft.com/research_themes/structuraldamping/PhDthesis.pdf>.

Bibliografía

[1] C. Mares, J. E. Mottershead and M. I. Friswell. Stochastic model updating: Part 1—theory and simulated example. *Mechanical Systems and Signal Processing*, 20 (2006) 1674–95.

[2] M. I. Friswell and J. E. Mottershead. Finite Element Model Updating in Structural Dynamics. *New York: Kluwer–Academic.* 1995.

[3] M. I. Friswell and J. E. Mottershead. Model Updating in Structural Dynamics: A Survey". *Journal of Sound and Vibration*, 167(2) (1993) 347-375.

[4] C. C. Chang, T. Y. P. Chang and Y. G. Xu. Adaptive neural networks for model updating of structures. *Smart Materials and Structures*, 9 (2000) 59–68.

[5] J. L. Zapico, M. P. González, M. I. Friswell, C. A. Taylor and A. J. Crewe. Finite element model updating of a small scale bridge. *Journal of Sound and Vibration*, 268 (2003) 993–1012.

[6] J. L. Zapico, F. J. Molina, M. P. González, S. Montes. Identification of a composite frame from a pseudodynamic test. *Mechanical Systems and Signal Processing*, 19 (2005) 579-595.

[7] J. Arora. Introduction to Optimum Design (2nd edn). *Hardbound*. 2004.

[8] G. R. Liu and X. Han. Computational Inverse Techniques in Nondestructive Evaluation. *CRC Press*. 2003.

[9] N. M. M. Maia and J. M. M. Silva. Theoretical and Experimental Modal Analysis. *Research Studies Press LTD.* 1997.

[10] R. I. Levin and N. A. J. Lieven. Dynamic finite element model updating using simulated annealing and genetic algorithms. *Mechanical Systems and Signal Processing*, (1998) 91–120.

[11] C. G. Koh, Y. F. Chen, C.-Y. Liaw. A hybrid computational strategy for identification of structural parameters. *Computers and Structures*, 81 (2003) 107 - 117.

[12] O. Begambre, J. E. Laier. A hybrid Particle Swarm Optimization Simplex algorithm (PSOS) for structural damage identification. *Advances in Engineering Software*, (2009). doi:10.1016/j.advengsoft.2009.01.004.

[13] K. Worden, G. R. Tomlinson. Nonlinearity in structural dynamics: detection, identification and modelling. *Taylor & Francis*. 2001 [ISBN:9780750303569].

[14] S. Zivanovic, A. Pavic, P. Reynolds. Vibration serviceability of footbridges under human-induced excitation: a literature review. *Journal of Sound and Vibration*, 279 (2005) 1‑74.

[15] ISO. Basis for design of structures-serviceability of buildings and pedestrian structures against vibration. *Geneva: ISO 10137 International Organization for Standardization*. 2007.

[16] FEMA-350E. Recommended seismic design criteria for new steel moment-frame buildings. *Washington (DC): Federal Emergency Management Agency*. 2000.

[17] H. Sohn, C. R Farrar, F. M. Hemez, D. D. Shunk, D. W. Stinemates, B. R. Nadler. A review of structural health monitoring literature: 1996‑2001. *Los Alamos National Laboratory Report LA-13976-MS*, 2003.

[18] J. A. Brandon. Towards a nonlinear identification methodology for mechanical signature analysis, damage assessment of structures. *Proceedings of the international conference on damage assessment of structures (DAMAS 1999), Dublin, Ireland*, (1999) 265–72.

[19] C. Modena, D. Sonda, D. Zonta. Damage localization in reinforced concrete structures by using damping measurements, damage assessment of structures. *Proceedings of the international conference on damage assessment of structures (DAMAS 1999), Dublin, Ireland*, (1999) 132‑41.

[20] P. A. Atkins, J. R. Wright, K. Worden. An extension of force appropriation to the identification of non-linear multi-degree of freedom systems. *Journal of Sound and Vibration*, 237 (2000) 23‑43.

[21] M. E. Platten, J. R. Wright, G. Dimitriadis, J. E. Cooper. Identification of multi-degree of freedom non-linear systems using an extended modal space model. *Mechanical Systems and Signal Processing*, 23 (2009) 8‑29.

[22] M. Peeters, G. Kerschen, J.-C. Golinval. Dynamic testing of nonlinear vibrating structures using nonlinear normal modes. *Journal of Sound and Vibration*, 330 (2011) 486‑509.

[23] M. Peeters, G. Kerschen, J.-C. Golinval. Modal testing of nonlinear vibrating structures based on nonlinear normal modes: experimental demonstration. *Mechanical Systems and Signal Processing*, 25 (2011) 1227‑47.

[24] S. Sehgal and H. Kumar. Structural Dynamic Model Updating Techniques: A State of the Art Review. *Archives of Computational Methods in Engineering*, 2015. doi 10.1007/s11831-015-9150-3.

[25] D. J. Ewins. Modal testing: theory, practice and application, 2nd edn. *Research Studies Press Limited, England, UK*. 2000.

[26] J. P. D. Hartog. Mechanical vibrations. *McGraw-Hill Book Company Inc, USA*. 1934

[27] M. Petyt. Introduction to finite element vibration analysis. *Cambridge University Press, Cambridge, UK*. 1998.

[28] A. Berman. Mass matrix correction using an incomplete set of measured modes. *Journal of American Institute of Aeronautics and Astronautics*, 17 (1979) 1147–1148.

[29] M. Baruch, I. Y. Bar-Itzhack. Optimal weighted Orthogonalization of measured modes. *Journal of American Institute of Aeronautics and Astronautics*, 16 (4) (1978) 346–351.

[30] A. Berman, E. J. Nagy. Improvement of a large analytical model using test data. *Journal of American Institute of Aeronautics and Astronautics,* 21 (1983) 1168–1173.

[31] B. Caesar. Update and identification of dynamic mathematical models. *Proceedings of the fourth international modal analysis conference. Los Angeles, USA,* (1986) 394–401.

[32] J. Carvalho, B. N. Datta, A. Gupta and M. Lagadapati. A direct method for model updating with incomplete measured data and without spurious modes. *Mechanical Systems and Signal Processing*, 21 (2007) 2715–2731.

[33] R. J. Allemang, and D. L. Brown. A Correlation Coefficient for Modal Vector Analysis. *1st International Modal Analysis Conference. Orlando, Florida,USA,* (1982) 110-116.

[34] J. C. Chen, C. P. Kuo and J. A. Garba. Direct structural parameter identification by modal test results. *Proceedings of the 24th structural dynamics and materials conference.* California, USA, (1983) 44–49.

[35] J. Sidhu and D. J. Ewins. Correlation of finite element and modal test studies of a practical structure. *Proceedings of the second international modal analysis conference. Orlando, USA,* (1984) 756–762.

[36] A. M. Kabe. Stiffness matrix adjustment using mode data. *Journal of American Institute of Aeronautics and Astronautics,* 23 (1985) (9) 1431–1436.

[37] C. Farhat, F. M. Hemez. Updating finite element dynamic models using an element-by-element sensitivity methodology. *Journal of American Institute of Aeronautics and Astronautics,* 31(9) (1993) 1702–1711.

[38] M. I. Friswell, D. J. Inman, D. F. Pilkey. The direct updating of damping and stiffness matrices. *Journal of American Institute of Aeronautics and Astronautics,* 36 (3) (1998) 491–493.

[39] Z. Xiamin. A best matrix approximation method for updating the analytical model. *Journal of Sound and Vibration,* 223 (5) (1999) 759–774.

[40] S. L. J. Hu, H. Li, S. Wang. Cross-model cross-mode method for model updating. *Mechanical Systems and Signal Processing,* 21 (2007) 1690–1703.

[41] H. Fang, T. J. Wang, X. Chen. Model updating of lattice structures: a substructure energy approach. *Mechanical Systems and Signal Processing,* 25 (5) (2011) 1469–1484.

[42] E. Jacquelin, S. Adhikari, M. I. Friswell. A second-moment approach for direct probabilistic model updating in structural dynamics. *Mechanical Systems and Signal Processing,* 29 (2012) 262–283.

[43] J. Jiang, H. Dai, Y. Yuan. A symmetric generalized inverse eigenvalue problem in structural dynamics model updating. *Linear Algebra and its Applications,* 439 (2013) 1350–1363.

[44] J. D. Collins, G. C. Hart, T. K. Hasselman, B. Kennedy. Statistical identification of structures. *Journal of American Institute of Aeronautics and Astronautics,* 12 (2) (1974) 185–190.

[45] J. C. Chen, J. A. Garba. Analytical model improvement using modal test results. *Journal of American Institute of Aeronautics and Astronautics,* 18 (6) (1980) 684–690.

[46] K. O. Kim, W. J. Anderson, R. E. Sandstrom. Non-linear inverse perturbation method in dynamic analysis. *Journal of American Institute of Aeronautics and Astronautics*, 21 (9) (1983) 1310–1316.

[47] R. M. Lin, M. K. Lim, H. Du. Improved inverse eigensensitivity method for structural analytical model updating. *ASME Journal of Vibration and Acoustics*, 117 (2) (1995) 192–198.

[48] R. M. Lin, D. J. Ewins. Model updating using FRF data. *Proceedings of 15th international modal analysis seminar. KU Leuven, Belgium*, (1990) 141–162.

[49] S. V. Modak, T. K. Kundra, B. C. Nakra. Prediction of dynamic characteristics using updated finite element models. *Journal of Sound and Vibration*, 254 (3) (2002a) 447–467.

[50] S. V. Modak, T. K. Kundra, B. C. Nakra. Comparative study of model updating methods using simulated experimental data. *Computer and Structures*, 80 (2002b) 437–447.

[51] M. Imregun, D. J. Ewins, I. Hagiwara, T. A. Ichikawa Comparison of sensitivity and response function based updating techniques. *Proceedings of 12th international modal analysis conference. Hawaii, USA*, (1994) 1390–1400.

[52] V. Arora, S. P. Singh, T. K. Kundra. Finite element model updating with damping identification. *Journal of Sound and Vibration*, 324 (2009) 1111–1123.

[53] V. Arora, S. P. Singh, T. K. Kundra. Damped model updating using complex updating parameters. *Journal of Sound and Vibration*, 320 (2009) 438–451.

[54] D. F. Pilkey. Computation of damping matrix for finite element model updating. *Ph.D. thesis, Virginia Polytechnic Institute and State University. Virginia.* 1998.

[55] V. Arora. Comparative study of finite element model updating methods. *Journal of Vibration and Control*, 17(13) (2011) 2023–2029.

[56] R. M. Lin, D. J. Ewins. Model updating using FRF data. *Proceedings of 15th international modal analysis seminar. KU Leuven, Belgium*, (1990) 141–162.

[57] S. Pradhan, V. Modak. Normal response function method for mass and stiffness matrix updating using complex FRFs. *Mechanical Systems and Signal Processing*, 32 (2012) 232–250.

[58] S. Pradhan, V. Modak. A method for damping matrix identification using frequency response data. *Mechanical Systems and Signal Processing*, 33 (2012) 69–82.

[59] S. V. Modak, T. K. Kundra, B. C. Nakra. Model updating using constrained optimization. *Mechanics Research Communications*, 27 (5) (2000) 543–551.

[60] S. V. Modak, T. K. Kundra, B. C. Nakra. Studies in dynamic design using updated models. *Journal of Sound and Vibration*, 281 (2005) 943–964.

[61] M. J. Atalla, D. J. Inman. On model updating using neural networks. *Mechanical Systems and Signal Processing*, 12 (1) (1998) 135–161.

[62] R. I. Levin, N. A. J. Lieven. Dynamic finite element model updating using neural networks. *Journal of Sound and Vibration*, 210 (5) (1998) 593–607.

[63] D. H. Besterfield, C. Besterfield-Michna, G. H. Besterfield, M. Besterfield-Sacre. Total quality management. *Prentice-Hall, Englewood Cliffs. NJ, USA*, 1995.

[64] W. L. Li. A new method for structural model updating and joint stiffness identification. *Mechanical Systems and Signal Processing*, 16 (1) (2002) 155–167.

[65] R. M. Lin, J. Zhu. Finite element model updating using vibration test data under base excitation. *Journal of Sound and Vibration*, 303 (2007) 596–613.

[66] E. Jamshidi, M. R. Ashory Comparative study of RFM and model updating method using base excitation test data. *Proceedings of the 27th international modal analysis conference. Orlando. USA,* (2009) 2399–2409.

[67] T. Marwala. Finite element model updating using particle swarm optimization. *International Journal of Engineering Simulation,* 6 (2) (2005) 25–30.

[68] K. S. Kwon, R. M. Lin. Robust finite element model updating using Taguchi method. *Journal of Sound and Vibration,* 280 (2005) 77–99.

[69] Q. Guo, L. Zhang Finite element model updating based on response surface methodology. *Proceedings of the 22nd international modal analysis conference. Michigan. USA,* (2004) 1990–1997.

[70] W. X. Ren, H. B. Chen. Finite element model updating in structural dynamics by using the response surface method. *Engineering Structures,* 32 (2010) 2455–2465.

[71] S. Shahidi, S. Pakzad. Generalized response surface model updating using time domain data. *ASCE Journal of Structural Engineering,* 140 (8) (2014).

[72] S. Chakraborty, A. Sen. Adaptive response surface based efficient finite element model updating. *Finite Elements in Analysis and Design,* 80 (2014) 33–40.

[73] G. H. Kim, Y. S. Park. An automated parameter selection procedure for finite-element model updating and its applications. *Journal of Sound and Vibration,* 309 (2008) 778–793.

[74] E. Fissette, C. Stavrinidis, S. Ibrahim. Error location and updating of analytical dynamic models using a force balance method. *Proceedings of the sixth international modal analysis conference. Orlando, USA,* (1988) 1063–1070.

[75] T. P. Waters. A modified force balance method for locating errors in dynamic finite element models. *Mechanical Systems and Signal Processing,* 12 (2) (1998) 309–317.

[76] G. H. Kim, Y. S. Park. An automated parameter selection procedure for finite-element model updating and its applications. *Journal of Sound and Vibration,* 309 (2008) 778–793.

[77] S. Adhikari, M. I. Friswell. Distributed parameter model updating using the Karhunen-Loeve expansion. *Mechanical Systems and Signal Processing,* 24 (2010) 326–339.

[78] J. E. Mottershead, M. Link, M. I. Friswell. The sensitivity method in finite element model updating: a tutorial. *Mechanical Systems and Signal Processing,* 25 (2011) 2275–2296. doi:10.1016/j.ymssp.2010.10.012.

[79] H. H. Khodaparast, J. E. Mottershead, K. J. Badcock (2011) Interval model updating with irreducible uncertainty using the Kriging predictor. *Mechanical Systems and Signal Processing,* 25 (2011) 1204–1226.

[80] D. E. Adams, R. J. Allemang. Survey of nonlinear detection and identification techniques for experimental vibrations structural dynamic model through feedback. *Proceedings of the International Seminar on Modal Analysis (ISMA). Leuven,* (1998) 269–281.

[81] K. Worden. Nonlinearity in structural dynamics: the last ten years. *Proceedings of the European COST F3 Conference on System Identification and Structural Health Monitoring. Madrid,* (2000) 29–52.

[82] P. Ibanez. Identification of dynamic parameters of linear and non-linear structural models from experimental data. *Nuclear Engineering and Design,* 25 (1973) 30–41.

[83] S. F. Masri, T. K. Caughey. A nonparametric identification technique for nonlinear dynamic problems. *Journal of Applied Mechanics,* 46 (1979) 433–447.

[84] F. M. Hemez, S. W. Doebling. Inversion of structural dynamics simulations: state-of-the-art and orientations of the research. *Proceedings of the International Seminar on Modal Analysis (ISMA). Leuven,* (2000).

[85] F. M. Hemez, S. W. Doebling. Review and assessment of model updating for non-linear, transient dynamics. *Mechanical Systems and Signal Processing,* 15 (2001) 45–74.